Alma Mater Studiorum - Università di Bologna

DOTTORATO DI RICERCA IN

Ingegneria elettronica, delle Telecomunicazioni, e Tecnologie dell'Informazione

Ciclo XXIX

Settore Concorsuale di afferenza: 09\F2

Settore Scientifico disciplinare: ING-INF\03

Cognitive-based Solutions to Spectrum Issues in Future Satellite Communication Systems

Presentata da: Vincenzo Riccardo ICOLARI

Coordinatore Dottorato
Prof. Alessandro
VANELLI-CORALLI

Relatore
Prof. Alessandro
VANELLI-CORALLI

Esame finale anno 2017

"...take the case of Thales, Theodorus. While he was studying the stars and looking upwards, he fell into a pit, and a neat, witty Thracian servant girl jeered at him, they say, because he was so eager to know the things in the sky that he could not see what was there before him at his very feet. [...], is a laughing-stock not only to Thracian girls but to the multitude in general, for he falls into pits and all sorts of perplexities through inexperience, and his awkwardness is terrible, making him seem a fool... "

Plato, Theaetetus, 174a-174c

Acknowledgements

The thesis is the end result of several fruitful collaborations and joint activities with researchers and people who are probably at the highest level in their research field. It is for this reason that I am really grateful to my supervisor Prof. Alessandro Vanelli-Coralli, without the support of which I would not have had the great opportunity of working in such motivating and high level environment. I believe sharing ideas and working as a part of a team aiming at common objectives is one of the most valuable and successful attitude to improve both personal and other's experience.

I would like to express gratitude to all the people I have met in my path as a PhD student with these few lines. First of all, I have to mention all the people from University of Bologna and, particularly, the Digicom group. Starting from Prof. Giovanni Emanuele Corazza, Prof. Daniele Tarchi, and Ing. Alessandro Guidotti, whose technical advices have been invaluable, to the other PhD students and researchers who everyday passionately spend their time on their research. List all of them would be impossible. However, I would like to mention some past and current members of the group with whom I shared most of the activities of my PhD: Giorgio, Sergio, Irene, Serena, Marco, Giacomo, Ala, Vahid, Stefano, Alberto, and Roberta.

Moreover, I would like to thank all the people within the CoRaSat consortium (University of Luxemburg, University of Surrey, Newtec, Thales Alenia Space, and SES), with whom I shared most of my activities from meetings to conference events. Secondly, I am really grateful to all the members of the TEC-ECT section, which have welcomed me during my stay at the European Spece Agency (ESA). I have to express particular gratitude to Ing. Daniel Pantelis-Arapoglou, Ing. Stefano Cioni, and Ing. Alberto Ginesi for their willingness and helpful contributions.

I am really thankful to Ing. Nader Alagha (ESA-ESTEC) and Ing. Eva Lagunas (University of Luxemburg), which have reviewed the thesis providing brilliant comments and suggestions.

Undertaking a PhD has been a truly life-changing experience and it would not have been possible without the support and guidance that I received from these people. There aren't enough words to express my gratitude and respect to them. I can really feel that all the experiences I had, have been worthwhile for my personal growth.

Finally, a special thanks to my mother, father, and brother. Thank you for supporting me and for being present everyday. Thank you for the valuable and constant help, in every occasion and even far away from home. Thank to Lorenza for being everyday at my side. Thank you for being always present, for supporting my choices, for being patient, and for all the efforts we make together. I am also really grateful to all my friends, who always believe and have believed (even more than myself) in me. Iacopo, Simone, with whom I share most of my interests; Marco, Andrea, for which I had to travel thousands of kilometers to meet them again; Antonello, Dylan, and Edoardo with whom I shared not only a house but many unforgettable moments in Bologna; and all the others who are now spread almost

in all Europe but any occasion would be good to meet them again: Paolo, Leslie, Marco, and so on.

Thank also to all the people that are reading these few lines. Thank to all the researchers that everyday put a lot of efforts and passion in what they do. I also hope that this thesis could be helpful and a good starting point for future researches. Thank you.

It is not the mountain we conquer, but ourselves.
Edmund Hillary.

Contents

List of Figures

List of Tables

List of Abbreviations

ACM	**A**daptive **C**oding **M**odulation
AWGN	**A**dditive **W**hite **G**aussian **N**oise
BSS	**B**roadcast **S**atellite **S**ervice
CAF	**C**yclic **A**utocorrelation **F**unction
CDF	**C**umulative **D**ensity **F**unction
CDR	**C**onstant **D**etection **R**ate
CEPT	**C**onference of **E**uropean **P**ostal & **T**elecommunications
CFAR	**C**onstant **F**alse **A**larm **R**ate
CFD	**C**yclostationary **F**eature **D**etection
CR	**C**ognitive **R**adio
CU[1]	**C**ognitive **U**ser
CU[2]	**C**apacity **U**nit
CRB	**C**ramer **R**ao **B**ound
CSI	**C**hannel **S**tate **I**information
DCA	**D**ynamic **C**arrier **A**llocation
DSA	**D**ynamic **S**pectrum **A**ccess
DVB	**D**igital **V**ideo **B**roadcasting
EC	**E**uropean **C**ommision
ECC	**E**lectronic **C**ommunications **C**ommittee
ED	**E**nergy **D**etection
EIRP	**E**quivalent **I**sotropically **R**adiated **P**ower
ES	**E**arth **S**tation
ESOMP	**E**arth **S**tations **O**n **M**obile **P**latform
EZ	**E**xclusion **Z**one
FAM	**F**FT **A**ccumulation **M**ethod
FCC	**F**ederal **C**ommunications **C**ommission
FD	**F**eature **D**etection
FFR	**F**ull **F**requency **R**euse
FFT	**F**ast **F**ourier **T**transform
FoM	**F**igure **o**f **M**erit
FS	**F**ixed **S**ervice
FSS	**F**ixed **S**atellite **S**ervice
GEO	**G**eostationary **E**arth **O**rbit
GW	**G**ate**W**ay
HDFSS	**H**igh **D**ensity **F**ixed-**S**atellite **S**ervice
HTS	**H**igh **T**hroughput **S**atellite
IA	**I**nterference **A**ccess
IC	**I**nterference **C**artography
INR	**I**nterference to **N**oise **R**atio
ITU	**I**nternation **T**elecommunication **U**nion
IU	**I**ncumber **U**ser
LHCP	**L**eft-**H**and **C**ircular **P**olarization
LNA	**L**ow **N**oise **A**mplifier

LNB	**L**ow **N**oise **B**lock
MGF	**M**oment **G**enerating **F**unction
MINLP	**M**ixed **I**nteger **N**on **L**inear **P**rogramming
ML	**M**aximum **L**ikelihood
MMSE	**M**inimum **M**ean **S**quare **E**rror
MSS	**M**obile **S**atellite **S**ervice
NCC	**N**etwork **C**ontrol **C**enter
NF	**N**oise **F**igure
NGEO	**N**on-**G**oestationary **E**arth **O**rbit
PDF	**P**robability **D**ensity **F**unction
PFD	**P**ower **F**lux **D**ensity
PL	**P**hysical **L**ayer
PU	**P**rimary **U**ser
QoS	**Q**uality **o**f **S**ervice
RF	**R**adio **F**requency
RHCP	**R**ight-**H**and **C**ircular **P**olarization
ROC	**R**eceiver **O**peration **C**haracteristic
RR	**R**adio **R**egulation
SatCom	**Sat**ellite **Com**munication
SatNet	**Sat**ellite **Net**work
SCC	**S**atellite **C**ontrol **C**enter
SCD	**S**pectral **C**yclic **D**ensity
SINR	**S**ignal to **I**nterference plus **N**oise **R**atio
SNORE	**S**ignal to **NO**ise **R**atio **E**stimator
SNOIRED	**S**ignal to **NO**ise and **I**nterference **R**atio **E**stimator and **D**etector
SNR	**S**ignal to **N**oise **R**atio
SoA	**S**tate **o**f the **A**rt
SS	**S**pectrum **S**ensing
SU	**S**econdary **U**ser
TTC	**T**elemetry, **T**racking & **C**ontrol
UT	**U**ser **T**erminal
WD	**W**aveform-based **D**etection

List of Symbols

Symbols in Chapter 3

$r(t)$	Received signal
$s(t)$	Received useful signal
$i(t)$	Received interference signal
$d(k)$	Training symbol sequence
$n(t)$	Thermal noise
W	Number of estimated pilot blocks
N_s	Number of symbols per pilot block
N_{slot}	Slot block length
N_{tot}	Number of total symbol pilots
P_0	Received signal power density
N_0	Noise power density
I_0	Interference power density
$\frac{I_0}{N_0}\|^t$	Target INR ratio
σ_ϵ^2	Error variance
$\bar{\sigma}_\epsilon^2$	Normalized error variance
B_W	Sensing bandwidth
L_{sat}	Satellite longitude
L_R	Pointing errors
θ_{3dB}	3 [dB] beamwidth angle
L_{FRX}	Feeder losses
L_{POL}	Polarization mismatch losses
A_{FSL}	Free space loss attenuation
A_P	Atmospheric attenuation
A_{TOT}	Total propagation attenuation
$EIRP_{SAT}$	Satellite EIRP
G/T_{ET}	Figure of merit of the receiver antenna
Δ_1	Additional $EIRP_{SAT}$ variation
Δ_2	Additional $(G/T)_{ES}$ variation
G_R	Receiver antenna gain
L_{POL}	Polarization losses
T_A	Terminal antenna temperature
T_{eRX}	Effective noise temperature
T_F	Terminal component temperature
T_0	Default temperature
T_{SKY}	Sky temperature
T_{GROUND}	Ground temperature
T_M	Temperature of the medium
NF	LNA Noise Factor
$\mathcal{F}$	Fisher distribution

$\mathbb{F}\{y\|a,b,c\}$	Fisher cumulative density function
D_{Fi}	i-th degree of freedom of the Fisher distribution
λ	Non-central distribution parameter
$I(z;a,b)$	Regularized incomplete beta function with parameters a, b
H_i	Decision hypothesis related to the i-th decision region $\mathcal{Z}_i$
$\mathcal{Z}_i$	i-th decision region
P_{fa}	Probability of False Alarm
$\hat{P}_{fa}$	Target Probability of False Alarm
P_d	Probability of Detection
$\hat{P}_d$	Target Probability of Detection
$p_x(x)$	Probability density function
$p_x(x\|\mathrm{X})$	Conditioned Probability Density Function
Q	Marcuum Q-function
ρ_N	Noise uncertainty
N_{oss}	Observation sensing samples
T_{oss}	Observation sensing time
γ	SINR
$\hat{\gamma}$	Estimated SINR
η	Detection threshold
η_{CFAR}	Detection threshold in the CFAR approach
η_{CFAR}	Detection threshold in the CDR approach
$\|\cdot\|_N$	Modulo-N operator
$\hat{\cdot}$	Estimated or target

Symbols in Chapter 4

n	User index
k	Carrier index
P_{nk}^{rx}	Received power at the antenna input
I_{nk}	Overall interference
I_{nk}^{EX}	External interference generated by other systems
I_{nk}^{CO}	Co-channel interference
I_{nk}^{AC}	Adjacent channel interference caused by imperfect filtering
I_{nk}^{other}	Other interference contributions
P_k	Satellite transmitted power
h_{nk}	Channel coefficient
N_B	Number of beams of the satellite
P_b^{max}	Maximum power assigned to the b-th beam
P^{sat}	Saturation power level
C_{tot}	Total achievable system capacity
C_n^{user}	User capacity
B_K	Total bandwidth per carrier
K	Number of carriers
N_k	Number of users allocated in the k-th carrier
w_{nk}	Allocation weight
SINR_{nk}^a	SINR in the assigned carrier
Q_n^{min}	Minimum QoS constraint of the n-th user
$\mathbf{S}_{N\times K}$	SINR matrix
$\mathbf{Q}_{N\times 1}$	QoS vector
$\mathbf{P}_{N\times 1}$	Transmission power vector
$\mathbf{S}^a$	SINR experienced by users vector

$\mathbf{T}^{a}_{N\times 1}$	Assigned slot vector
N_U	Number of users per carrier
$\hat{R}_m$	Target rate of the m-th user
R_{km}	User rate
$\mathbf{R}_{1\times M}$	QoS requirements in terms of minimum data rate vector
N_{max}	Total number of time slots
B_W	Total bandwidth per carrier
N_m	Assigned slots per user
$N_{tot,k}$	Assigned slots per carrier
N_{max}	Maximum number of available slots in each carrier
η_{km}	DVB-S2X MODCOD spectral efficiency
R^T_k	Achieved sum-rate per carrier
R^S	System sum-rate
t_m	User availability in changing the selected carrier
F_T	Fitness function
β	Reduction parameter
M	Number of users
N_{ch}	Total number of channels
N^{ort}_{ch}	Orthogonal channels
B^{ort}_w	Orthogonal available bandwidth
R	Outer radius
r	Inner radius
h_r	Channel coefficient threshold for zone selection
C_{ort}	Achieved capacity in orthogonal channels
C_{pr}	Achieved capacity in precoded channels
h_{ij}	Channel coefficient j-th beam / i-th user
P_i	Allocated power to the user
$\mathbf{h_i}$	Channel coefficients vector of the i-th user
$\mathbf{u_i}$	Precoding weights vector of the i-th user

To my family,

Chapter 1

The need for *"space"*

1.1 Introduction

This thesis is the outcome of three years work focused on developing solutions and strategies for improved spectrum efficiency of wireless communication systems. With particular attention to Satellite Communications (SatComs), *cognitive*-based solutions are investigated. With *cognitive*-based solutions we refer to all those techniques that aim at improving spectrum utilization of the available spectrum and rely on the knowledge of the environment in which the systems operate. As a matter of fact, an improved spectrum utilization enables higher throughput capacities that will satisfy the future markets and demands of an increasingly connected world.

The definition derives from the concept of Cognitive Radio (CR) [1, 2, 3, 4] but it is not strictly related only to it. Allowing a more flexible and efficient utilization of the spectrum is widely accepted as major solution to the *spectrum scarcity issue*, which is becoming a major problem for wireless communication systems. This higher efficiency needs to be pursued both improving the utilization of the already assigned spectrum and allowing systems to operate in wider bandwidths. Spectrum is a scarce resource and assigning wider bandwidths to different services would not be possible unless coexistence is allowed on a *shared* or *non exclusive/unlicensed* basis. However, this latter approach would be in contrast with the typical *exclusive* assignment of spectrum bands to different services defined by regulatory bodies. Among the many solutions proposed, Dynamic Spectrum Access (DSA) and Cognitive Radio (CR) are foreseen as feasible approaches to cope with a more flexible usage of the radio spectrum. As a matter of fact, the implementation of CR techniques providing an effective utilization of the spectrum, is considered as a potential enabler for future communication systems. In fact, this flexibility can contribute to the fulfilment of the challenging requirements established by the new and future communication standards as in case of 4G and 5G networks, which have recently captured the attention of scientific, standardization, and regulatory communities, [5, 6, 7].

Due to the changing environment in which communication systems have to satisfy more and more stringent and demanding requirements, cognitive radios as designed by its creator J. Mitola in [1] seem a *"wireless communication Chimera"*. However, his idea is evolved and, based on the same concept of sharing the spectrum, similar solutions are still proposed and under investigation within several contexts. The basic idea proposed by

Mitola in [1] was to design a radio, later the concept was extended by Akyildiz in [4] to entire networks and systems, with an improved level of cognition. This additional level of cognition, in particular, aims at improving spectrum utilization enabling systems to operate in the same bands both exploiting opportunistically chunks of spectrum not used by others and avoiding inter-systems interference. Thanks to the proposed approach, it would be possible to supersede the fixed spectrum allocation policy that limits the efficiency of the spectrum and enabling new spectrum opportunities to meet future requirements. The fixed allocation policy now in use is regulated and established by regulatory bodies as FCC, CEPT, and ITU, which, however, are already modifying the actual regulatory to cope with the increasing demands by means of amendments and proposing in several standards the use of *shared* and *non exclusive* bands. Of course, either an additional complexity or adaptations with respect to the typical design of a communication system are required for achieving the necessary cognition. In particular, features to cope both with the knowledge of other systems exploiting the resources in the same environment, and with the common transmission and receiving operations, are required. In the parlance of CR, all these features usually refer to the *"cognitive cycle"* as depicted in Figure 1.1. The *"cognitive cycle"* is the framework on which the correct functioning of cognitive radios is based on. It includes different phases that are repeated depending on the status of the environment in which the system operates. From a general point of view, the system has to operate alternating two main phases, namely *spectrum awareness* and *spectrum exploitation*, which include all the tasks to be performed for the correct exploitation of the shared spectrum. Consequently, dedicated techniques need to be designed with respect to the different phases. In particular, *spectrum awareness* refer to all the operations needed to cope with the knowledge of other systems operating in the environment. On the other side, *spectrum exploitation* techniques aim at establishing the proper communication between cognitive transmitter and cognitive receiver. Of main importance for cognitive systems is the knowledge of the different systems operating in the same environment. Especially in case these latter have priority in using the spectrum, namely the *Incumbent* or *Primary Users*. The cognitive radio or system, also known as *Secondary User* (SU) must avoid unwanted inter-system interference, which is one of the main issues in cognitive radios since spectrum will still be regulated on a priority and hierarchy basis. Thus, the additional cognition supplied to the system is mainly intended to cope with coexistence of different systems in the same spectrum allocation.

With particular focus on SatCom systems exploiting either on an *exclusive* or a *non exclusive* basis the available spectrum portions, techniques aiming at an improved spectrum utilization based on the knowledge of the environment in which they operate, *i.e.*, *cognitive*-based solutions, are here investigated. In particular, the high rate demands of future markets would be satisfied by improving the utilization of bands already assigned to SatCom on an *exclusive* basis, which, however, are becoming limited, and exploiting wider bandwidths coexisting with other systems. In particular, the latter solution will be necessary as far as the environment will be populated by an increased number of services and several different systems. In the context of satellite communications, the application of cognitive radio concepts is still a rather unexplored area and only in the last years attention is raised

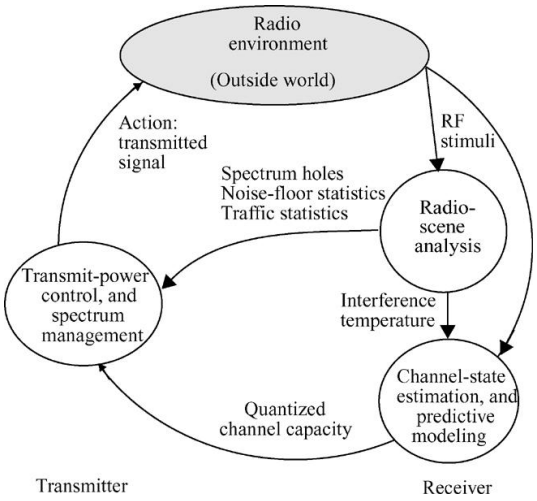

FIGURE 1.1: The cognitive cycle [2]: basic operations of a *cognitive*-based systems.

on the topic. As a matter of fact, a considerable number of areas to be investigated are still open. Although initially few opportunities have been conceived on the application of CR in SatCom scenarios, the interest on the topic is recently increased. In fact, despite the wide literature in the case of terrestrial systems (see, as an example, [2, 3, 4, 8]), its application in Satellite Communication scenarios has raised attention only in the last years, [9, 10]. Introducing cognitive capabilities in a satellite environment certainly allows exploitation of new dimensions for the coexistence with other systems but also provides new challenges to be addressed. On the other side, an improved spectrum exploitation of the available *exclusive* bandwidth is also investigated. With this aim, interference management techniques and a higher frequency reuse can provide even in spectrum limited scenarios higher gains rather than the common frequency deployment of SatCom systems. The considered approach has been recently investigated in [11, 12, 13, 14, 15]. However, the application of the proposed techniques in spectrum limited scenarios and with respect to system architectures that flexibly can exploit the available resources, is raising interest only recently. Either in case of *exclusive* or *non exclusive* bands, the foreseen spectrum efficiency is enabled by knowledge of the environment, which requires knowledge of Channel State Information (CSI). Thus, following the approach advocated by CRs, which is based on the *cognitive cycle* and alternates awareness and exploitation of the available spectrum, techniques have been designed and adapted to the considered case of studies.

The thesis is divided in three main chapters. Chapter 2 focuses on the description of the reference systems and scenarios considered as starting point of the analysis carried out through the thesis. Two systems, one in case of Ka-band and the other operating in L-band, are considered. The reference Ka-band system, for which cognitive features are developed and built as additional tools to operate in a cognitive environment, is presented in section 2.1. On the other side, the L-band system architecture, which exploits its flexibility to improve spectrum efficiency but no modification of the system architecture is considered, is presented in section 2.3.1. Different scenarios are addressed for both. In sections 2.2 and 2.3.2, three different

scenarios affected by possible spectrum allocation issues (two in case of the Ka-band and one for the L-band scenario), are described. As demonstrated through the thesis, the two reference satellite systems can take advantage of the additional *cognitive*-based capabilities in the considered scenarios. The additional cognition is achieved by the implementation of *spectrum awareness* and *spectrum exploitation* techniques as described in Chapter 3 and Chapter 4, respectively. In Chapter 3, a technique based on the joint estimation and detection of the Signal-to-Noise-plus-Interference Ratio (SINR) for *spectrum awareness* is developed. The studies are related to the design of the proposed techniques for an improved knowledge of the environment in case of shared bandwidth scenarios (section 2.2). Practical impairments and uncertainties are taken into account and analysis are carried out. In Chapter 4, techniques aiming at an improved spectrum exploitation are investigated. As will be clarified throughout the thesis, Dynamic Carrier Allocation (DCA) techniques are considered as effective solutions to cope with the spectrum exploitation in the selected cognitive scenarios in Ka-band. First, a technique for carrier allocation purposes based on complete knowledge of the CSI is reviewed. To this aim and avoiding redundancy on the feed back to the gateway, a technique on genetic algorithms is also proposed, section 4.3.3. In addition, solutions for spectrum limited scenarios are investigated in case of *exclusive* bands in the L-band scenario. With particular interest in hot spot scenarios, flexible configuration exploiting higher frequency reuse and interference mitigation techniques are studied in section 4.4. Finally, Appendix A reviews the main findings in literature concerning the application of cognitive-based techniques in SatComs. The proposed references have been considered as starting point of the studies and analysis proposed in the thesis.

1.2 Motivations and Objectives

Satellite Communication systems have always played a major role in service delivery either for common or more specific markets. The importance of SatCom reflects the uniqueness of the system, which would never be replaced by terrestrial systems and which would still have a main role in future communications. However, densification of the spectrum and a critical exploitation of the medium will affect similarly, if not worse in case of SatComs, both. The new generation of satellite communication systems need to be designed to deliver higher throughputs to the user terminals. In particular, satellite systems are nowadays more integrated with other communication systems and play a fundamental role in creating a global digital society. SatComs fullfil a range of user needs, which go from commercial to military purposes also supporting diverse user requirements and use cases. Services as broadcasting or internet access are supported by satellite operators, which can deliver services to costumers that are at specific deployed locations, also when not reachable by terrestrial networks or where those networks experience performance and capacity limitations.

Moved by the fundamental role of SatComs for future wireless communications, this thesis proposes solutions to the increasing densification of the radio spectrum, which will be a limiting factor in the deployment of future systems. The proposed way forward foresees the necessity by satellite

systems to acquire, first, cognition of the environment in which they operate and, secondly, apply techniques for a correct spectrum utilization aiming at higher spectrum efficiencies and coexisting with other systems when spectrum is shared. SatComs will thus benefit either from an improved use of the *exclusive* spectrum and from exploiting additional bands in case new spectrum opportunities are enabled.

The specific characteristics of satellite systems make them essential in future wireless communication. Nowadays, according to the service they provide, different spectrum portions are allocated to satellite services. In the last years, lot of interest has been put in higher frequencies as Ka-bands. In these bands a wide spectrum is still available. However, also terrestrial systems are allocated in Ka-bands and even more will be in the future. Due to the fast deployment of new communication systems that will saturate these bands as already happened in case of lower frequencies, a more flexible approach in exploiting the spectrum is necessary. On the contrary, in lower frequency bands, which are almost saturated due to the higher number of services deployed, an improved efficiency on a *exclusive* basis would be more feasible even in case of limited available spectrum.

Considerable advantages and an improved exploitation of the spectrum are foreseen by means of the application of cognitive radio techniques in satellite communications. In particular, it is necessary to investigate how a more flexible usage of the spectrum for these systems is possible since different and additional dimensions of the spectrum can be exploited. As an example, one of the main advantages of satellite systems is linked with their capability to illuminate also areas in which terrestrial systems can not be able to transmit. Thus, the space or angular dimensions can provide additional gain allowing different systems to coexist in the same spectrum bandwidth but in different areas. Thus, it will be possible, based on the only additional cognitive capability provided to the system, to enhance the spectrum usage without incurring to regulatory actions.

This work investigates several approaches aiming at an improved utilization of the assigned bandwidths in SatCom scenarios affected by spectrum issues. The main objective of the thesis is to develop feasible solutions with respect to the scenarios presented in section 2.2 and 2.3.2. These solutions have been conceived aiming both at a short and long term perspective. Thus, what is proposed in this thesis are, first of all, solutions that take into account feasible applicability in real scenarios and their practical impairments. With respect to the current SatCom system architecture and possible future modifications, both the spectrum awareness and exploitation phases are addressed. The thesis goes through the analysis of the whole cognitive cycle, *i.e.*, first being aware of the available opportunities and, then, their exploitation. The effectiveness of the proposed techniques in the considered scenario has to be addressed by means of appropriate Figures of Merit (FoM). Thus, specific FoM to evaluate the application of cognitive techniques in a satellite environment are also proposed in the thesis.

Achieving the objective of defining a real cognitive radio satellite system need a long process that involves, among others, regulatory and standardization bodies. However, from a technical point of view, proposing feasible and practical solutions in the short term gives a real motivation both for further investigations and for developing a truly operational cognitive satellite system. Thanks to the flexibility that can be provided by satellite

communications, establishing the possibility of a dynamic spectrum usage also considering presence of other systems have a dual advantage. First of all, a wider spectrum can be allocated to SatComs since the application of cognitive techniques allows not to interfere or be interfered by other systems. This can provide a wider bandwidth that can be exploited by several services with a consequent gain in capacity. Secondly, a better exploitation of the *exclusive* spectrum that will be scarse in a near future due to the increasing number of different services that are raising, would be possible.

1.3 Personal Contributions

This thesis is the end result of several fruitful collaborations and joint researches performed during my PhD activities. The studies carried out during the first and second year have contributed to the positive conclusion of the project CoRaSat (Cognitive Radio for Satellite Communication) [16]. The project founded by the European Commission (EC) aimed at "investigating, developing, and demonstrating cognitive radio techniques in satellite communication systems for spectrum sharing". The outcomes of the study also aimed at "driving the definition of strategic roadmaps to be followed towards regulatory and standardization groups in order to ensure that the necessary actions are undertaken to open new business perspectives for SatCom through cognitive radio communications in support of the Digital Agenda for Europe", [17].

During the project, the spectrum awareness technique described in Chapter 3 has been proposed and investigated with respect to the selected scenarios. A complete characterization of the proposed technique, namely SNOIRED, has been carried out. The technique relies on the joint estimation and detection of interfering users. Although the technique has been developed for the considered scenarios, general applicability would be possible from a theoretical point of view as well. Thus, the technique has been modeled firstly ideally for a general application in cognitive radio systems and, secondly, its assessment in the considered SatComs scenarios has been provided. With respect to the specific case of SatComs, an analysis under practical uncertainties has also been performed. The proposed spectrum awareness is assessed in terms of the typical Figures of Merit of estimation and detection. Due to the novelty of the application of cognitive radios in SatComs, an additional analysis is carried out in terms of geographic performance, which is of main importance in the considered topic. The geographic assessment quantifies the area that can be exploited by the cognitive satellite to provide services in already used spectrum bandwidths. With respect to considered cognitive-based SatCom scenarios, the adaptation of other existing techniques as Energy Detection (ED) and Cyclostationarity Feature Detection (CFD) has been investigated and assessed during the project as starting point for the development of the new proposed technique. Personal contributions regarding the proposed awareness technique and the assessment of existing techniques in a SatCom environment are [18, 19, 20], and the project deliverables [21, 22, 23], where additional information can be found.

Chapter 4 addresses the development of exploitation techniques for an efficient use of the available spectrum in cognitive-based SatCom scenarios. The exploitation part is strictly related to the architecture of the system and the scenarios taken into account. Thus, the exploitation of additional frequency bands in which the presence of other systems can occur, could entail the modification of several segments of the satellite system. For the considered cognitive-based scenarios, we focussed on developing new algorithms for carrier allocation. The proposed algorithm based on Genetic Algorithms (GAs) and for which additional information can be found in [24], aims at minimizing the feed back signals due to the redundancy of the information that the user terminals need to feed back. Analysis with respect to algorithms based on the complete knowledge of the channel state information are provided as well. In addition, the third year of the PhD was focussed on the study of a more flexible exploitation of the available resources of L-band Mobile Satellite Systems (MSS) in case of limited spectrum scenarios. The studies, which have been carried out during a stay of eight months in ESA-ESTEC where I joined the TEC-ETC section as visiting researcher, aimed at investigating intra-system interference mitigation techniques in hot spots. In particular, the joint application of linear precoding techniques for MSS systems and the flexible use of the system's resources has been investigated. With respect to the application of precoding techniques, several analysis have been carried out also including studies on the impact of impairments and on comparing the performance of the technique in different scenarios. Some of the main outcomes of these research activities has been included in [25].

Further personal contribution with respect to the development of techniques for cognitive-based SatCom system and the related spectrum issues are [10, 26, 27, 28, 29, 30]. These works provide additional and complementary results related to the work performed during the PhD activities. The works [10, 26, 28, 30] are related to the main outcomes obtained as part of the CoRaSat consortium during the project. On the contrary, [27, 29] include some additional analysis on parallel aspects of my research.

Chapter 2

System and Scenario Definition

In this chapter are introduced both the system and the scenarios that are taken into account for the development of the proposed *cognitive*-based solutions for spectrum issues in SatCom environments. The design of techniques in Ka-band SatCom environments is related to Scenario 1 and 2, whereas the third scenario, Scenario 3, addresses solutions for L-band systems in case of spectrum limited scenarios. These scenarios are considered as baseline for the development of *cognitive*-based techniques to be included in the system architecture for an improved spectrum efficiency. With particular focus on the two former scenarios, the reference Ka-band system architecture for future developments is taken into account as starting point [31, 32]. Each segment is analyzed and the necessary modifications are described in the chapter. Spectrum policies and regulatory issues are taken into account in order to highlight which spectrum opportunities are present and how regulatory bodies cope with the problem of spectrum scarcity. Following, coexistence of different systems in the selected scenarios is studied and feasible approaches to the problem, which would be analyzed in depth through the thesis, are proposed. With respect to the third scenario, the analysis does not take into account presence of different systems in the same spectrum but addresses a limited spectrum availability for the selected system. The issue, as in the previous scenarios, is related to the stringent spectrum policies that are limiting the availability of *exclusive* bands. As a matter of fact, improving the spectral efficiency of satellite systems in spectrum limited scenarios would also allow SatCom systems to cope with the higher demands of future markets. In Table 2.1 the main aspects of each scenario, which will be detailed in the following sections, are resumed.

2.1 Ka-band System Architecture

The typical architecture of satellite systems operating in Ka-bands is assumed to be the baseline for future developments in which include cognitive features. Due to the growing importance of higher frequencies, which provide significant spectrum allocations and higher capacities, future satellite systems are foreseen to operate in these bands. As in case of new *"High Throughput Satellite"* (HTS) systems, which have been developed thanks to the significant advances in SatComs in the recent years, the advantages of SatComs systems let them having a leading role in communication markets. In particular, satellites have different missions, either civil or military, and provide globally a wide range of services, from broadcast and broadband transmissions to navigation services.

	Scenario 1	Scenario 2	Scenario 3
Spectrum Range GHz	[17.3-17.7]	[17.7-19.7]	[1.6]
Primary User	BSS	FS	MSS
Cognitive User	FSS	FSS	none
Spectrum Issue	Different System Coexistence		Limited Availability
Interfering links	BSS toward FSS	FS toward FSS	Intra-system Interference
Awareness applicable techniques	Database, Sensing, other		CSI feedback at the GW
Exploitation applicable techniques	Carrier Allocation, Power Control, other		Higher Frequency Reuse, Interference Mitigation
Policies and Amendment for spectrum coexistence	ECC/DEC/(05)08 ECC/DEC/(13)01	ERC/DEC/(00)07 ECC/DEC/(13)01	FCC and CEPT Spectrum Policies

TABLE 2.1: Main aspects of the selected scenarios.

A typical satellite system foresees three different segments: the ground, the space, and the user segment. In Figure 2.1 the three segments are illustrated. The reference SatCom system architecture foresees a star topology where gateways (GW) establish a point-to-multipoint connection with the user terminals (UTs). The elements in charge to manage all the functionalities of the system, to control communications on ground, and to supervise the correct functioning of the overall system are included in the ground segment. More in details, one or more high-capacity gateways, which are Earth Stations (ES) with large-antennas that feed the space segment; the Telemetry, Tracking and Control (TTC) station in charge of the management of the satellite; a Network Control Center (NCC) and a Satellite Control Center (SCC) aiming at a correct functioning of the system; are taken into account. These elements are also connected through an interconnection network, which provides connectivity to other infrastructures as terrestrial telecommunication networks. The space segment includes the satellite payload. Modern Ka-band systems are typically Geostationary Earth Orbit (GEO) satellites, which are positioned to a specific longitude and at an altitude of around $36\,000$ Km. In addition, modern payloads are designed to be multi feeds and to support multiple beams, which provide continuous coverage over a specific geographic area. The satellite can generate by tens to hundreds of spot beams. The spot beams are overlapping and frequency reuse of the available user bandwidth, i.e., the available Space-to-Earth spectrum toward the user terminals, is exploited to reduce co-channel interference among adjacent beams avoiding to allocate the same bandwidth to them. Portions of the user bandwidth repeat according to a specific pattern over the beams as shown in Figure 2.2 in case of a 4 and 3 color reuse. The user segment includes all the end User Terminals (UTs) that are spread along the beam coverage of the satellite and to which communication is provided. The satellite can provide different services to the UTs, which can be either fixed or mobile, regardless their location. When a two-way communication with the ground segment is established, the traffic from the ground segment to the UTs, namely the forward link, passes through the satellite, while return links from the UTs to the GW, which are in general asymmetric, can be provided either by the satellite or terrestrial networks. The forward and the

return links are organized and subdivided in carriers and in carrier groups in the forward and return link, respectively. The reference air interface in case of forward links is the DVB-S2 standard and its extension DVB-S2X [33, 34], whereas the DVB-RCS(2) [35] is used on the return link.

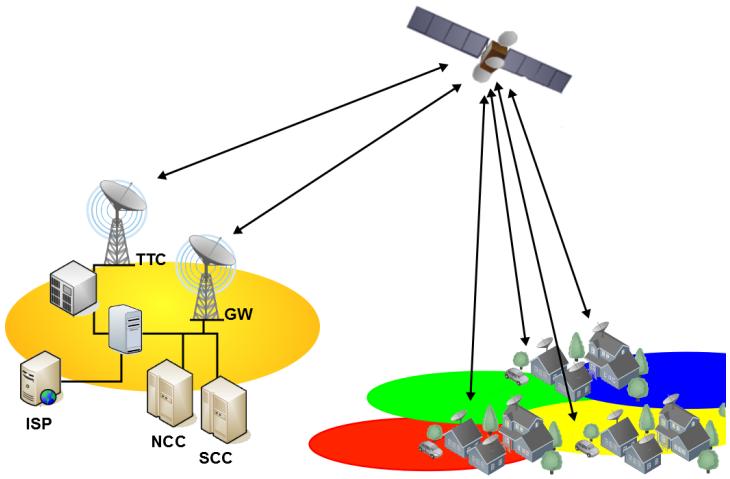

FIGURE 2.1: Ka-band Reference System Architecture.

The deployment of satellite systems in Ka-band allows wider bandwidths to be exploited. From a regulatory point of view, the spectrum in which priority is given to satellite systems goes from 27.5 to 30 GHz in case of Earth-to-Space Fixed Satellite Services (FSS) transmission links and from 17.7 to 20.3 GHz for Space-to-Earth downlinks [36, 37]. In particular, user links, *i.e.*, from the satellite to the UTs and vice-versa, exploit on a *exclusive* basis the bands from 19.7 to 20.2 GHz on the downlink and from 29.5 to 30 GHz on the uplink. The feeder links from the gateways to the satellite use the other portions of the assigned Ka-band spectrum but higher bands as Q/W bands are meant to be exploited in future. Figures 2.3 and 2.4 present a typical frequency plan for uplink and downlink in Ka-band, respectively. With focus on the user link, the downlink toward the UTs supports 250 MHz per beam and a four color reuse frequency is usually taken into account allowing frequency reuse with reduced co-channel interference between adjacent spot beams. Half of the available user bandwidth, and one of the two available circular polarizations (RHCP and LHCP), is assigned to each beam. The number of colors and the related frequency reuse is a trade-off between system capacity and acceptable amount of interference. As described in [29] other colors can be exploited as well.

Spectrum congestion will also affect future Ka-band deployments. In fact, HTS are already starting to suffer from spectrum scarcity in Ka-band and downlink spectrum availability is a major issue. The 500 MHz of *exclusive* spectrum for the deployment of FSS systems are the only available in all ITU Regions and might not be able to cope with the high demands of future markets. Thus, access to further spectrum could potentially allow more efficient utilization. As will be clarified in the next paragraph 2.2, regulatory bodies are currently modifying in some countries the spectrum allocation policy allowing FSS satellite systems to use terrestrial spectrum on a *non-protected*, *non-interference* basis both in case of satellite feeder and user

links. These decisions are based on national agreements and granted landing rights, but no general standardized solutions exists. The exploitation of these additional bandwidths, namely *non exclusive*, would be possible thanks to additional features to be included at system level [38]. Satellites have evolved thanks to numerous technological innovations that have led SatComs-based systems to be one of the most important service provider in the communication market. However, several modification would be necessary to cope with the problem of spectrum scarcity and system densification. Assuming satellite systems with additional cognitive capabilities in order to exploit wider bandwidths, implies modification to the present architecture. These modifications allow coexistence of non-coordinated but prioritized systems in the same spectrum portion. In particular, this coexistence would be mainly based on the necessary knowledge of the activities from other systems and on the flexible capability of the system to modify its transmission parameters. Some major modification to the system are foreseen for all the segment of the system. With respect to the ground segment, in order to provide this additional knowledge, an external cognitive radio database as additional network element or an interference access (IA) database can be included. Thanks to a database, a priori information on other systems can be exploited even thought additional processing capabilities would be necessary [39, 40, 41, 42, 43]. Concerning the space segment, the payload needs to be capable to process wider bands or handle more spectrum portions. *Exclusive* and *non exclusive* bandwidths can be independently exploited as different Satellite Networks (SatNets) over the same payload. Thus, it would be possible to associate different transmissions according to the availability of each SatNet. The usage of both *exclusive* and *non-exclusive* frequency bands, however, provides additional cost and complexity of the space segment due to the introduction of further frequency bands. The user segment would be also affected by the exploitation of additional bands. Bandwidth limitations of the forward link carriers for the UTs will occur due to receiving and processing capabilities of the terminals. For the receiver front-end, in fact, the antenna system has to take into account the wide frequency band over which the terminal has to receive and transmit. Terminals need to be capable of tuning into either the *exclusive* or the *non-exclusive* bands. In addition, new processing capabilities providing improved spectrum awareness and exploitation need to be developed both in the ground and the user segments.

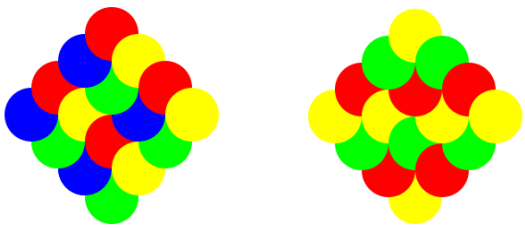

FIGURE 2.2: Examples of frequency reuse patterns.
4 Color (left) and 3 Color (right) frequency reuse.

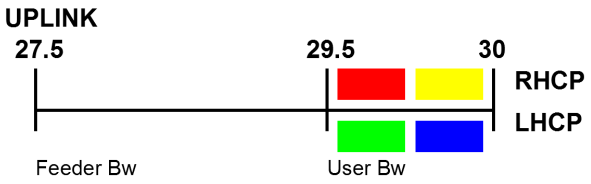

FIGURE 2.3: Reference Uplink Spectrum Allocation

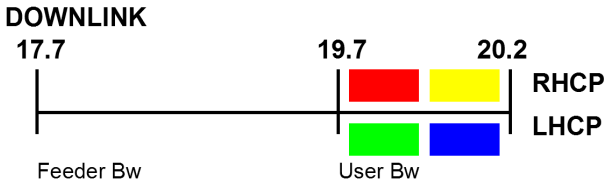

FIGURE 2.4: Reference Downlink Spectrum Allocation

2.2 Ka-band Scenarios

In the context of cognitive radios, the consolidation of feasible scenarios in which a cognitive system or network can operate is fundamental. Regulatory bodies as ITU, CEPT and FCC establish by spectrum allocation policies [36, 37] the coordination of the different services among the radio spectrum. However, they are currently modifying the present spectrum allocation by means of amendments. The allocation policies are constantly evolving defining portion of spectrum in which different systems can coexist because allowing system to operate in wider bandwidth would cope with the higher spectrum demands. Thanks to the application of cognitive techniques coexistence would be enabled. In the following, the two reference scenarios taken into account for the development of the proposed techniques for cognitive-based satellite systems, are detailed.

2.2.1 Scenario 1: CR Satellite user downlink Ka-band [17.3 – 17.7 GHz]

Scenario 1 foresees the deployment of cognitive satellite user downlink in the range of spectrum between 17.3 and 17.7 GHz. The considered spectrum is assigned to uplink feeder links (Earth-to-Space) of Broadcasting Satellite Services (BSS). However, cognitive satellite systems can exploit the same bands for downlink purposes providing services to mobile or fixed satellite terminals. The scenario allows a possible implementation of cognitive systems due to recent decisions at regulatory level. In particular, CEPT has adopted the Decision ECC/DEC/(05)08 [44], which gives guidance on the use of this band by "high density applications in the Fixed-Satellite Service" (HDFSS). The Decision stipulates that the designation of the band 17.3 – 17.7 GHz is without prejudice to the use of this band by Broadcasting Satellite Service (BSS) feeder uplinks and that it is not allocated to any terrestrial service on an incumbent basis (except in some countries). The deployment of uncoordinated Fixed-Satellite Service (FSS) Earth stations is also authorized in these bands. Thus, the presented scenario, foresees

the possibility of deploy uncoordinated FSS stations that could increase frequency exploitation by flexible usage of the spectrum portion through the adoption of cognitive radio techniques. Moreover, with regard to satellite terminals on mobile platforms, the ECC Decision ECC/DEC/(13)01 [45] addresses the harmonized use of Earth Stations On Mobile Platforms (ESOMPs) operating within the given frequency band.

The interfering links that can occur in the deployment of different systems in the same spectrum bandwidths need to be evaluated. The assessment allows the adaptation of the desired cognitive radio techniques to the selected scenario. In case of Scenario 1, Figure 2.5 represents the useful and interfering links that can occur. In particular, no interference from space to ground FSS links to the BSS system occurs since the BSS satellite is GEO and is not interfered by the downlink of other GEO or NGEO FSS satellites. Hence, the issue of incumbent protection can be sufficiently guaranteed under this scenario. On the contrary, the cognitive system needs to employ appropriate techniques to avoid interference from the BSS feeder station since in the vicinity of BSS feeder stations, the FSS terminals can receive harmful interference.

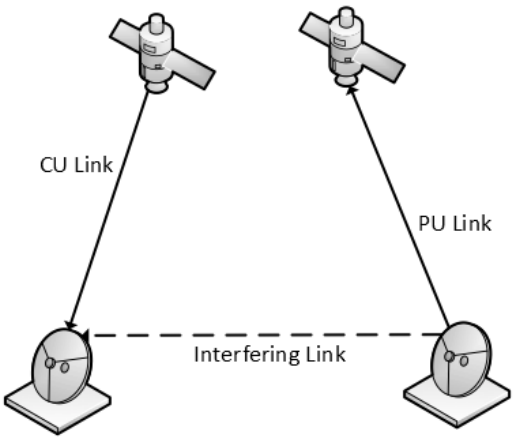

FIGURE 2.5: Scenario 1 interference link representation

As depicted in Figure 2.6, it can be assumed that only few cognitive terminals will be interfered since a limited number of BSS feeder GWs are deployed. In this context, Exclusion Zones (EZ) can be defined [46]. An Exclusion Zone is defined as the area around a BSS feeder or a general incumbent user where the SINR margin of the cognitive FSS terminals is not satisfied. The geographical density of the BSS feeders is low and a vast geographical area outside the EZ becomes available for cognitive downlink communications in the band from 17.3 to 17.7 GHz. The exclusion zones can be defined by a contour around the feeders. These contours can be assumed limited since BSS feeders antennas are highly directional. A more accurate definition of them would, therefore, allow the deployment of cognitive UTs. By acquiring information about existing BSS gateway stations, RF maps can be created in order to find out the spectral holes in the geographical space domain. Thus, an Interference Cartography (IC) map, which can be subsequently used to find out the regions where the cognitive satellite system can operate by satisfying the QoS requirement of the users, can be created. Subsequently, the cognitive FSS terminals can be deployed

outside this zone. The combination of a database and a coordination approach can be applied for this scenario in which the jointly exploitation of a priori and dynamic information gathered by the UTs on the BSS gateway activities, can achieve an overall improved exploitation of the spectrum. With this aim, since the cognitive radio is active in downlink while the incumbent user is the uplink BSS feeder and the chance of interference from the cognitive GEO satellite to the incumbent GEO satellite is almost zero, the awareness phase acquires a fundamental importance for the cognitive transmission. In fact, in this scenario, no spectrum awareness is required to protect the incumbent user. However, the FSS terminal can receive interference from the BSS feeders. Therefore, spectrum awareness can be employed by the FSS in order to avoid the interference coming from the BSS feeders. Contrary to the exploitation of a priori information from databases, we refer to *sensing* techniques as those awareness techniques performed by the cognitive users that can generate or suffer harmful interference in order to directly have knowledge of other systems' spectrum activities. Following, the correct exploitation of the detected spectrum opportunities would be enabled by techniques that allow transmissions in case of no or acceptable interference, *i.e.*, outside the exclusion zones.

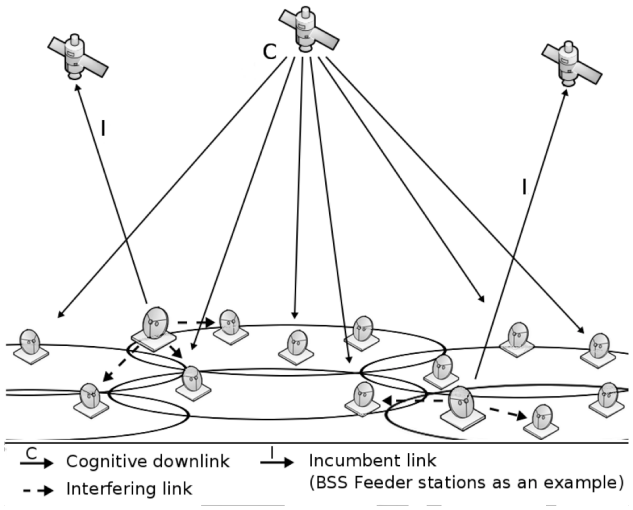

FIGURE 2.6: Detailed Scenario 1 and interference links

2.2.2 Scenario 2: CR Satellite user downlink. Ka-band [17.7 – 19.7 GHz]

Scenario 2 addresses the deployment of cognitive radio satellite downlinks in the spectrum portion between 17.7 and 19.7 GHz. Contrary to the previous scenario, scenario 2 can be considered as an extension of the FSS exclusive frequency band 19.7 – 20.2 GHz by adding significant spectrum in the 17.7 – 19.7 GHz bandwidth. The cognitive-based satellite systems has to cope with terrestrial Fixed Services (FS), which have priority in the considered band. However, CEPT has adopted a Decision, ERC/DEC/(00)07 [47], which gives guidance on the use of this band by both Fixed Satellite Services (FSS) and Fixed Services (FS). The Decision stipulates that stations of the FSS can be deployed anywhere, but without right of protection from

interference generated by FS radio stations. This Decision sets the conditions under which the 17.7 – 19.7 GHz spectrum is used by: coordinated and protected Earth stations (Earth-to-Space, forward link), terrestrial FS links, and uncoordinated and unprotected end-user Earth stations (Space-to-Earth links, forward link). The latter links, which are not coordinated through a national frequency assignment process, shall not claim protection from FS stations. In order to decrease the probability of interference to uncoordinated FSS Earth stations, the FS, when practical, shall implement mitigation techniques such as automatic transmitter power control, high performance (low side lobe) antennas and EIRP limited to the minimum necessary to fullfil performances of FS link. On the contrary, uncoordinated Earth stations, when practical, shall implement mitigation techniques such as dynamic channel assignment (to select a non-interfered channel when available), site shielding or high performance (low side lobe) antennas in order to limit the interference from FS stations. With this aim, cognitive radio techniques could significantly increase the spectrum usage by enabling FSS to access into the same frequency spectrum of terrestrial transmitters. Thus, cognitive radio techniques could act as a dynamic and flexible protection of FSS downlink from FS interference. With regard to satellite terminals on mobile platforms, also in this scenario the ECC Decision ECC/DEC/(13)01 [45] addresses the harmonized use of ESOMPs operating within the given frequency band.

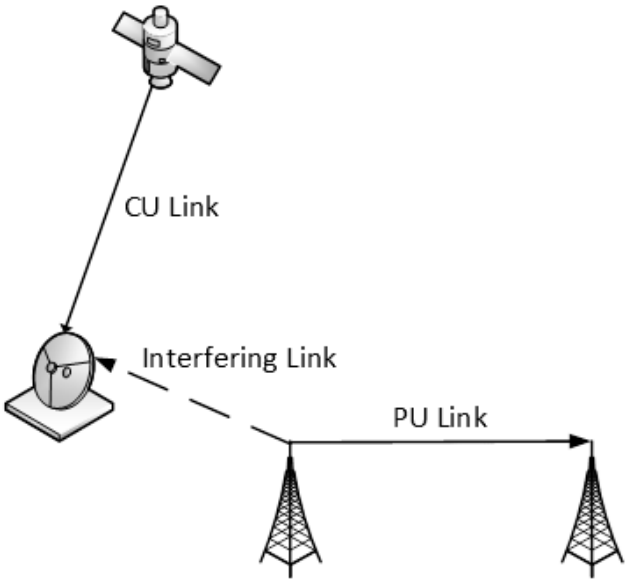

FIGURE 2.7: Scenario 2 interference link representation

In Figure 2.7, the interfering links between the two deployed systems are shown. In this scenario, either the satellite or the FS transmission links can interfere each other. Article S21 of the ITU Radio Regulations [48] defines Power Flux Density (PFD) limits for emissions in various frequency bands up to 40 GHz in order to limit interfering emissions from transmitting FSS Space-to-Earth links to FS terrestrial receivers. The limitation are posed in terms of ground PFD for the given frequency band from 17.7 to

19.7 GHz. Considering the worst case scenario, the EIRP density that corresponds to a limit of ground power flux density amounting to $-115\ [\frac{dBW/m2}{MHz}]$ for an elevation of $5\ \mathrm{deg}$ is greater than $47\ [\frac{dBW}{MHz}]$, while the maximum EIRP density of Ka-band satellite systems typically never exceeds $40\ [\frac{dBW}{MHz}]$ [21]. As a results, typically, the FSS downlink would not interfere with the FS link. In this scenario, the downlink interference from the cognitive satellite to terrestrial FS receivers is assumed negligible due to limitation in the maximum EIRP density of the current Ka band satellite system. The only harmful interference to handle in this scenario is, therefore, the interference received by the satellite user terminals from the FS transmitters.

The approach followed for Scenario 1 would be similar for Scenario 2. The application of cognitive techniques aims at avoiding interference from incumbent users, which in the selected scenario are FS transmitters. The EZ is, thus, defined as the area around an FS link where the SINR margin of the cognitive FSS terminal is not satisfied. As in Scenario 1, depending on the knowledge on the FS links, a more effective approach to coexistence is possible. However, different link budget properties apply. as an example, it has to be taken into account a different directivity of the FS interfering link. The interference from FS transmitters to the cognitive satellite terminal needs to be taken into account in order to guarantee the QoS of the cognitive users. Thus, the combination of database and sensing seems to be promising also in this scenario. Based on the available information on FSs, which however would be wide-ranging due to the multiple application of microwave links, from the regulators and operators, an initial database can be created and sensing can be employed in the regions where clear geographical spectrum holes are not present and periodically to provide updated information if needed. As in Scenario 1, spectrum sensing is necessary in order to avoid activities in those bands where the receiving interference from the FS microwave links are higher than a specific threshold rather than protect the incumbent user. Also exploitation would be performed similarly to Scenario 1.

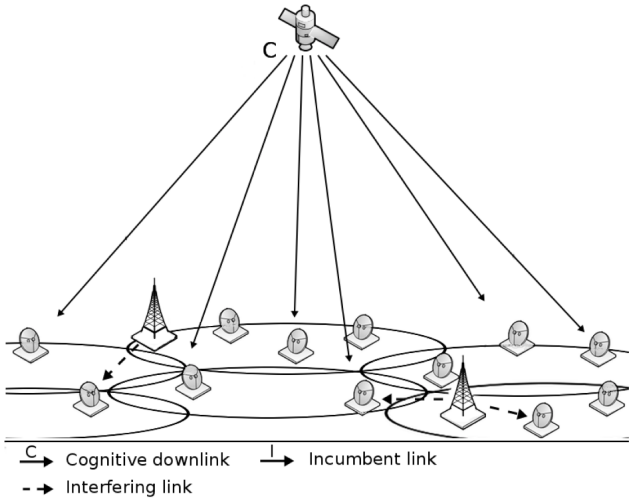

FIGURE 2.8: Detailed Scenario 2 and interference links

Fixed Service (FS) system review

Microwave point-to-point radio are line of sight radio terrestrial communication links. Due to their deployment since the beginning of wireless communications history, Fixed Services (FS) can be either analog or digital transmissions, while broadcasting, telephone service, and backhauling are the most common services provided by these systems. Moreover, due to the great number of different services, transmission parameters as bandwidths, modulations, transmission power, or transmission ranges vary as well. From a general point of view, microwave point-to-point radio links are directive links, which would highly interfere FSS terminals only if FSS are deployed along the link direction. Some guidance on the deployment of FS links, which can be used as useful reference to derive models, are provided. As a matter of fact, knowledge of transmission parameters and antenna radiation patterns is essential to perform detailed interference analysis from which derive and design cognitive techniques aiming at system coexistence. Some of the recommendation are:

- Recommendation ITU-R F.758-5 [49], *"System parameters and considerations in the development of criteria for sharing or compatibility between digital fixed wireless systems in the fixed service and systems in other services and other sources of interference"* presents parameters for Point-to-Point FS systems in the band 17.7-19.7 GHz;
- Recommendation ITU-R F.699 [50], *"Reference radiation patterns for fixed wireless system antennas for use in coordination studies and interference assessment in the frequency range from 100 MHz to about 70 GHz"*;
- Recommendation ITU-R F.1245 [51], *"Mathematical model of average radiation patterns for line-of-sight point-to-point radio-relay system antennas for use in certain coordination studies and interference assessment in the frequency range from 1 GHz to about 70 GHz"*;
- Recommendation ITU-R F.1336 [52], *"Reference radiation patterns of omnidirectional, sectoral and other antennas in point-to-multipoint systems for use in sharing studies in the frequency range from 1 GHz to about 70 GHz"*.

2.3 L-band System Architecture and Scenario

2.3.1 L-band system architecture

We consider a typical Mobile Satellite System (MSS) operating in L-band where a GEO multibeam and multifeed satellite covers with hundreds of beams a wide geographical area. In particular, we refer to an INMARSAT-like payload as described in [53, 54, 55] and depicted in Figure 2.9. Of interest is the flexibility that the system can achieve at the payload level, while all the other segments are similar as in case of the reference Ka-band architecture. This flexibility is achieved thanks to the capability of assigning dynamically channels within the spot beams. In detail, the assignment is according to the traffic demand and a granularity of 200 KHz is considered for the channels. In terms of power, we assume the system can assign to each channel a reference EIRP (Equivalent Isotropic Radiated Power) proportional to the maximum attainable EIRP per spot beam, which is 67 dBW.

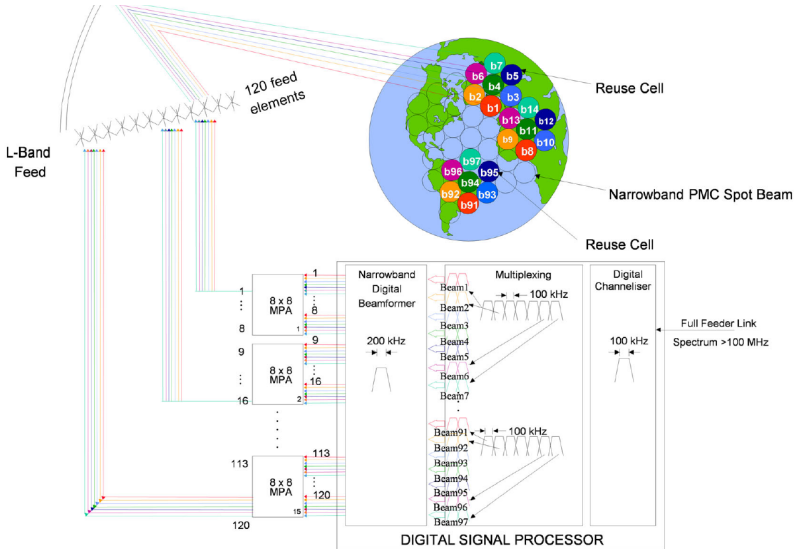

FIGURE 2.9: L-band satellite payload architecture [53]

The channel reference EIRP is not fixed and the payload can flexibly adjust the power within a wider dynamic range of values depending on the number of active channels. In particular, the number of 200 KHz channels that can be processed in parallel by the payload, is assumed to be limited to 630. This constraint apart from the on board processing capability, may be also driven by the fact that the feeder bandwidth is limited.

2.3.2 Scenario 3: Limited downlink user bandwidth

An unbalanced rate demand is present within the coverage, even more noticeable due to the increasing and changing requests of the market. In this scenario, the system has to cope both with low and very high rate demands areas along the coverage. In particular, the focus is on these latter, which can be the bottleneck of the system and are called hot spots. The hot spot is, in general, a limited geographical area, for which the system does not have sufficient resources in terms of spectrum and power to satisfy the users' high demands. Since the hot spots are few with respect to the whole coverage and they are usually surrounded by areas with lower demands, this causes an ineffective functioning of the system with respect its overall capabilities. Assuming all the active users of the hot spot limited within the same spot beam, we consider as reference scenario the beam that covers the hot spot plus the six adjacent beams as shown in Figure 2.10a, where different colors represent their standard coverage. For the considered scenario, the system is limited by a frequency reuse factor of 7. This implies that the available bandwidth can not be reused in different beams within the same cluster. We refer to this frequency allocation plan as *reference configuration*.

With respect to the spectrum allocation plan in the forward link of L-band mobile systems, the total bandwidth is divided in orthogonal channels of 200 KHz, which can be flexibly allocated among the beams according to the frequency reuse of the *reference configuration*. Thus, a different number of channels according to the required bandwidth can be allocated in each beam but obeying the reuse constraint. From the regulatory point of view, the spectrum allocated to L-Band MSS is between 1525 MHz and

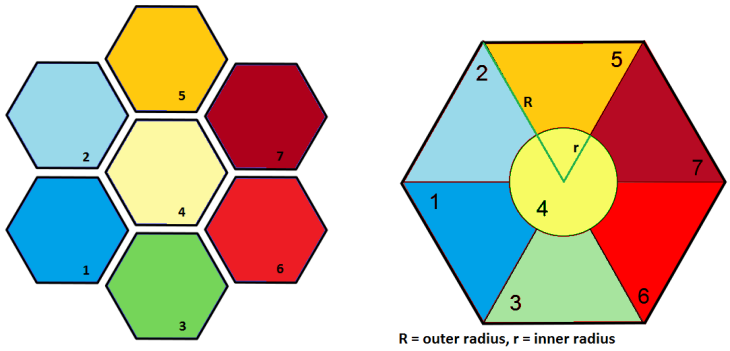

(A) *Cluster of 7 Beams*

(B) *Zone selection within the central beam coverage.*

FIGURE 2.10: Representation of the 7 beams cluster and of the 7 zones of the central beam

1559 MHz, i.e., an available bandwidth of 34 MHz, plus an additional bandwidth of 7 MHz from 1581 MHz to 1525 MHz [37]. Thus, the total available spectrum for the forward downlink in L-Band is equal to 41 MHz, which translates into 205 orthogonal channels of 200 KHz each. This frequency plan, however, faces with some limitation according with the different regions. Regulatory bodies give priority to different services within the same bandwidth and, thus, we assume as worst case a limited spectrum availability of only 7 MHz, i.e., 35 orthogonal channels, in some areas [37].

As described in section 4.4.1, the system can achieve high level of flexibility even in the *reference configuration*. However, depending on the demands and with particular focus on hot spots, limitations occur. Either spectrum or power availability can affect the performance of the system. The following scenarios, which take into account the main constraints posed by the system, have been identified and addressed.

Spectrum limited scenarios:

- scenarios limited due to regulatory issues. In some regions only part of the total available spectrum, which is 41 MHz, is allocated to L-band satellite systems. The minimum allocated bandwidth in these regions is assumed to be equal to 7 MHz.

Power limited scenarios:

- scenarios limited by the capability of the system. The total EIRP, which is 67 dBW, has to be shared among each channel and the beams.

These limitations penalize the *reference configuration* in the hot spot scenario. However, the flexibility of the considered system can be exploited according to a new framework aiming at improving spectrum efficiency and system performance. This new framework, as will be explained in 4.4.1 and assessed in 4.4.3, identifies new configurations, namely *flexible configurations*, able to better exploit the flexibility of the system based on a higher frequency reuse and the application of interference management techniques.

Chapter 3

Spectrum Awareness

3.1 Introduction

Spectrum awareness techniques provide improved knowledge of other systems' spectrum activities. This knowledge enables the following phases of the cognitive cycle exploiting those available spectrum opportunities. With respect to the scenario in which the cognitive user operates, different techniques can be designed according to the constraints, the requirements, and the performance to be achieved. Thus, targeting specific Figure of Merits (FoM), spectrum awareness techniques must be designed to satisfy them.

In this chapter, a novel approach for spectrum awareness in cognitive-based scenarios is developed. A complete characterization of the technique, namely **SNOIRED**, in terms of the common indicators that are used to asses awareness techniques performance, is provided. The proposed technique is based on the joint Signal to Interference plus Noise Ratio (SINR) estimation and detection of primary users at the cognitive receiver side and it is particularly effective for underlay scenarios, in which cognitive users are allowed to operate in already deployed frequencies if the interference generated against licensed users does not exceed a predefined threshold [3]. The definition of underlay scenario fits the two scenarios described in 2.2. Thus, in these scenarios, an additional awareness capability is provided to the end-user terminals, which would be able to be autonomously aware of the spectrum activities within the bands of interest. The proposed technique, even if designed focusing on satellite cognitive-based scenarios, has a general applicability. Thus, in the following paragraphs, the technique is first designed from a general point of view and, secondly, specific analysis are carried out for the selected satellite cognitive-based scenarios.

The remainder of the chapter is the following. Paragraphs 3.2 and 3.3 present the motivations that have pushed towards the proposed novel approach and the State of the Art of spectrum sensing techniques, respectively. From a general point of view and applicability, in paragraphs 3.4.1, 3.4.2, and 3.4.3 are presented the system model, the design of the estimation, and the design of the detection stages of the proposed technique. Analysis on its performance are carried out in section 3.5. In the subsequent sections 3.6 and 3.7 the technique is assessed on specific SatCom scenarios under ideal and in presence of impairments conditions, respectively. The results obtained are then resumed in 3.8. In the appendix 3.9.1 and 3.9.2 are provided additional and complementary details on the technique design. Finally, a review of the typical spectrum awareness techniques in literature, focussing on their applicability in satellite cognitive-based scenarios, is included in section 3.9.3.

3.2 Motivations

In the last years, CRs and spectrum sensing have received significant attention within the scientific and industrial communities, resulting in the production of a wide literature and a plethora of ad-hoc techniques, [56, 57, 58, 59, 60, 61]. The capability of a communication system to improve its performance by means of a cognitive approach is based on an intelligent exploitation of the available resources according to what the system senses and is aware of. In particular, the latter feature is the capability to acquire awareness of other users' spectrum usage and occupancy. As a matter of fact, knowledge on the activity of licensed and unlicensed users is critical for spectrum sharing, as it shall:

- i) avoid harmful interference towards incumbent users;
- ii) respect national and international regulatory policies;
- iii) enhance the efficiency in spectrum utilization.

In this context, spectrum sensing techniques and the use of databases are widely considered as a valid and effective solution, [2, 3, 4, 56, 57, 58, 59, 60, 61, 62, 63, 64].

As detailed in the following, some issues can be identified in current spectrum awareness approaches. Spectrum sensing techniques usually only refer to a binary *i.e.*, on-off, information on the availability of a specific band, without providing interference levels that would allow to fully exploit it in the subsequent resource allocation phase. As for databases, they might be able to provide such information, but the main issues are: i) confidentiality aspects, as they might not be disclosable to the public or to the database owner; and ii) their accuracy, as they might be not up to date. These considerations lead to the need for an extended spectrum awareness approach, in which not only the band is detected as available or not, but estimation techniques are implemented to gather information on the actual interference that is present. This approach could even enable different exploitation techniques and a more flexible and effective usage of the spectrum. As an example, depending on the output of both the estimation and the detection phases of the algorithm, Adaptive Coding Modulation (ACM) [65] or dynamic carrier allocation [66, 67] can be implemented.

3.3 State-of-the-Art and Rationale

Several techniques have been proposed in literature with respect to detection of primary users in cognitive radio scenarios. With respect to their application in a satellite context, an analysis of the main proposed techniques applied in the considered scenarios is provided in the Appendix 3.9.3 of this chapter. In particular, Energy Detection (ED) [62], Cyclostationary Feature Detection (CFD) [68], and Feature and Waveform-based Detection (FD and WD) [61] are among the most common techniques for spectrum sensing and each of them has specific features related to what the cognitive user aims at:

- i) energy detection has the advantage of low complexity and general applicability, but it becomes inefficient in case of uncertainties (noise, in particular);
- ii) cyclostationary detection achieves a more robust detection at the expense of higher complexity and larger sensing times since it is based on the detection of periodic features included within signals (*e.g.*, modulation, carrier, etc.);
- iii) feature or waveform detection that can reduce the sensing time without decreasing the performance are based on the knowledge of a-priori patterns to be detected, which, however, might not be available.

These techniques aim at detecting primary users (PUs), thus allowing the cognitive system to exploit unused frequencies. In this context, unused refers to unused resources either in time or space. In particular, the detection is performed periodically when no transmission among the cognitive users is requested, or alternating sensing and transmission periods in order to keep track of any change in the environment. Typically, the optimization of the duty cycle between the two periods, as proposed in [69], or sensing by means of a dedicated hardware, are usually employed. In [64], the authors approach the problem from an architectural point of view, proposing a simultaneous spectrum sensing and transmission scheme based on an hybrid architecture for CR transceivers. However, these solutions lead to a throughput reduction or to an increased complexity of the system, which are drawbacks that should be avoided or minimized. The above spectrum sensing techniques only provide a binary information on the availability of a specific band, *i.e.*, whether it can be allocated to a cognitive user or not. However, estimates on the power levels (*i.e.*, noise and, eventually, other signals) that are present on the considered band would greatly enhance the overall performance of a cognitive system. In fact, this information, if made available to the resource allocation engine, would allow to identify the bands providing higher capacities and select the most suitable technique to exploit them. A similar approach to the problem here addressed, has been considered in [70], where the authors approach the estimation and detection of malicious (*i.e.*, jamming) users with a non data-aided approach based on the Moment Generating Function (MGF) of the received signal.

In this context, we propose an extended spectrum sensing approach, which performs a joint estimation and detection at the cognitive receiver side. Starting from the SNORE (Signal-to-NOise Ratio Estimator) technique presented in [71, 72], we develop an extension, named SNOIRED (Signal-to-NOise plus Interference Ratio Estimator and Detector), for cognitive scenarios. In [71], it has been demonstrated that it is possible to analytically estimate the Signal-to-Noise Ratio (SNR) by resorting to the Maximum Likelihood (ML) approach, while it has been exploited in [72] as enabler of adaptive coding and modulation in satellite communication scenarios. Different from the SNORE [71], our approach can be modeled and designed aiming at solving the joint estimation and detection problem with respect to cognitive scenarios. In particular, the proposed algorithm aims at jointly estimating and detecting the presence of the noise plus interference caused by the primary transmission, if present. The estimation is performed in a data aided fashion, preventing the system to interrupt the transmission or to rely on

a dedicated sensing hardware. This choice is driven by the fact that the data aided estimation performs better in case of low signal to interference plus noise ratios with respect to the non data aided estimation, resulting in a more advantageous approach. In particular, pilots commonly used for channel state estimation can also be employed to identify both the most reliable channel for cognitive transmissions, *i.e., estimation*, and the presence of primary or incumbent users, *i.e., detection*. It is worth to be noticed in fact, that the presence of pilot symbols can be assumed true for most of the standardized communication systems, e.g., DVB-S2 [33], DVB-S2X [34], LTE [73], and DVB-T2 [74].

As detailed in the following sections, with particular focus on the considered cognitive-based SatComs scenarios, we provide a complete characterization of the proposed technique in terms of the parameters that define the sensing phase of the cognitive engine. In fact, the design of the number of pilots required for a proper Signal to Interference plus Noise Ratio (SINR) estimation is an important aspect to be taken also into account besides from the estimation performance of the algorithm. Moreover, combining detection capabilities is also fundamental in case of cognitive radio scenarios, where multiple users share the spectrum and a reliable but prompt knowledge of them is required. In fact, variations of the environment, as changes in the licensed user activities or the arrival of new licensed users, might occur and have to be monitored so as to both protect the licensed system and maximize the cognitive potential. Thus, the cognitive system has to periodically sense the spectrum and detect these variations. In addition, it should also rely on a sensing technique capable to identify the spectrum portion that allows to minimize the interference against licensed user transmissions. To these aims we propose the joint estimation and detection of the SINR γ and interference levels. Thus, thanks to the proposed technique, the cognitive user achieves a broader knowledge of the environment and of the spectrum utilization. In particular, estimates of the SINR provide a quality index for the transmissions in the selected bandwidth, and it is able to distinguish the source of the degradation, *i.e.*, if in presence of only noise or also other interfering users (as other cognitive terminals, licensed users, or jamming sources).

3.4 SNOIRED Technique Design

A general signal model, which allows general applicability of the proposed technique, is consider. The technique is based on the jointly estimation of the SINR and the detection of PUs according to the estimated metric. In particular, the estimation process is first addressed and, following, the detection included. The main parameters that have an impact on the design of the proposed technique are mathematically derived for both the stages.

3.4.1 Signal Model

In CR systems, the cognitive user has to define whether the licensed user is present or not, represented by hypotheses H_1 and H_0 in which, respectively: i) both noise and the licensed signal(s) are present; and ii) only noise is present. However, since our aim is also to estimate the interference level,

we include the useful (intended) signal into both hypothesis, since it will be exploited so as to provide the objective estimates in a data aided approach. Thus, we can represent the base-band equivalent expression of the signal at the cognitive receiver denoted as $r(t)$ as follows:

$$r(t) = \begin{cases} s(t) + n(t) & H_0 \text{ (PU absence)} \\ s(t) + \sum_{m=1}^{N_i} i_m(t) + n(t) & H_1 \text{ (PU presence)} \end{cases} \tag{3.1}$$

where: $s(t) = \sqrt{P_0} v(t) e^{j\phi_0}$ is the useful signal; $i_m(t) = \sqrt{I_m} \iota_m(t) e^{j(2\pi f_m t + \phi_m)}$ is the m-th interferer, with $m = 1, \ldots, N_i$ and N_i denoting the number of the interferers; P_0, I_m, for $m = 1 \ldots, N_i$, denote the received power on the useful and the m-th interfering links, respectively; ϕ_0, ϕ_m, for $m = 1, \ldots, N_i$, denote the phase of the useful and m-th interfering signal, respectively, and we assume $\phi_0 = 0$ without loss of generality; f_m, $m = 1, \ldots, N_i$, is the frequency shift between the useful signal carrier ($f_0 = 0$ since we have low-pass equivalents) and the m-th interfering signal carrier; and $v(t), \iota_m(t)$, with $m = 1, \ldots, N_i$, denote the lowpass complex signals of the cognitive and m-th interfering signals, respectively.

Under this general model and according to the typical modeling in cognitive radio scenarios [60], we can assume that the interfering signals have white spectral density in their band, and they can thus be modeled by means of the central limit theorem as a Gaussian random variable with variance I_0, which includes all of the previous interfering contributions. The Additive White Gaussian Noise (AWGN), represented by $n(t)$, is modeled as a Gaussian random variable with zero mean and power spectral density equal to N_0 as well.

3.4.2 SNOIRED Design - Estimator

The design of the estimator part of the proposed SNOIRED technique is here derived starting from the results, which are here briefly reported for sake of completeness, obtained in [71, 72]. In case of cognitive radio systems a complete characterization of the parameters that influence the sensing phase, *e.g.*, the sensing period, is of main importance.

As highlighted in [72], the data aided variant of the SNORE algorithm improves its performance and is based on the exploitation of pilot symbols embedded within the cognitive communication stream. It is assumed, as commonly foreseen in many communication standards [33, 74, 73], that blocks of pilots having the same length are embedded in the transmitted signal $s(t)$ and alternated with data symbols. We further assume that the cognitive receiver is synchronized with the transmitter and is able to decode the symbols as required for the algorithm. Based on these assumptions, $s(t)$ can be written as:

$$s(t) = \sum_{l=1}^{W} \sum_{k=1-lN_{slot}}^{N_s - lN_{slot}} d\left(|k|_{N_{slot}}\right) \tag{3.2}$$

where: W represents the number of pilot blocks; N_s is the number of pilot symbols in each pilot block; N_{slot} denotes the slot block length, which includes both pilot and data symbols; and $d\left(|k|_{N_{slot}}\right)$ represents the k-th complex symbol belonging to a certain pilot block. The notation $|\cdot|_{N_{slot}}$

FIGURE 3.1: Frame structure of the proposed cognitive transmission. Alternating data and pilot blocks.

defines the modulo-N_{slot} operator. A representation of the cognitive transmission framing structure with both data and pilot blocks is provided in Figure 3.1.

The real SINR γ is defined as the ratio between the useful received signal power P_0 and the noise plus interference power $N_0 + I_0$, *i.e.*, $\gamma = P_0/(N_0 + I_0)$ and its ML estimation, $\hat{\gamma}$, can be calculated as in [71, eq. (2)], here reported in equation (3.3) for sake of completeness.

$$\hat{\gamma} = \frac{\hat{P}_0}{\hat{P}_R - \hat{P}_0} \tag{3.3}$$

where:

$$\begin{aligned} \hat{P}_0 &= \left[\frac{1}{WN_s} \sum_{l=1}^{W} \sum_{k=1-lN_{slot}}^{N_s - lN_{slot}} r(k) d\left(|k|_{N_{slot}} \right) \right]^2 \\ \hat{P}_R &= \frac{1}{WN_s} \sum_{l=1}^{W} \sum_{k=1-lN_{slot}}^{N_s - lN_{slot}} |r(k)|^2 \end{aligned} \tag{3.4}$$

$\hat{P}_0$ and $\hat{P}_R$ in (3.4) represent the estimated useful power (power of $s(t)$) and the overall estimated received power (power of $s(t) + \sum_{m=1}^{N_i} i_m(t) + n(t)$), respectively. The SNORE algorithm is a Maximum Likelihood (ML) estimator for which a deeper characterization can be found in [18, 71].

Starting from the relationship between the error variance σ_ϵ^2 [1], the SINR, and the number of pilot blocks W that allow to reach the Cramer-Rao Bound (CRB), the explicit expressions for the design of the proposed cognitive technique are derived following the approach described in the Appendix 3.9.1. Eqs. (3.5) - (3.6) provide the minimum number of total symbol pilots $N_{tot} = WN_s$ required to reach the CRB and the target error variance σ_ϵ^2, respectively. With respect to (3.6), roots of the equation are not shown due to their complexity. Thanks to (3.5) and (3.6), an upper and lower bound of the symbols are required to achieve a reliable or targeted estimation, are obtained. According to these equations is therefore possible to optimize the frame structure of the cognitive transmission for estimation and detection of the incumbent users purposes.

$$N_{tot} = \left(\frac{3}{2} + \frac{SINR^2}{CRB} \left(\frac{2}{SINR} + 1 \right) \left(\frac{1}{2} + \sqrt{1 + \frac{6CRB}{SINR\,(2 + SINR)}} \right) \right) \tag{3.5}$$

[1] The error variance is defined as the square difference between the estimated and the real value, $(\hat{\gamma} - \gamma)^2$. In the following, we usually refer to the normalized value $\bar{\sigma}_\epsilon^2$, which is equal to $\left(\frac{\hat{\gamma} - \gamma}{\gamma} \right)^2$

$$N_{tot}^3 - \left(\frac{11}{2} + \frac{SINR}{\sigma_\epsilon^2}(SINR+2)\right) N_{tot}^2 + \cdots$$
$$\cdots + \left(\frac{39}{4} - \frac{1}{2\sigma_\epsilon^2} + 2\frac{SINR}{\sigma_\epsilon^2}\right) N_{tot} - \frac{45\sigma_\epsilon^2 - 4}{8\sigma_\epsilon^2} = 0 \tag{3.6}$$

3.4.3 SNOIRED Design - Detector and Threshold Derivation

The cognitive user usually relies on the output of the spectrum sensing phase in order to identify the presence of licensed users. In particular, a test statistic able to discern presence or not is derived from the received signal $r(t)$. Two different hypotheses, *i.e.*, H_0 and H_1, can be defined in the proposed scenario at the receiver input. For the former, we consider that the received signal is not interfered by the primary user and comprises only the useful signal $s(t)$ and the AWGN noise $n(t)$ while, in the latter, the licensed interfering signal $i(t)$ and other (possible) interfering contributions, which have been expressed as $\sum_m^{N_i} i_m(t)$ in (3.1), are also present. Since either H_0 and H_1 is true, we should derive a decision criterion, which, after observing the outcome in the observation space, is able to guess which hypotesis is true. In case of binary hypotesis problems, the comparison between a test statistic and a threshold is the common approach. The proposed test statistic, to be compared with the threshold η, is the estimated signal to noise plus interference ratio $\hat{\gamma}$ computed with the SNOIRED algorithm.

In the context of the detection theory, the probabilities of false alarm, P_{fa}, and correct detection, P_d, are considered as performance indicators to be guaranteed and used to evaluate the effectiveness of the algorithms. Thus, P_{fa} and P_d are derived in the following. Stating that the observation in the region associated to H_1 is lower than the one associated to H_0 according to (3.1) and as explained in the Appendix 3.9.2, the two probabilities can be defined as:

$$P_{fa} = \text{Prob}\{\hat{\gamma} < \eta | H_0\} = \int_0^\eta p_{\hat{\gamma}|H_0}(\hat{\gamma}|\, H_0) d\hat{\gamma} \tag{3.7}$$

$$P_d = \text{Prob}\{\hat{\gamma} < \eta | H_1\} = \int_0^\eta p_{\hat{\gamma}|H_1}(\hat{\gamma}|\, H_1) d\hat{\gamma} \tag{3.8}$$

where: $\hat{\gamma}$ is the test statistic; η is the detection threshold; and $p_x(x|H_i)$ is the Probability Density Function (PDF) of x conditioned to hypothesis H_i, with $i = 1, 0$.

An analytical expression of the threshold η can be derived from the conditioned probability density functions of the test statistic, $p_{\hat{\gamma}}(\hat{\gamma}|H_0)$ and $p_{\hat{\gamma}}(\hat{\gamma}|H_1)$. From [71], the statistical distribution of $\hat{\gamma}$ is given by a non-central Fisher distribution, $\mathcal{F}$, with degrees of freedom 1 and $2N_{tot} - 1$, and non-central parameter $\lambda = 2N_{tot}\gamma$:

$$\hat{\gamma} \sim \frac{1}{2N_{tot} - 1} \mathcal{F}_{1, 2N_{tot}-1}(2N_{tot}\gamma) \tag{3.9}$$

where γ represents the real SINR to be estimated and N_{tot} the number of pilot symbols used for the estimation. γ can be written as:

$$\gamma = \frac{S}{N_0 + I_0} = \frac{S}{N_0}\left(\frac{I_0}{N_0} + 1\right)^{-1} \tag{3.10}$$

and we can state that, under the hypothesis H_0, the SINR coincides with the SNR due to the absence of the interferer, *i.e.*, $I_0 = 0$, while, under H_1, the SINR also includes this contribution. Thus, λ_{H_i}, the non-central parameter under the selected hypothesis H_i with $i = 1, 0$, becomes

$$\lambda_{H_i} = \begin{cases} 2N_{tot}\, SNR = 2N_{tot}\, \frac{S}{N_0} & \text{if } H_0 \\ 2N_{tot}\, SINR = 2N_{tot}\, \frac{S}{N_0}\left(\frac{I_0}{N_0} + 1\right)^{-1} & \text{if } H_1 \end{cases} \tag{3.11}$$

In conclusion, taking into account that (3.7) and (3.8) are the definition of the Cumulative Density Functions (CDFs) conditioned by H_0 and H_1 respectively, we can reformulate them as:

$$P_{fa} = \text{Prob}\left\{\hat{\gamma} < \eta | H_0\right\} = \mathbb{F}\left\{\hat{\gamma} | 1, 2N_{tot} - 1, \lambda_{H_0}\right\} \tag{3.12}$$

$$P_d = \text{Prob}\left\{\hat{\gamma} < \eta | H_1\right\} = \mathbb{F}\left\{\hat{\gamma} | 1, 2N_{tot} - 1, \lambda_{H_1}\right\} \tag{3.13}$$

where $\mathbb{F}\left\{\hat{\gamma} | D_{F1}, D_{F2}, \lambda\right\}$ is the non-central Fisher CDF of the random variable $\hat{\gamma}$ with degrees of freedom D_{F1}, D_{F2} and non-central parameter λ. A complete representation of the CDF is given in (3.14), where $I(z; a, b)$ is the regularized incomplete beta function with parameters a, b. According to (3.9), the CDFs derived in (3.12) and (3.13) are already normalized with respect to the multiplicative constant $1/\left(2N_{tot} - 1\right)$.

$$\mathbb{F}\left\{\hat{\gamma} | D_{F1}, D_{F2}, \lambda\right\} = \sum_{j=0}^{\infty}\left(\frac{\left(\frac{1}{2}\lambda\right)^j}{j!} e^{-\frac{\lambda}{2}}\right) I\left(\frac{D_{F1}\hat{\gamma}}{D_{F2} + D_{F1}\hat{\gamma}}; \frac{D_{F1}}{2} + j, \frac{D_{F2}}{2}\right) \tag{3.14}$$

Finally, the threshold selection can be obtained by means of the Neyman-Pearson theorem [75]. A target probability of false alarm or detection are usually fixed in order to maximize the other, leading to the two different approaches for the threshold selection: Constant False Alarm Rate (CFAR) and Constant Detection Rate (CDR), respectively.

By focusing on the CFAR approach, the threshold η_{CFAR} is derived for a target $\hat{P}_{fa}$. The selected threshold allows to obtain the maximum value for P_d. From (3.11) - (3.12), it is possible to derive such threshold as:

$$\eta_{CFAR} = \frac{1}{2N_{tot} - 1}\mathbb{F}^{-1}\left\{\hat{P}_{fa} | 1, 2N_{tot} - 1, 2N_{tot}\, SNR\right\} \tag{3.15}$$

where $\mathbb{F}^{-1}\left\{y | D_{F1}, D_{F2}, \lambda\right\}$ is the non-central Fisher inverse cumulative density function of the corresponding probability y with parameters D_{F1}, D_{F2}, and λ.

Similarly, for the CDR approach, a target probability of detection $\hat{P}_d$ is taken into account trying to minimize the P_{fa}. In this case, the threshold can be calculated from (3.11) and (3.13) as:

$$\eta_{CDR} = \frac{1}{2N_{tot} - 1}\mathbb{F}^{-1}\left\{\hat{P}_d | 1, 2N_{tot} - 1, \lambda_{CDR}\right\} \tag{3.16}$$

where $\lambda_{CDR} = 2N_{tot}\, SNR \left(\frac{I_0}{N_0}|^t + 1\right)^{-1}$ is the non-central parameter and $\frac{I_0}{N_0}|^t$ the minimum Interference-to-Noise Ratio (INR) to be detected with a probability equal to $\hat{P}_d$. Indeed, the threshold selected by means of the CDR is dependent on the interference power I_0, which is not known *a priori*. Thus, in order to define the threshold η_{CDR}, a minimum detectable value I_0 has to be selected. This value can be identified taking into account recommendation and regulatory requirements. As an example, in [76] the $\frac{I_0}{N_0}$ values that should not be exceeded for guaranteeing the maximum allowable error performance and availability degradation are defined in case of Fixed Satellite Services (FSS). Thus, considering a target $\frac{I_0}{N_0}|^t$, by means of the CDR threshold selection approach we guarantee the desired probability of detection $\hat{P}_d$ for all the values above the chosen threshold $\frac{I_0}{N_0}|^t$.

For both threshold selection approaches, the SNR is considered known *a priori*. A description on how the estimation degrades in the presence of errors in the SNR estimates can be found in section 3.7.

3.5 SNOIRED Performance Analysis

3.5.1 Estimator Performance Analysis

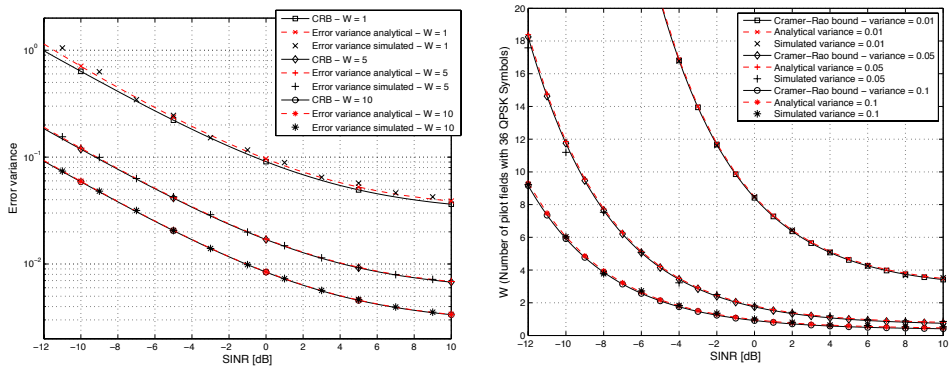

(A) Normalized error variance

(B) Number of pilot blocks

FIGURE 3.2: DA-SNORE performance bounds. Normalized error variance and Number of pilot blocks as a function of the SINRs.

In this section we discuss the numerical results concerning the estimation part of the proposed technique. In Figure 3.2, the performance of the SNORE algorithm is assessed in the proposed scenario. In particular, Figure 3.2a shows the normalized estimated error variance as a function of the SINR for $W = 1, 5, 10$ pilot blocks, *i.e.*, the estimation of the SINR accumulating a different number W of pilot blocks, each constituted by 36 QPSK symbols as in the DVB-S2x standard [34]. The performance is derived by comparing the CRB with both analytical and Monte Carlo simulation results. In this figure, the solid line shows the normalized Cramer-Rao bound evaluated from (3.27), the dashed line represents the analytical error variance derived in (3.28), whereas the computer simulated results are represented by the dots. The algorithm provides very good results, very close to the Cramer-Rao Bound. Moreover, as expected, the error variance for

a fixed SINR decreases by using more pilot blocks, as this ensures better performance of the estimation process.

In Figure 3.2b, the behavior of W is represented in terms of the Cramer-Rao Bound, as derived in (3.5) with a solid line, compared with the results in terms of analytically derived estimation error variance, as derived in (3.6), with a dashed line, as a functions of the SINR. The computer simulation results are shown with dots. Different values of normalized error variance $\bar{\sigma}_\epsilon^2$ equal to 0.1, 0.05, and 0.01 to be achieved, are considered. The simulated results perfectly fit the analytical results. In accordance with the previous figure, the number of required pilot blocks decreases for increasing values of the error variance. Based on this algorithm, the estimation can be performed with the minimum number of W equal to the nearest integer number with respect to the value obtained from (3.6) for the desired variance and, as we expected, in order to obtain a better variance a higher W is required.

3.5.2 Detector Performance Analysis

In this section, the performance of the proposed joint estimation and detection technique, whose block diagram is shown in Figure 3.3, is evaluated by means of the typical figures of merits used in the field of detection theory, whereas the assessments on its estimation capabilities have been assessed in section 3.5.1. The Receiver Operating Characteristics (ROC) are assessed for different values of the number of symbols N_{tot} and of the SNIR. Then, in order to compare the proposed algorithm with the ED, the performance in terms of probability of detection P_d as a function of the INR is shown. Finally, a comparison between the CFAR and the CDR approaches as described in Section 3.4.3 for threshold selection is also provided. The parameters used for the evaluation of the proposed technique are listed in Tab. 3.1.

We assume that the cognitive receiver is synchronized with the cognitive transmitter and able to decode the received symbols. This is a reasonable assumption if the proposed algorithm is performed to detect new incoming licensed users when the cognitive transmission is already established, or in case of underlay scenarios where the two transmissions can coexist and the cognitive system has to adapt itself to the information gathered during the sensing phase. We also assume that the pilot symbols of the cognitive transmission for SINR estimation are QPSK modulated and embedded within the communication stream.

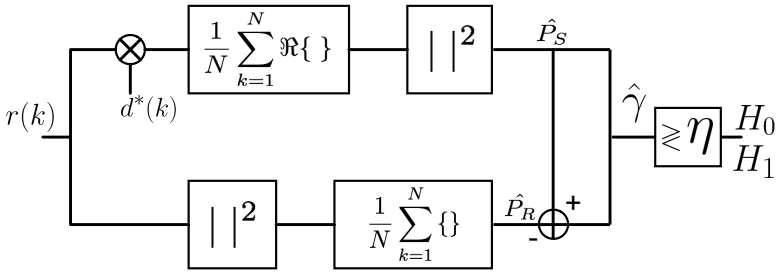

FIGURE 3.3: Block diagram of the SNOIRED technique.

TABLE 3.1: Detector performance assessment: simulation parameters.

Parameter	Value
N_s	36
W	1, 5, 10
I_0/N_0 [dB]	from -15 to 15
$I_0/N_0\|^t$ [dB]	-10
S/N_0 [dB]	-10, 0, 5, 10
P_{fa}^t	0.1
P_d^t	0.9

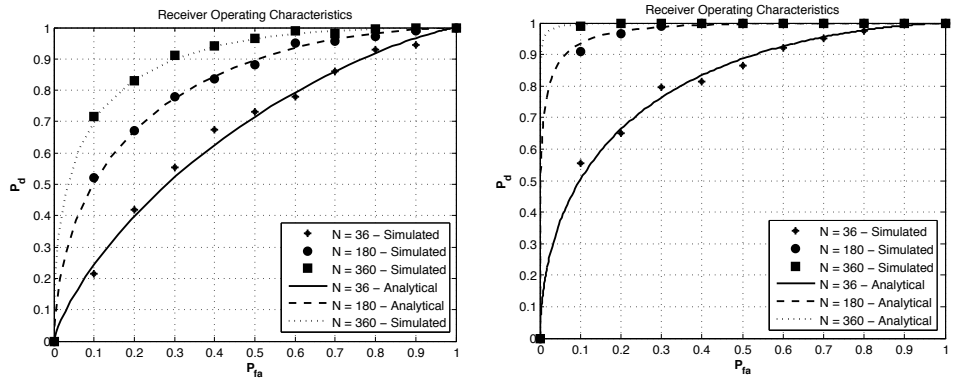

(A) SNR = -5 dB and INR = -5 dB

(B) SNR = 5 dB and INR = -5 dB

FIGURE 3.4: Detector performance assessment: ROC curves.

In Figs. 3.4a and 3.4b the ROC curves for different values of N_{tot} are shown by considering an INR equal to -5 dB and a SNR equal to -5 dB and to 5 dB, respectively. As expected, in both cases, given a selected probability of false alarm, a higher number of samples N_{tot} provides a higher probability of detection due to the better estimation of $\hat{\gamma}$. Moreover, the SNR also affects the probabilities of the ROC curves. In fact, comparing the two figures, we can highlight that for higher SNRs the estimation of $\hat{\gamma}$ is more accurate and leads to a higher detection performance of the interfering signal. In the two figures, the numerical results obtained through Monte Carlo simulations are compared with the analytical curves derived from (3.7) - (3.8). It can be noticed that the simulated results almost perfectly match the analytical curves.

A comparison between the proposed SNOIRED technique and the ED is shown in Fig. 3.5. The two techniques are assessed as a function of the interference to noise ratio INR since, while the SNOIRED algorithm operates in presence of both the useful and the interfering signal, no presence of the useful signal occurs in case of the energy detector. Moreover, for the proposed technique we consider different values of SNR, here fixed to 0 and 10 dB for simulation purposes. The threshold is evaluated for both the techniques by means of the CFAR approach taking into account a target probability of false alarm $\hat{P}_{fa}$ equal to 0.1 and different number of samples N_{tot}. In particular, the figure shows the results obtained for the SNOIRED algorithm and the ED in case of $N_{tot} = 36$ (W=1) and $N_{tot} = 360$ (W=10) samples, respectively. It can be noticed that the performance of the two techniques is

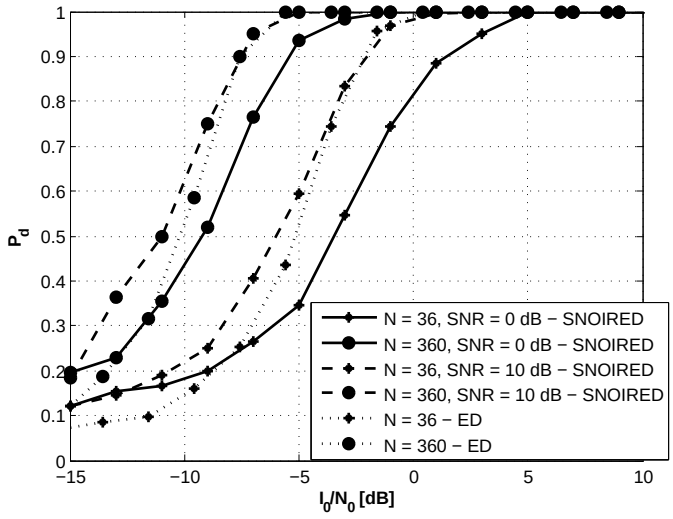

FIGURE 3.5: Detector performance assessment: P_d as a function of the interference to noise ratio INR.

similar in terms of probability of detection above a given INR. In particular, they converge to the same probability for higher SNRs independently of the number of samples considered for estimation, whereas, in case of lower SNRs, the probability of detection slightly worsen for the former technique. On the contrary, in case of low INRs, for which the probability of detection decreases in both cases, the performance of the proposed technique converges to the same probability of detection independently of the SNR, and such probability is slightly higher than that achieved by the ED.

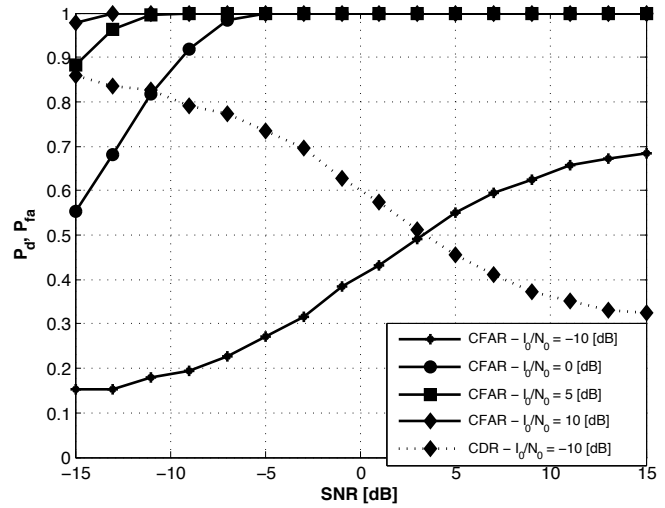

FIGURE 3.6: Detector performance assessment: P_{fa} and P_d as a function of the SNR for CFAR and CDR threshold selection.

Since the previous results show that the performance of the algorithm depends either on the SNR and the number of samples N_{tot}, the probability of detection is further assessed as a function of the SNR for different interfering power levels. Thus, in order to assess how the INR affects the performance of the proposed technique, P_d and P_{fa} are evaluated as a function of the SNR for different INRs and for both the CFAR and CDR approaches in

Fig. 3.6, where the x-axis refers to P_d in case of CFAR and to P_{fa} in case of CDR. A number of samples N_{tot} equal to 360 and the interference threshold $I_0/N_0|^t$ fixed to -10 dB in case of the Constant Detection Rate (CDR) approach are considered. As expected, the probability of detection is an increasing function of the SNR and, for a given value, a stronger interferer is detected more easily. On the other hand, it can be noticed that the probability of false alarm obtained with the CDR approach guarantees a probability of detection equal to 0.9 for all the values of INR higher than -10 dB. In this case, P_{fa} is a decreasing function of the SNR independently from the interference level.

3.6 Assessment on real SatCom scenarios

Both the estimation and the detection capabilities of the proposed technique are now evaluated in the different SatCom scenarios, for which the technique is designed and adapted. The assessment of the SNOIRED technique with respect to the considered SatCom environments would highlight its advantages in terms of applicability and enabled spectrum opportunities. Geographical maps showing in each grid point the selected FoM, are presented. In case of estimation, real values of INR from database data and the values estimated by the UTs are compared to show the effectiveness of the technique. On the other side, a similar analysis is performed also in case of detection for which percentages of *spatial probability of false alarm* and *detection* are provided [27]. Both Scenario 1 and 2 are addressed and similarities and differences concerning their spectrum opportunities are highlighted.

With respect to the assessment of the proposed technique and the numerical results provided, we assume a multibeam satellite with hundreds of beams covering the whole Europe as reference system architecture (see section 2.1). We assume that the payload operate with different SatNets both in the *exclusive* and *non exclusive* spectrum bandwidths. The reference 4 color frequency reuse is used in the *exclusive* bandwidth and a similar pattern can be considered for the *non exclusive* bandwidth. However, not all the *non exclusive* spectrum is considered but only portion of it. Either the spectrum available in case of Scenario 1 or 2 can be exploited in case of spectrum opportunities. Thus, portion of spectrum either from the spectrum from 17.3 to 17.7 GHz or from 17.7 to 19.7 GHz are assigned to the considered cognitive-based satellite system on a secondary basis. The system exploits a four-color frequency reuse scheme and DVB-S2x [34] air interface for forward downlinks. The FSS Earth terminals of the cognitive system are equipped with a receiving chain able to scan all the frequencies of interest with a sensing sub-band, B_W, equal to 36 MHz, which is the typical bandwidth of DVB-S2 [33] and DVB-S2x [34] communications. Although the wide spectrum considered in case of the two scenarios, we assume that only part of the available user bandwidth is scanned. This allows a trade-off between the number of carriers to be evaluated and the spectrum opportunities that can be present. As an example, considering a user bandwidth to be scanned of 500 MHz, this band is divided in 13 adjacent carriers. For each of these carriers, the SNOIRED algorithm is performed considering a proper number of pilots N_{tot} in order to assess whether primary users are present or not and to estimate the interference they generate. The algorithm

exploits the known symbols included in each pilot block, which are always present in the DVB-S2x Super-Frame (SF) structure and regularly inserted and composed by 36 symbols or a multiple, [34]. Thus, in the considered scenarios 1 and 2, the FSS terminal downlink might be interfered by incumbent links. This condition occurs if the FSS terminal partially/fully shares the same bandwidth with the PUs. However, exploiting the geographical reuse in order to achieve a better spectrum utilization would be possible due to the wide coverage of the satellite beams. To this aim, the FSS terminal are equipped with a receiving chain able to scan all the frequencies of interest and for each of such bands define whether PUs activities are present or not. In this context, it is assumed that the user terminals have an awareness additional capability, which allows them to sense and evaluate the spectrum. Therefore, the user bandwidth is sensed and spectrum opportunities are detected directly by the user terminals. The awareness phase has to cope with the detection of a frequency band in which the maximum interference that the PU may cause against the FSS terminal does not exceed a specific limit defined by ITU Recommendation S.1432-1 [76]. Since in this scenario the main problem is not due to the interference from the cognitive to the incumbent, but the interference generated by the incumbent towards the cognitive system, it would be sufficient to detect/estimate such interference in each band, and identify those bands in which the interference level is more tolerable. Then, one of the possible bands should be chosen providing the best performance at the FSS terminal. Therefore, FSS terminals that usually operate in the *exclusive* frequency bands, can additionally use the *non exclusive* if room is found in order to get additional capacity. The scan operation can be performed periodically with a duty cycle defined according to the variation of the activities of the PUs in order to guarantee the desired capacity and satisfy QoS requirements. More specifically, a first more accurate evaluation can be performed along all the frequency range when no data transmission is required. In particular, all the terminals of the system may be activated to perform a synchronized sensing by means of a broadcast channel. After this, such terminals can send back to the Network Control Center (NCC) the information on the spectrum utilization and the NCC could allocate, for each user, the most reliable band according to the selected resource allocation algorithm. This operation may be identified as the *i*nitial sensing phase. However, if a transmission is established in a *non exclusive* band, the potential interference caused and the quality of the transmission parameters should be periodically detected/estimated as well. We refer to this operation as a *f*ast in-band sensing. Consequently, if during this phase an interference level higher than expected is detected, another band should be selected for the downlink transmission. To this aim, it is possible to perform a second initial sensing phase, in order to scan the entire spectrum again or to rely on the decision made during the former one choosing another frequency band. It is worthwhile highlighting that while the terminal performs the spectrum scan phase, the NCC decides when and how to perform it and which frequencies are the most suitable for transmission. Hence, terminals should provide all the values of the detected/estimated interference to the NCC by means of the signaling channel. The NCC then collects them and decides the frequency assignment to be used. The initial and in-band fast sensing operations above described are shown in Figure 3.7. The flow diagram shows the sequential operations performed by the

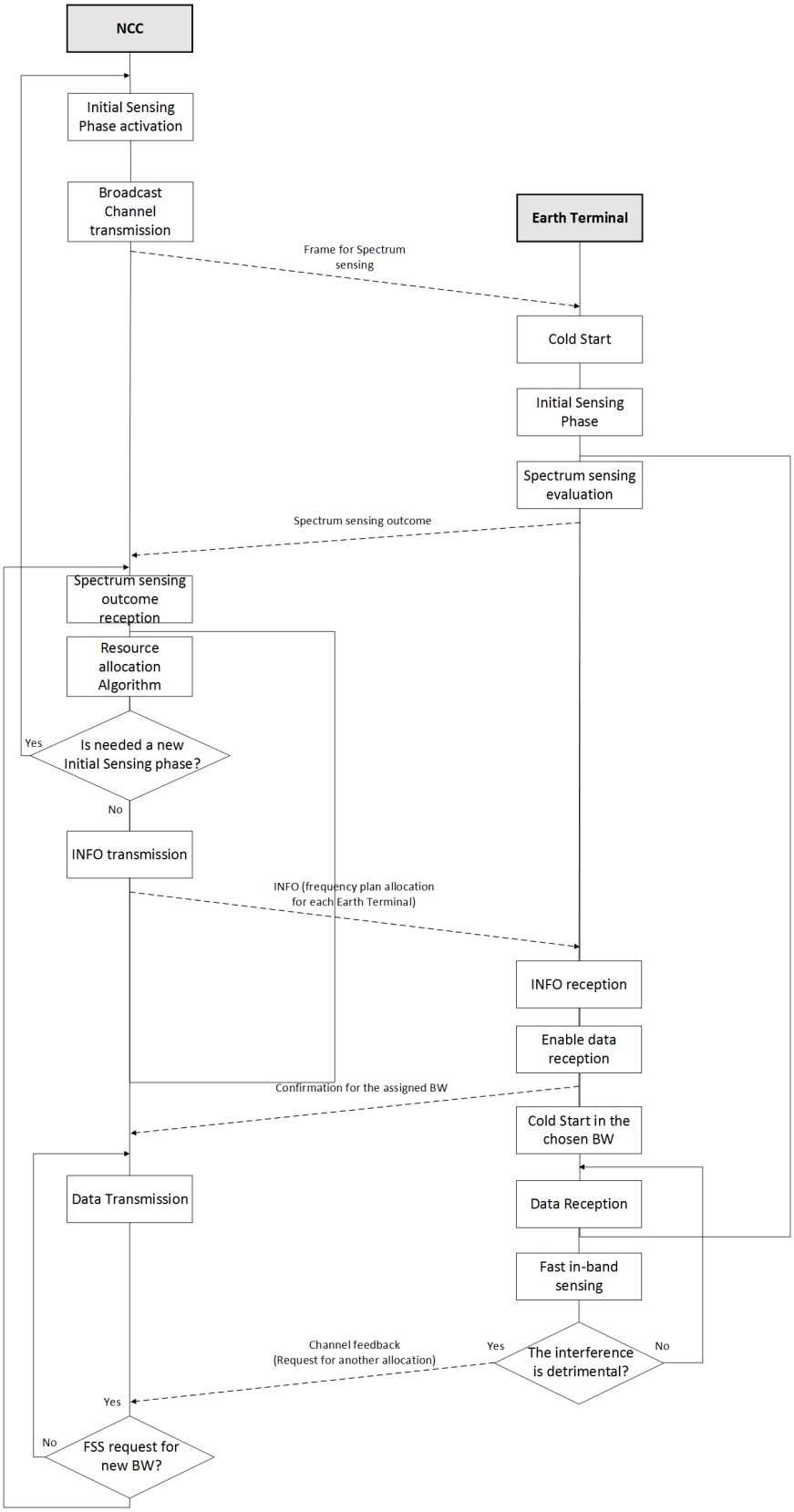

FIGURE 3.7: Awareness operational work flow in the considered cognitive-based SatCom scenarios.

NCC and the Earth terminal. Moreover, the exchanged messages, represented by dashed lines, between the NCC and the Earth terminals are highlighted and we suppose that these information messages can be exchanged by means of the signaling channel. On the other hand, the diamonds represent different alternatives according to the changes in the environment and the boxes represent the operations of the sensing technique and data transmission. From the terminal point of view, it is important to define the bandwidth to be scanned and the sensing time in order to compute a reliable estimation of the PU interference. In this case, typical bandwidths of 36 MHz channel bandwidth for downlink transmissions are considered.

3.6.1 Estimation

Simulations on the applicability of the SNOIRED technique to the proposed scenarios have been performed. In order to assess the performance of the SNORE based estimation algorithm, a comparison with data representing the ground interference values for a certain cognitive scenario has been made according to the following approach. The interference levels to be estimated with the SNORE algorithm at a given geographical location has been obtained in [21, 22] by assuming the presence of incumbent systems and by computing the interference level through ITU-R Recommendation P.452-15 [77]. The input parameters to be initialized are related to the terminal antenna that performs SINR estimation; as inputs it is possible to set the FSS terminal coordinates *(latitude, longitude)*, the longitude of the FSS satellite L_{sat} that the terminal points at, the SNR defined as signal to noise ratio P_0/N, and the number of pilot blocks W. Thus, the corresponding values estimated by the SNORE estimation block and those used as a reference are compared. These reference interference values are evaluated from the interference model proposed in ITU-R Recommendation P.452-15 [77] used for modeling the interference path losses.

TABLE 3.2: Assessment in SatCom scenarios: Frequency assessments parameters

	Parameters Figure 3.8a	Parameters Figure 3.8b
Frequency $[GHz]$	from 17.3 to 17.7	from 17.3 to 17.7
SNR [dB]	4, -2, -8	-8
FSS Terminal latitude [°]	51.73N	51.73N
FSS Terminal longitude [°]	-0.17E	-0.17E
L_{sat} $[degree]$	53E	-34E
W	10	1, 5, 10
B_W $[MHz]$	36	36
Frame Modulation	QPSK	QPSK
N_{pilot} $\left[\frac{symbol}{pilot\ block}\right]$	36	36

In particular, this approach aimed at understanding how accurate the estimation process is for a fixed terminal antenna in the frequency range to be scanned, and which bands are temporarily/geographically vacant. Tab. 3.2 lists the parameters used for the simulation setup, which considers Scenario 1 for first assessments. Figure 3.8a compares the estimated and real SINR values (dashed and solid lines, respectively) for different SNRs as a function of the frequency being scanned. The estimation is performed by

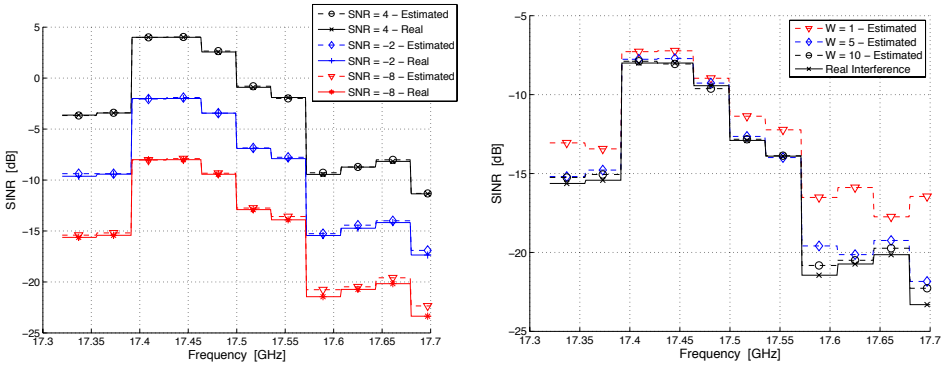

(A) for different values of SNR. (B) for different values of W.

FIGURE 3.8: Assessment in SatCom scenarios: Frequency assessments

accumulating 10 pilot blocks in each 36 MHz band. Numerical results confirm that errors decrease for increasing values of the SNR. Moreover, also in low SNR regimes, the algorithm provides good performance, correctly estimating the interference level in strong interference scenarios (*i.e.*, for low SINR values). As an example, from (3.6) it is obtained, by setting W equal to 10, that a target normalized error variance equal to 0.1 can be guaranteed up to SINR equal to -12.4 dB. These values are also confirmed by the simulation showed in Figure 3.8a. In Figure 3.8b, the SNR is fixed at -8 dB, and different pilot blocks dimensions W are taken into account. As expected, by accumulating more pilot blocks, the estimated SINR values (dashed lines) get closer to the real values (solid line), especially in low SINR environments where an higher number of pilots is required as demonstrated in Figure 3.2b.

Some considerations on the time required to estimate the SINR in each band and along all the frequency range shall be provided as well. Since the pilot blocks are inserted in the PHY framing of the DVB-S2x [34] between data slots, namely *capacity units* (CUs), a higher W can lead to a very long sensing time. Considering as an example the Format Specification 2, by starting the estimation algorithm at the *Start of Super-Frame*, the first pilot block occurs after the six replicas of the PL header[2], *i.e.*, after 1104 symbols. The first block is constituted by five blocks of 36 symbols each, *i.e.*, 180 symbols, whereas the other pilot blocks are constituted by 36 symbols and occur every 956 symbols inside the bundled PL-Frame. Thus, for each bundled PL-Frame included in the considered Super Frame structure 71 pilot blocks that allow the accumulation of 10 pilot blocks and the SINR estimation in each band, are included.

In addition to the previous results in the frequency domain, some geographic evaluations have been performed. In particular, the potential geographic reuse factor of a specific carrier frequency as a function of the relative location between interferer sources and the interfered terminal are provided. Table 3.4 lists the parameters used for these simulations. In Figs. 3.9,3.10, and 3.11 the maps describing real SINR values obtained from databases and those estimated by a terminal in each point of the area, for different pointing antenna angles, are compared. The results highlight that

[2]The PL (*Physical Layer*) header identifies the start of the bundled PLFRAME.

TABLE 3.3: Assessment in SatCom scenarios: Geographic assessments parameters

	Parameters Figs. 3.9-3.10
Frequency $[GHz]$	17.634
SNR [dB]	4
FSS Terminal latitude [°]	from 51.4 to 52.4
FSS Terminal longitude [°]	from -1.0 to 0.2
L_{sat} $[degree]$	53E, 0E, 34W
W	10

different pointing angles generate different interference patterns, which, therefore, demonstrate how different spectrum opportunities can be enabled according to the scenarios. The three figures evaluate the spectrum opportunities with respect to the same area but different pointing angles of the terminal antenna of the UTs. Thus, a correctly estimated area leads to a better exploitation of geographically available spectrum. This area can be evaluated in terms of percentage comparing the number of users that have performed the estimation within a targeted estimation error and the total. With respect to the considered scenario, the percentages of terminals that have performed the estimation with an error higher than the target normalized error estimation, $\bar{\sigma}_{\epsilon}^2$, equal or lower than 0.1, are 0.57% in Figure 3.9, 0.34% in Figure 3.10, and 0.39% in Figure 3.11. Thus, thanks to an accurate estimation of the SINR, the FSS system would be able to avoid high interferences and effectively reuse geographically available spectrum resources.

3.6.2 Detection

Assuming that the system relies on the proposed joint estimation and detection technique, an increased knowledge of the incumbent presence is given. However, to select the most favorable carrier in which the Earth terminal can receive the satellite signal, not only spectrum activities need to be estimated but also PUs detected. In order to assess the capability of detecting PUs, we consider that the Ka-band FSS cognitive system exploits the frequency bands from 17.7 to 19.7 GHz, already allocated to terrestrial Fixed Services (FS), for downlink transmissions, *i.e.*, Scenario 2. In particular, the presence of PUs and their transmission parameters is more irregular and makes their detection more challenging in Scenario 2. The cognitive system is able to scan the spectrum of interest and to estimate the interference levels by means of the proposed technique identifying those frequencies suitable for the transmission, *i.e.*, those where the interferer is weak or not present. Thus, the proposed technique not only is evaluated with respect its estimation performance but also detection is taken into account.

In the depicted scenario, due to the wide beam coverage of the satellite system with respect to the terrestrial link, the reuse of spectral resources on a geographical basis would provide a better spectrum efficiency. This is also due to the highly directive antenna radiation patterns of both incumbent and cognitive Earth terminals. For this reason, the applicability of the technique is assessed in terms of the geographical area that can be exploited by the cognitive users and be correctly estimated and detected. In particular, the potential geographic reuse factor is assessed for a specific carrier frequency as a function of the relative location between interfering sources

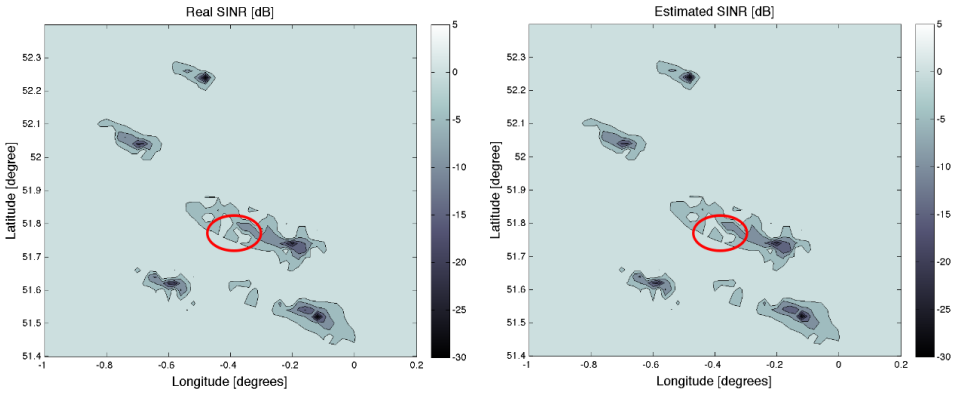

(A) *Database interference values* (B) *Estimated interference values*

FIGURE 3.9: Assessment in SatCom scenarios: Geographic domain assessments. $L_{sat} = 53E$.

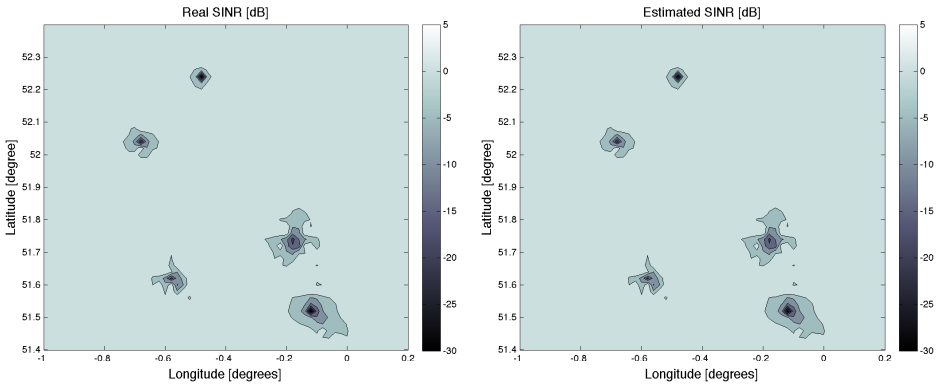

(A) *Database interference values* (B) *Estimated interference values*

FIGURE 3.10: Assessment in SatCom scenarios: Geographic domain assessments. $L_{sat} = 0E$.

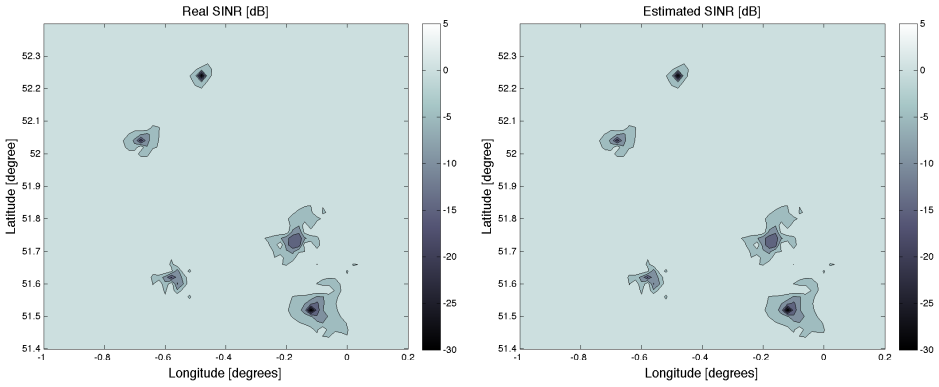

(A) *Database interference values* (B) *Estimated interference values*

FIGURE 3.11: Assessment in SatCom scenarios: Geographic domain assessments. $L_{sat} = 34W$.

TABLE 3.4: Assessment in SatCom scenarios: system and simulation parameters for geographic assessments of the detection stage

System Parameters	
Frequency Range	from 17.7 to 19.7 GHz
Frequency reuse factor	4
Air Interface	DVB-S2X
Geographical unavailable area	30%
Simulation Parameters Figs. 3.13 and 3.12	
Carrier Frequency [GHz]	18.4
FSS Terminal latitude [°]	from 47.2 to 47.6
FSS Terminal longitude [°]	from 18.8 to 19.6
B_W [MHz]	36
Frame Modulation	QPSK
N_{tot}	360
W	10
Simulation Parameters Figs. 3.12a and 3.12b	
$\sigma^2_{\epsilon}\|_t/\text{SINR}^2$	0.1
Simulation Parameters Figs. 3.13a and 3.13b	
$\hat{P}_{fa}$	0.1
$\hat{P}_d$	0.9

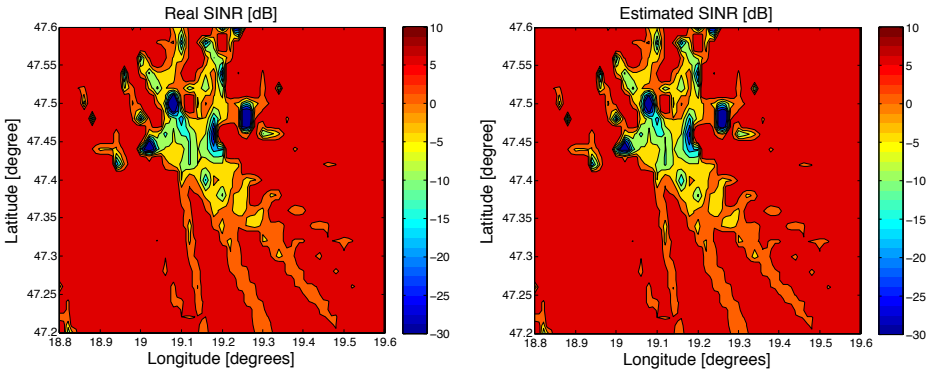

(A) *Database SINR values* (B) *Estimated SINR values*

FIGURE 3.12: Assessment in SatCom scenarios: Geographic assessments - estimated areas

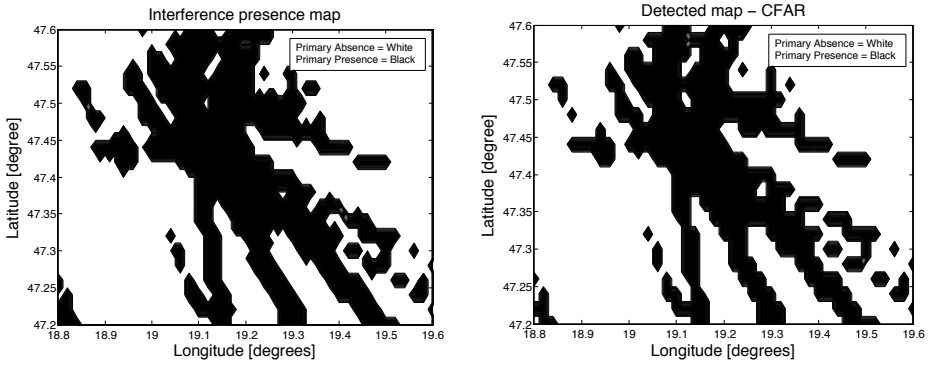

(A) *Database values* (B) *Detected values*

FIGURE 3.13: Assessment in SatCom scenarios: Geographic assessments - detected areas

and the interfered terminal. Thus, a comparison with data representing the ground interference values for a certain cognitive scenario has been made also in case of the detection stage.

The geographic assessments has been carried out considering a portion of Hungary limited from 18.8 to 19.6 of longitude and from 47.2 to 47.6 of latitude and a frequency carrier centered in 18.4 GHz. About 30% of the considered region is occupied by the primary FS systems, providing a wide area that can be reused by cognitive satellite terminals. This percentage, namely the *Geographical unavailable area*, is calculated by the database data as the ratio between the grid points for which $\frac{I}{N}|_t \geq -10\ [dB]$ and the whole coverage. All the parameters used for simulations are listed in Table 3.4.

Figures 3.12a and 3.12b compare the maps of the considered region showing the SINR values obtained from databases and those estimated by assuming a terminal at each location of the area. The results confirm that the estimation technique gives a reliable awareness of the SINR levels in the considered area, in which the primary and cognitive systems share the same frequency and the primary users interfere the satellite links. In particular, considering a target normalized estimation error $\bar{\sigma}_\epsilon^2$ equal to 0.1, the percentage of points not correctly estimated is 0.69%. The results demonstrate that SINR values are correctly estimated and a wide area for satellite cognitive transmissions can be exploited even in absence of the primary users. Thus, a better exploitation of geographically available spectrum can be achieved if this large area is correctly estimated. Subsequently, primary users are detected in the second stage of the algorithm in order to provide additional information on the spectrum activities within the area of interest.

Thanks to an accurate estimation of the SINR, the FSS system would be able to avoid highly interfered areas and thanks to the detection effectively reuse geographically the available spectrum resources. This can be achieved by the joint estimation and detection technique, which provides an additional knowledge about presence of other users. Results are shown in Figs. 3.13a-3.13b, where the data from the database are compared with those obtained through simulations. Target probabilities of false alarm $\hat{P}_{fa}$ and of detection $\hat{P}_d$ are fixed to 0.1 and 0.9, respectively. In Fig. 3.13a the white and the black areas indicate primary user absence and presence, respectively. The values from the database can be compared with those obtained from simulations, shown in Fig. 3.13b. The areas where the interference is detected with a probability $\hat{P}_d$ higher than 0.9 are shown in black, whereas the white area represents the area where the primary user has not been detected or is absent. By recalling the figures of merit *spatial detection rate* R_d^S (eq.) and the *spatial false alarm rate* R_{fa}^S (eq.), introduced in [27], and defined, respectively, as the ratio between the area correctly detected as interfered $A|_{\hat{H}_1|H_1}$ and the total interfered area $A|_{I/N \geq I/N|_t}$, and the ratio between the area wrongly detected as interfered $A|_{\hat{H}_1|H_0}$ and the total area not interfered $A|_{I/N \leq I/N|_t}$, it is possible to evaluate the effectiveness of the proposed approach in a realistic area.

$$R_d^S = \frac{A_{\hat{H}_1|H_1}}{A|_{I/N \geq I/N|_t}} \tag{3.17}$$

$$R_{fa}^S = \frac{A_{\hat{H}_1|H_0}}{A|_{I/N \leq I/N|_t}} \tag{3.18}$$

With respect to the performed evaluations, in the proposed scenario the CFAR threshold allows to achieve a percentage of spatial detection ratio equal to 81.7%. On the contrary, the spatial false alarm ratio is zero and no points in which the interfering signal is not present are (wrongly) considered as occupied. Thus, considering the probabilities of missed detection and rejection (dual to false alarm and correct detection, respectively), the selected threshold guarantees that all points in which the primary user is absent can be correctly detected as free, while a percentage of approximately 18.3% of points in which the primary user is present are not correctly detected. Similar results can be obtained in different areas and scenarios in accordance to the percentage of occupied area and the parameters set for the estimation of the SINR and the threshold selection. In particular, it has to be stated that estimation and detection errors occur in opposite situations and can therefore compensate each other. In particular, estimation errors are due to highly interfering users, which can be easily detected since high INRs occur. On the opposite, detection errors take place in case of weak interferers, *i.e.*, resulting in higher SNIR values, for which the estimation error variance is lower.

3.7 Impairments Analysis

Even if the proposed SNORIRED technique achieves promising performance as shown in the previous sections, its application in a realistic environment would be affected by the presence of several impairments. Thus, performance assessments under realistic impairments should be performed. In particular, the spectrum sensing based on measuring the SNIR requires a baseline calibration in order to handle practical uncertainties.

In the following, we do not refer to any specific knowledge of the incumbent, *e.g*, its presence and spectrum activities, for the sensing task. First, spectrum sensing is performed during the first carrier lineup procedure of the terminal installation. The overall expected link performance is assumed known from planning and previous link budget exercises, which do not take into account presence of PUs. This results in an expected signal to noise ratio that has to be met at the installation of the terminal. During the terminal installation and after the antenna pointing task, we obtain the expected and measured signal to noise ratio. A residual difference between the two values has to be correctly interpreted by the NCC. This difference may result from different perturbations or inaccuracies, which are listed in Table 3.5, in the overall system and they need to be addressed with the NCC integration of the spectrum sensing techniques and its proper calibration. Additional mechanisms have to be defined in this context to address all possible sources of practical errors to devise a reliable detector of the interference generated by PUs.

The focus is on the effect of perturbations and impairments that may occur to the proposed spectrum sensing technique and previously described. Thus, the SNORIRED technique is here reviewed taking into account changes and adaptations required with respect to the reference technique under ideal conditions in order to cope with possible impairments that will affect

the cognitive satellite system. The link budget of Earth terminals is affected by typical issues that may arise also during set up procedure as:

- Pointing errors
- Fading uncertainties
- G/T and sat. gain uncertainties over coverage area

Impairments that affect the SINR estimation process during terminals installation and the sensing phase performed during the common transmissions, are here introduced and summarized in Table 3.5. Further details can be found in [31, 32].

Imperfect alignment of the transmitting and receiving antennas could cause *pointing errors* that are sources of additional losses. These losses are due to a reduction of the antenna gain with respect to its maximum and are function of the misalignment of the angle of reception θ_R, and can be evaluated as:

$$L_R = 12\left(\frac{\theta_R}{\theta_{3dB}}\right)^2 \quad [dB] \tag{3.19}$$

where θ_{3dB} is the 3 [dB] beamwidth angle between the maximum gain direction and the 3 [dB] antenna gain direction. Other losses that could affect Earth Terminals (ET) due to non idealities, are the feeder losses L_{FRX} between the antenna and the receiver, and the polarization mismatch losses L_{POL}.

Potential contributing factor to measured SNIR delta perturbation	**Order of inaccuracy**	**Mitigation measure**
Rainfade and atmospheric attenuation during terminal installation	Several [dB]	Long-Term averaging, additional learning procedure at NCC
Inaccurate antenna pointing of the terminal	1 [dB]	
Cross polarization interference	0.5 [dB]	
Bias in expected SNIR value from margins at different levels	1 [dB]	Reference terminals, overall system learning
Interference from other satellite downlinks or adjacent beams of the same system	2 [dB]	Planning tools, measurements of expected levels
Interference from other systems (Scenario 1/2)	Scenario dependent	
Receiver gain variation	1 – 2 [dB] (seasonal)	
LNB gain variation	1 – 2 [dB]	

TABLE 3.5: Potential perturbations contributing to incorrect SNIR estimation of the SNOIRED technique

Atmospheric events cause additional attenuation and variation with respect to the common free space loss propagation. Several effects are present but an overall contribution affecting the received power can be taken into account by adding to the free space loss attenuation A_{FSL} the contribution A_P that includes all the atmospheric attenuation:

$$A_{TOT}[dB] = A_{FSL}[dB] + A_P[dB] \tag{3.20}$$

These losses are significant above 10 GHz as in case of the Ka bands, which are used in the considered scenario. In such bands, tropospheric phenomena are the main contributions of the link availability and service quality degradation. These phenomena are i) attenuation, ii) scintillation, iii) depolarization and iv) increase of the antenna temperature in the receiving Earth terminal. A more detailed description of these phenomena is included in [31, Chapter 3]. Link budget is affected by these contribution in many ways. In the downlink case, the carrier to noise ratio can be expressed as:

$$\left(\frac{C}{N_0}\right)_{DOWNLINK}[dB] = (1-\Delta_1)EIRP_{SAT} - A_{TOT} + (1-\Delta_2)\left(\frac{G}{T}\right)_{ET} - k_B \quad (3.21)$$

and can be rearranged in order to separate the ideal, or expected value $\left(\frac{C}{N_0}\right)_{FSL}$ calculated in free space loss conditions, from contributions that cause its variation. The downlink carrier to noise ratio is, therefore, expressed as

$$\left(\frac{C}{N_0}\right)_{DOWNLINK}[dB] = \left(\frac{C}{N_0}\right)_{FSL} - \Delta_1 EIRP_{SAT} - A_p - \Delta_2\left(\frac{G}{T}\right)_{ET} \quad (3.22)$$

where $EIRP_{SAT}$ is the satellite EIRP, $\left(\frac{G}{T}\right)_{ET}$ the figure of merit of the Earth Terminal receiver and Δ_1 and Δ_2 a possible decrease of the satellite $EIRP_{SAT}$ and the figure of merit $\left(\frac{G}{T}\right)_{ET}$, respectively. In particular, the figure of merit $\left(\frac{G}{T}\right)_{ET}$, *i.e.*, including also losses of the receiving chain, can be expressed as

$$\left(\frac{G}{T}\right)_{ET} = \frac{G_{R_{\max}}/L_R L_{FRX} L_{POL}}{T_{TOT}}[K^{-1}] \quad (3.23)$$

where T_{TOT} is the total downlink system noise temperature at the receiver input and it is function of the antenna temperature T_A, the feeder temperature T_F, and the effective input noise temperature of the receiver T_{eRX}

$$T_{TOT} = \frac{T_A}{L_{FRX}} + T_F\left(1 - \frac{1}{L_{FRX}}\right) + T_{eRX} \quad (3.24)$$

Temperature variations of the environment cause variation from the nominal value of $\left(\frac{G}{T}\right)_{ET}$ besides other impairments already been addressed as pointing errors. In particular, T_A and T_{eRX} are defined as

$$T_A = \frac{T_{SKY}}{A_p} + T_M\left(1 - \frac{1}{A_p}\right) + T_{GROUND} \quad (3.25)$$

$$T_{eRX} = (NF - 1)T_0 \quad (3.26)$$

Where in the former equation T_{SKY}, T_M, and T_{GROUND} are respectively the sky, the medium and the ground temperatures whereas in the latter equation the NF is the noise figure and T_0 the default noise temperature fixed at 290 K. Variations of these effects can be included in Δ_2.

Parameter Name	Abbreviation	Value
Sky Temperature	T_{SKY}	15 [K]
Ground Temperature	T_{GROUND}	45 [K]
Temperature of the Medium	T_M	275 [K]
Downlink Frequency		18.4 - 18.8 GHz
Satellite EIRP	$EIRP_{SAT}$	50 – 70 [dBW]
Carrier Bandwidth		36 [MHz]
Terminal Efficiency		0.65
Terminal Antenna Diameter		0.6 meters
Figure of merit	G/T_{ET}	34.9 [dB/K]
Additional $EIRP_{SAT}$ variation Additional $(G/T)_{ES}$ variation	Δ_1 Δ_2	[dB] 0 – 2 [dB]
Antenna gain	G_R	50˘62 [dB]
Polarization Losses	L_{POL}	0 – 0.5 [dB]
Pointing Losses	L_R	0 – 1 [dB]
Feeder Losses	L_{FRX}	0 [dB]
Terminal Antenna Temperature	T_A	78 [K]
Effective noise temperature	T_{eRX}	262 [K]
Terminal Component Temperature	T_F	290 [K]
Default Temperature	T_0	290 [K]
LNA Noise Factor	NF	1.4 [dB]
QPSK Symbols per pilot		36

TABLE 3.6: System Reference Parameters for SNOIRED technique in presence of impairments assessments

3.7.1 Interference estimation in presence of impairments

After having reviewed the impairments that may occur at the receiver during the estimation process, we performed simulations in order to verify the robustness of the proposed technique. We provide a comparison between the ideal case, i.e., without impairments, and several worst case scenarios that include different subsets of impairments. In particular, the SINR estimated in the ideal case can be considered as the expected value that differs from the real estimated value due to the presence of impairments. System reference values taken into account for simulations are reported in Table 3.6.

In Figures 3.14 and 3.15 the performance of the SNORE algorithm in presence of three specific impairments cases, which are resumed in Table 3.7 and have been selected among all the possible for their significance, is depicted. In particular, Figure 3.14 shows the normalized error variance $\bar{\sigma}_{\epsilon}^2$ as a function of the SINR when 5 and 20 pilot blocks of 36 symbols each are used for the estimation, Figures 3.14a and 3.14b, respectively. On the other side, Figure 3.15 describes the minimum required number of pilot blocks in order to achieve a target normalized error variance, i.e., $\bar{\sigma}_{\epsilon}^2$, of 0.1 as a function of the SINR. In both figures, the solid line represents the Cramer Rao Bound, the dashed one the analytic value derived in [18], and the dots the simulated values under different impairments conditions. Under the ideal case the link budget is calculated without impairments and is considered as reference value, whereas in cases 1, 2, and 3 are introduced respectively the uncertainties shown in Table 3.7, where combinations of the possible uncertainties are considered.

The SNORE technique is also assessed in presence of impairments with respect to its applicability in specific SatCom scenarios. Both evaluations in the frequency domain for a specific Earth Terminal scanning the available user bandwidth, and in the geographic domain considering a wide region

Impairment	Ideal case	Case 1	Case 2	Case 3
Polarization Losses (L_{POL}) [dB]	0	0.5	0.5	0.5
Pointing Losses (L_R) [dB]	0	1	1	1
Additional $(G/T)_{ES}$ variation (Δ_2) [dB]	0	2	2	2
Additional atmospheric attenuation (A_p) [dB]	0	0	5	10

TABLE 3.7: SNOIRED assessment in presence of impairments: selected impairments cases of studies

covered by the satellite beam pattern, are performed. The followed approach is similar to the one considered in case of ideal conditions of the ETs and database data are considered for comparison purposes. The estimation capabilities of the terminal antenna under the different impairments listed in Table 3.7, are assessed. These simulations aimed at describing how accurate would be the estimation process for a fixed terminal antenna. The analysis are carried out with respect data for Scenario 2.

In case of the frequency assessments of a fixed terminal, we consider the portion of spectrum from 18.4 GHz to 18.8 GHz along which the estimation process is performed in carriers of 36 MHz. The FSS terminal is positioned in 47.5N latitude and 19E longitude. The estimation process is performed under the different impairments listed in Table 3.7, accumulating 1 and 10 pilot blocks of 36 symbols. In Figures 3.16a and 3.16b, the results obtained are shown. As expected, in each band the SINR value estimated is lower than the real value due to impairments that cause additional losses. However, in case of high SINR values the estimated value even in presence of impairments can be considered reliable while, otherwise, to obtain the desired uncertainty target for lower values of the SINR, more pilot blocks have to be accumulated. In fact, considering bands 5 and 6, it can be noticed that in Figure 3.16a, i.e., in case of 1 pilot block is accumulated, the estimated SINR in presence of impairments is similar to the real value, whereas in Figure 3.16b, i.e., where 10 pilot blocks are considered, the estimation is more accurate. Thus, an inappropriate estimation of the SINR in presence of impairments causes a misunderstanding in detecting presence of impairments or interference due to incumbent users.

In addition to frequency analysis, geographic assessments are performed to evaluate the SINR estimation process within the beam coverage. Thus, the area from 47N to 48N of latitude and from 19E to 20E of longitude is considered. Real SINR values that Earth terminals experience within the coverage, are presented in Figure 3.17. It can be noted the presence of a directive incumbent link and of some incumbent-free regions. Figure 3.18 show results in the cases listed in Table 3.7 when performing the estimation algorithm with 10 pilot blocks. Also the results obtained from geographic simulations confirm link budget losses due to the presence of impairments and a more reliable estimation due to longer observation periods. Percentages of the SINR values estimated that differ from the real value more than $\bar{\sigma}_{\epsilon}^2 = 0.1$, where the normalized error variance is the difference between the real value and the estimated value under uncertainties conditions, are shown in Table 3.8, where the results with 1 pilot block are also reported.

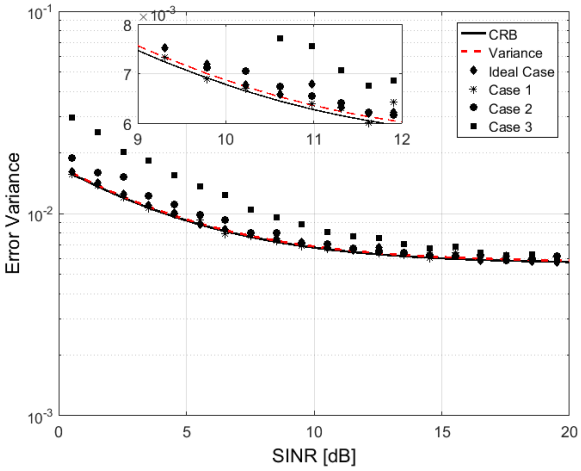

(A) *Number of pilot blocks - W = 5*

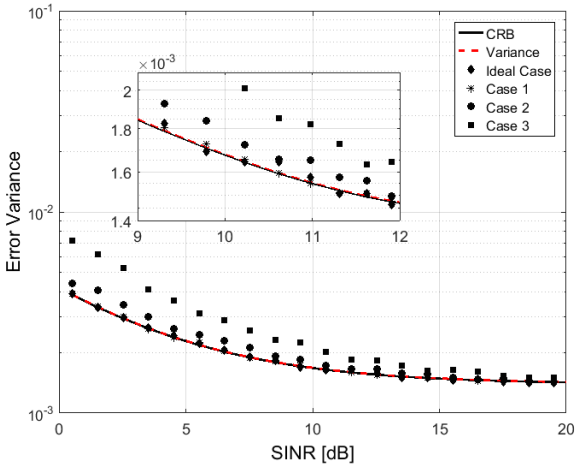

(B) *Number of pilot blocks - W = 20*

FIGURE 3.14: SNOIRED assessment in presence of impairments: normalised error variance as a function of the SNIR.

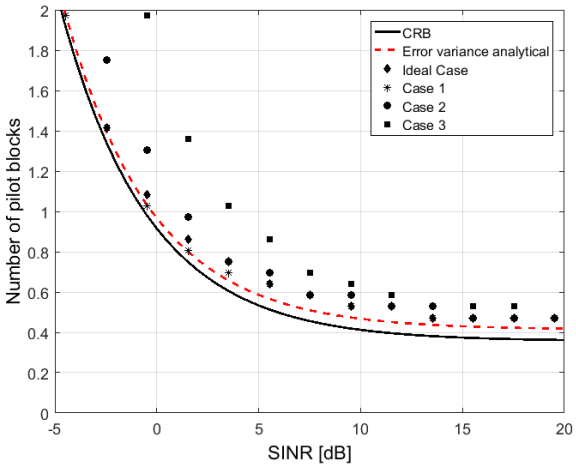

FIGURE 3.15: SNOIRED assessment in presence of impairments: minimum number of pilots for a given target error variance

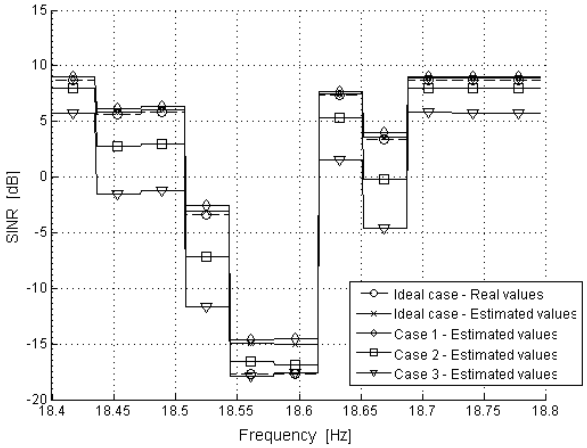

(A) *Number of pilot blocks - W = 1*

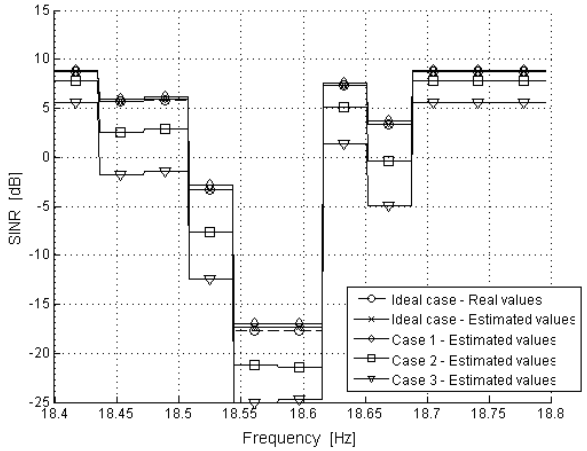

(B) *Number of pilot blocks - W = 10*

FIGURE 3.16: SNOIRED assessment in presence of impairments: assessments of the sensed spectrum.

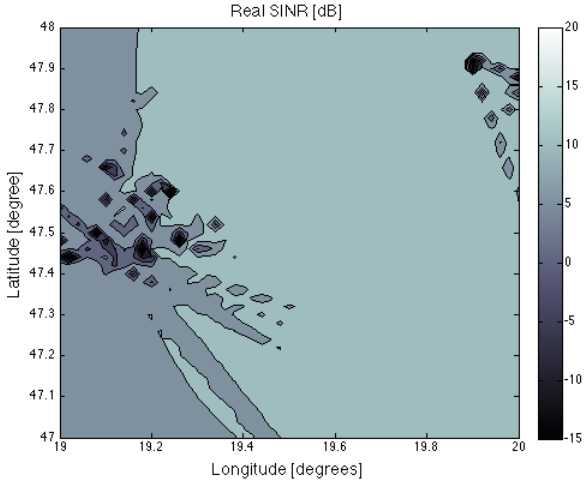

FIGURE 3.17: SNOIRED assessment in presence of impairments: Real SINR values along the selected geographic region

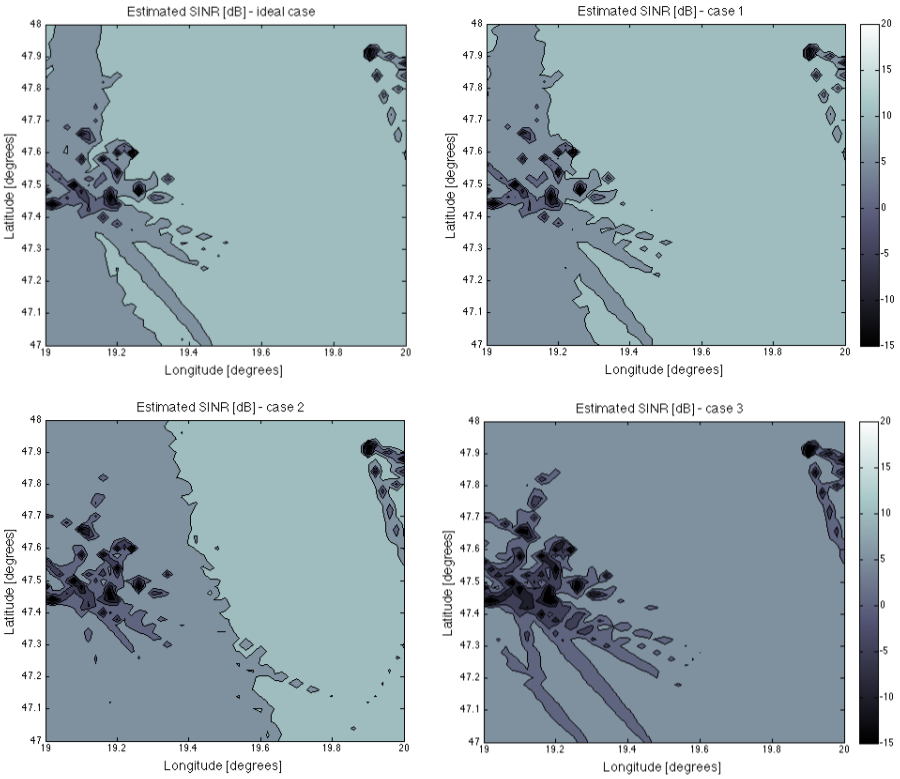

(A) Number of pilot blocks - W = 1

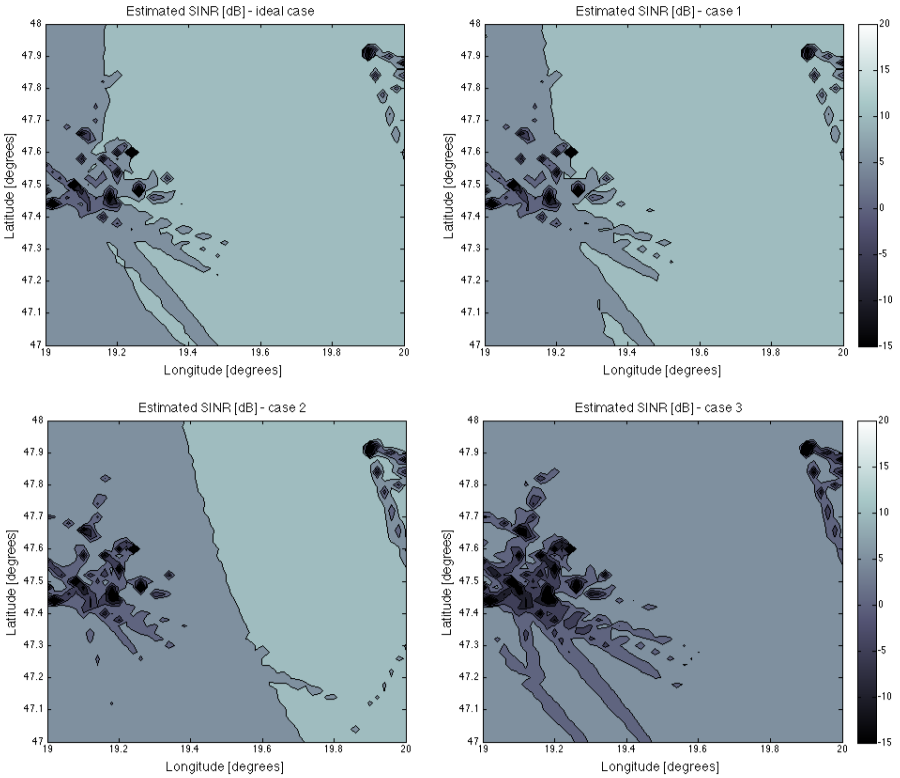

(B) Number of pilot blocks - W = 10

FIGURE 3.18: SNOIRED assessment in presence of impairments: comparison between estimated values.

Case	1 pilot block	10 pilot blocks
Ideal case	0.48%	0.19%
Case 1	0.71%	0.56%
Case 2	2.42%	2.46%
Case 3	3.67%	3.71%

TABLE 3.8: SNOIRED assessment in presence of impairments: geographic assessments results

Results show that in both cases impairments lead to a degradation of the percentages of points correctly estimated. However, in presence of low impairments losses as for the Ideal case and Case 1, longer estimations provide more reliable estimations whereas in case of higher impairments losses the estimated values do not satisfy the target reliability even in case of longer sensing periods.

3.8 Concluding Remarks

A joint estimation and detection technique, named SNOIRED, is designed for cognitive radio systems. The technique is based on the estimation of the SINR levels and the detection of primary users, thus providing a complete knowledge of the spectrum utilization in underlay cognitive scenarios. In fact, the applicability of the proposed technique is particularly suited in scenarios where the cognitive systems can coexist with the primary users without creating an harmful interference to them. The technique prevents the cognitive user to rely on additional hardware or to alternate transmission and sensing phases, which are common approaches in cognitive radios. An analytical description of the detector based on the SINR estimation is provided and the decision threshold is subsequently derived. Receiver operating characteristics plots and performance in terms of probabilities as a function of the power levels of the primary and the cognitive users are obtained both through Monte Carlo simulations and analytical computations. The numerical results perfectly match the theoretical analysis, substantiating the proposed algorithm. Moreover, a comparison between the proposed technique and the energy detector shows that, in terms of probability of detection, the two approaches are similar. The technique, which has been described from a general applicability point of view, is studied in the cognitive-based SatCom scenarios under investigation. To evaluate the spectrum opportunities in the considered scenarios, analysis in the frequency and the geographic domain are carried out. The assessments provide knowledge of the opportunities for a selected user over the available *non exclusive* spectrum and the opportunities over the same carrier along the whole covered area, respectively. The application of the technique to the proposed scenario is effective and provides good results either in terms of knowledge of the estimated signal to noise plus interference ratio and of interference detection. Notably, the proposed technique can be used along with dynamic resource allocation to enhance the system throughput with the exploitation of shared spectrum [9, 28] The results show that, for a selected user, the levels of interference vary along the scanned bandwidths. This results in a complete knowledge of the spectrum opportunities of each

user. On the other side, the assessment in terms of geographic area evaluates the spectrum opportunities for the whole system. In fact, two main outcomes are derived from these analysis. First, a wide geographical area, as expected, can be reused and, secondly, the techniques provides good results in terms of estimation and detection of the available spectrum opportunities. After introducing the SNORE based interference estimation technique, that results particularly effective for the selected heterogeneous terrestrial-satellite scenario, the presence if impairments is introduced. The numerical results shows that the proposed techniques is robust even in the case of the main impairments that may arise in the practical implementation of the technique. However, a first calibration and set up during installation are required. In fact, the presence of unknown interferences or impairments that affect the link budget during the installation need to be distinguished.

3.9 Appendix

3.9.1 Appendix I

In this appendix we provide some guidelines to derive Eqs. (3.5) and (3.6) from [71, Eqs. (20), (14)], respectively. For the sake of completeness, we report these two latter equations hereinafter.

The Cramer-Rao-Bound (CRB), [71, eq. (20)], of the ML estimator is:

$$CRB = \frac{4N_{tot}\left(2SNIR + SNIR^2\right)}{(2N_{tot} - 3)^2} \tag{3.27}$$

while the variance of the estimated SNIR, [71, eq. (20)], is:

$$\sigma_\epsilon^2 = \frac{N_{tot}^2\left(8SNIR^2 + 16SNIR\right) + N_{tot}\left(4 - 16SNIR\right) - 4}{8N_{tot}^3 - 44N_{tot}^2 + 78N_{tot} - 45} \tag{3.28}$$

Both are functions of the SINR and of the total number of symbols N_{tot}:

$$CRB = f\left(SINR, N_{tot}\right) \tag{3.29}$$

$$\sigma_\epsilon^2 = g\left(SINR, N_{tot}\right) \tag{3.30}$$

The domain of both $f(\cdot)$ and $g(\cdot)$ with respect to N_{tot} given the SINR, is the set of natural numbers $\mathbb{N}$. However, without loss of generality, we can simplify the problem relaxing N_{tot} to be continuous and, thus, extending its domain to $\mathbb{R}^+ - \left\{\frac{3}{2}\right\}$ and $\mathbb{R}^+ - \left\{\frac{3}{2}, \frac{5}{2}\right\}$[3], respectively. The images of (3.27) and (3.28), *i.e.*, the set of all values assumed by the CRB and σ_ϵ^2, is $\mathbb{R}^+$. Under this assumption, the partial derivatives of $f(\cdot)$ and $g(\cdot)$ with respect to N_{tot}, which solutions are omitted due to the length of their expressions, are polynomial since derivatives of polynomial functions as well. These resulting derivatives are piecewise positive or negative in intervals limited by zeros, which are rational and, thus, not of interest as solutions of N_{tot} in case of real scenarios. Considering each interval separately, the functions are continuous and strictly increasing or decreasing with no local maxima

[3]The roots of the denominator, which are not acceptable values of the domain, are $\left(\frac{3}{2}\right)$ and $\left(\frac{3}{2}, \frac{5}{2}\right)$ for (3.27) and (3.28), respectively.

or minima. As a consequence, within these intervals, $f(\cdot)$ and $g(\cdot)$ are invertible and their inverse functions $f^{-1}(\cdot)$ and $g^{-1}(\cdot)$, which are unique for the property of uniqueness, exist and can be derived thanks to the common inversion rules. Thus, are valid:

$$N_{tot} = f^{-1}(SINR, CRB) \tag{3.31}$$

$$N_{tot} = g^{-1}\left(SINR, \sigma_{\epsilon}^2\right) \tag{3.32}$$

and Eqs. (3.5) and (3.6) are derived.

3.9.2 Appendix II

In this appendix, the equations of P_{fa} and P_d defined in eqs. 3.7 and 3.8 are demonstrated. The binary hard decision problem considered for the derivation of the proposed detector, foresees the detection of an interference signal by means of the estimated signal to interference plus noise ratio $\hat{\gamma}$ as output of the observation space $\mathbb{Z}$. From [75], P_{fa} and P_d are conditional probabilities depending on the hypotesis H_0 and H_1, and are generally defined as:

$$P_{fa} = \int_{\mathbb{Z}_1} p_{\bar{r}|H_0}(\bar{R}|H_0)\, d\bar{r} \tag{3.33}$$

$$P_d = \int_{\mathbb{Z}_1} p_{\bar{r}|H_1}(\bar{R}|H_1)\, d\bar{r} \tag{3.34}$$

where $\bar{r}$ is the vector of the observations; $\mathbb{Z}_i$ is the decision region for H_i; and $p_{\bar{r}|H_i}(\bar{R}|H_i)$ is the conditional probability density of $\bar{r}$ conditioned by H_i, with i either 0 or 1. In particular, $\mathbb{Z}_0$ represents the region in which we decide for the interferer signal absence, while $\mathbb{Z}_1$ the one in which we decide for the interference presence.

For our observation $\hat{\gamma}$, $\hat{\gamma} \in \mathbb{R}^+$ and

$$\hat{\gamma} = \begin{cases} \frac{S}{N_0} & \text{if } H_0 \\ \frac{S}{N_0+I_0} = \frac{S}{N_0}\left(\frac{I_0}{N_0}+1\right)^{-1} & \text{if } H_1 \end{cases} \tag{3.35}$$

Since $\left(\frac{I_0}{N_0}+1\right)^{-1} < 1$ and $\hat{\gamma} \in \mathbb{R}^+$, it is possible to state that the decision regions $\mathbb{Z}_1$ and $\mathbb{Z}_0$ are respectively $[0, \eta]$ and $[\eta, +\infty]$, where η is the decision threshold, which separates the two regions. In conclusion, eqs. (3.7) and (3.8) are derived substituting $\mathbb{Z}_1$ in (3.33) and (3.34) with the corresponding extremes of the integral and stating that the obtained equations are the conditional probabilities Prob $\{\hat{\gamma} < \eta|H_0\}$ and Prob $\{\hat{\gamma} < \eta|H_0\}$, by definition.

3.9.3 Appendix III - Review of the application of Spectrum Awareness Techniques

In this appendix, a review of two of the main cognitive radio spectrum sensing techniques proposed in literature, *i.e.*, *Energy Detection* (ED) and *Cyclostationary Feature Detection* (CFD), are assessed. Analysis with respect to their adaptation into the considered SatCom scenarios are included in order to verify their applicability.

Energy Detection: An Energy Detector (ED) aims at detecting the presence of incumbent signals based on the energy estimated at the antenna input of the cognitive terminal [62, 78]. It is a blind detection technique, as it does not require a-priori knowledge on the incumbent signal, and therefore has a general applicability in CR-based systems. However, it is highly susceptible to Signal-to-Noise Ratio (SNR) wall problem, that prevents from achieving the desired target probabilities P_d or P_{fa}, as the uncertainty in noise power estimation, ρ_N, can easily erroneously trigger the detection [63]. We consider two different ED threshold selection approaches: i) Constant False Alarm Probability (CFAR), in which P_{fa} is fixed and parameters are set so as to reach the desired probability of detection; and ii) Constant Detection Rate (CDR), where P_d is fixed and a target probability of false alarm shall be reached. From [63], P_d and P_{fa} are given by (3.37) and (3.36), respectively, where $Q(\cdot)$ is the Marcuum Q-function, η_{thr} is the detection threshold, σ_ϵ^2 is the noise variance, $N_{oss} = 2BT$ is the number of observed samples, and γ is the SNR at the end of the receiving RF chain i.e., it includes the RF chain noise. In our case, we have considered the SNR at the end of the receiving RF chain including its noise contribution. A critical parameter is the sensing (observation) time, T_{oss}, related to N_{oss}. With particular focus on the detection threshold η_{thr}, equations (3.39) and (3.38) represent the CFAR (Constant False Alarm Rate) and the CDR (Constant Detection Rate) approaches, respectively. The two different approaches target a desired probability of false alarm or detection, while the other parameters are set in order to satisfy the sensing phase requirements. These parameters, in particular, affect the performance of the technique in the considered scenario.

$$P_{fa} = Q\left(\frac{\eta_{thr} - \sigma^2}{\sqrt{\frac{2}{N_oss}}\sigma^2}\right) \tag{3.36}$$

$$P_d = Q\left(\frac{\frac{\eta_{thr}}{\sigma^2} - (\gamma+1)}{\sqrt{\frac{2}{N_oss}}}(\gamma+1)\right) \tag{3.37}$$

$$\eta_{thr}^{CFAR} = \sqrt{\frac{2}{N_{oss}}}Q^{-1}(\hat{P}_{fa}) + 1 \tag{3.38}$$

$$\eta_{thr}^{CDR} = (\hat{\gamma}+1)\left(\sqrt{\frac{2}{N_{oss}}}Q^{-1}(\hat{P}_d) + 1\right) \tag{3.39}$$

Although, the energy detector is a blind spectrum sensing detection technique that does not need any a priori knowledge of the incumbent signal and has general applicability, specific sensing characteristics have to be set properly in the particular case of SatComs. As an example:

- the sensing time (or equivalently the samples that the receiver processes). We should fix a minimum and a maximum sensing time.

These bounds are related, respectively, to the time necessary to obtain the desired probability of the detection and the fragmentation between cognitive spectrum sensing and the effective secondary transmission;

- the typical cognitive station,*i.e.*, the UTs, characteristics that influence the energy detector such as noise power estimation, sensed bandwidth, threshold, receiver chain, geographical positions and distance from the incumbent user.

Assessments with respect to the specific SatCom scenario need to be performed in order to evaluate the effectiveness of the technique. The parameters considered in the energy detector assessment are shown in Table 3.9. In case of the CFAR approach, the first relationship that has been considered is the probability of detection P_d as a function of the signal to noise ratio when the desired probability of false alarm $\hat{P}_{fa}$ and the sensing time T_{oss} are fixed (see Figure 3.19). This choice is also driven by the need to detect an interfering signal whose power level, and, hence, the SNR at the antenna input receiver, should not be greater than a known threshold. The probability of detection is also a function of the sensing time and its behavior is evaluated in Figure 3.20. The minimum sensing time for a given signal to noise ratio is addressed to guarantee for the fixed probability of false alarm, the probability of detection that the detector requires. From the cognitive station point of view, the observation time T_{oss} and the bandwidth B_W, according to the ADC sampling frequency and other physical architecture's constraints, are set in the following way:

$$B_W T_{oss} << 1 \tag{3.40}$$

$$2B_W T_{oss} = N_{oss} \tag{3.41}$$

where N_{oss} is the number of observed samples, and the minimum sampling frequency is equal to twice the bandwidth (Nyquist frequency). In fact it is known [62] that a process, whose bandwidth B_W is sensed for a period equal to T_{oss}, is nearly described by a set of $2T_{oss}B_W$ samples. Hence if we consider the baseband signal, these samples are obtained by sampling the process every $\frac{1}{2B_W}$. Nevertheless the SNR and the related minimum sensing time could be also analytically derived from the following equation having fixed the desired probability of false alarm and of detection

$$N_{min} = 2\frac{[Q^{-1}(P_{fa} - Q^{-1}(P_d)(\gamma + 1)]^2}{\gamma^2} \tag{3.42}$$

In scenarios 1 and 2 the cognitive users have to detect an interference signal themselves. Thus, it would be sufficient detecting a signal, whose received power is equal to the maximum interference that the cognitive station can tolerate. When this maximum interference level is present and detected in the sensed band, the cognitive system should be able to detect another spectrum hole in which the transmission could be provided. Considering first a target probability of detection, we can refer to the CDR threshold selection approach, which can be fixed according to the ratio of the power of the signal to be detected and the noise. In the considered

Data	Value	Name
Target Probability of false alarm	0.1	$\hat{P}_{fa}$
Target Probability of detection	0.9	$\hat{P}_{d}$
Sensing time	0.6 ms	T_{oss}
Detection threshold CFAR paradigm	1.0331	η_{thr}^{CFAR}
Detection threshold CDR paradigm	1.0636	η_{thr}^{CDR}
Sensed Bandwidth	5 MHz	B_W
Noise Uncertainty	0-2 dB	ρ_N
Maximum long term interference over noise (I/N) at FSS station antenna input	-10 dB	$\frac{I}{N}\|_t$

TABLE 3.9: Evaluation of ED technique in SatCom environment: system parameters

scenario, the power to be detected is the interfering one for which a I/N threshold is defined by regulations and requirements.

Thus, while the discussion and the previous results refer to the CFAR methodology, having defined the I/N threshold, we can also take into account the CDR that would provide a constant probability of detection. Thanks to this approach, we fix a target probability of detection and for a given I/N threshold we can achieve the desired probability of detection for all the values above this threshold. As a consequence, we guarantee with a certain probability the detection of the incumbent user. However, we need to achieve the target false alarm probability as a function of the sensing time and similar considerations with respect to the CFAR case hold.

Despite of its simplicity and general applicability, the energy detector is mainly affected by the SNR wall phenomenon that prevents us from achieving the desired probabilities [63]. This phenomenon is caused by the uncertainty in noise power estimation and in case of a finite observation time the desired probabilities cannot be guaranteed. In our case, we have to guarantee that the SNR wall should be lower than the SNR needed for the detection of the minimum interfering incumbent signal. In fact, if the SNR wall is higher we are not going to detect an interfering incumbent signal causing disruptive interference to the cognitive system. In [79] it is stated that 1 [dB] of uncertainty is equivalent to a variation from the noise temperature of about $20°K$ and the main causes on which it depends are: calibration errors, thermal variations, changes in Low-Noise Amplifier (LNA) gain, and interference. In our simulations, we consider the nominal noise variance variable in the interval $[1/\rho_N; \rho_N]\sigma_n^2$ where σ_n^2 is the nominal noise variance and $\rho_N > 1$ the noise uncertainty. Besides the ideal behavior of the detection technique, we show the results under noise uncertainty having fixed σ_n^2 and varying the estimated noise at the receiver between this range of values. In particular under noise uncertainty estimation a proper threshold able to guarantee the desired false alarm $\hat{P}_{fa}$ equal to 0.1 in the CFAR approach, while a $\hat{P}_d$ of 0.9 in the CDR is taken into account. The system parameters used for the numerical results are listed Table 3.9.

From simulations for the CFAR approach, we can state that in low SNR conditions the energy detector is strongly affected by the SNR wall effect. In this case it is not possible to guarantee the detection with the desired probability even with long sensing observation periods. Figure 3.19 shows

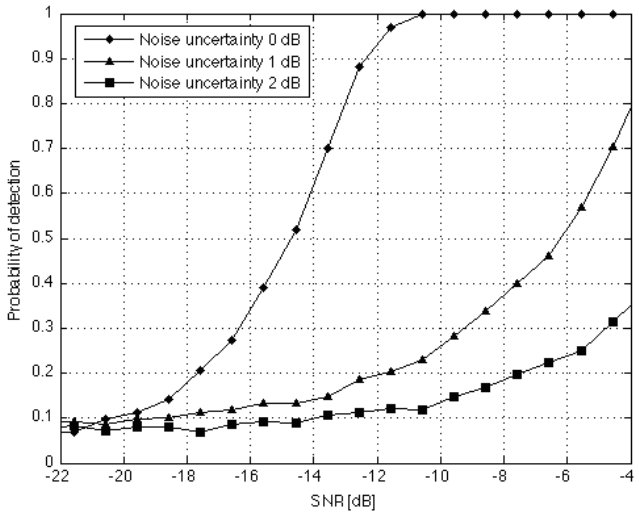

FIGURE 3.19: P_d for given P_{fa} and sensing time T_{oss} by varying the SNR with different noise uncertainty levels in the CFAR approach.

the probability of detection as a function of the SNR for a given observation time equal to 0.6 ms and a given false alarm probability equal to 0.1. In this case the noise uncertainty worsens the probability of detection, hence increasing the observation period should be a feasible solution. However, as shown in Figure 3.20 also in this case the noise uncertainty will prevent achieving the desired probability of detection. In particular, Figure 3.20 shows the probability of detection as a function of the sensing time in the worst-case condition, i.e. when the power received is equal to the interference threshold that is the minimum power signal level we must detect, $I/N = -10[dB]$. Both in the ideal case and with low noise uncertainty, $\rho_N[dB] = 0.1[dB]$, the desired probability is achieved. Instead in the high uncertainty case, $\rho_N[dB] = 1[dB]$, an asymptote at 0.3 prevents to achieve the desired probability of detection 0.9 even with long sensing periods.

The CDR methodology, which allows to fix the threshold for the energy detector such that it guarantees the desired probability of detection for the I/N threshold, has been also considered. Differently from the CFAR, in this case we need to reach the target false alarm probability. Since the false alarm probability depends only on the sensing time, we show in Figure 3.21 the guaranteed probability as a function of the sensing time. Since the CDR methodology guarantees a certain detection probability target for all the SNR values above a certain threshold, it is possible to avoid evaluation for different values of the SNR. Simulations have shown that with a signal under the threshold or in its absence the behavior is the same as the one shown in the figure. Hence, thanks to the CDR methodology the algorithm after a given sensing time is able to correctly decide for the absence of the interferer while in the opposite case its detection is a priori guaranteed. However also in this case the SNR wall phenomenon is present for strong noise uncertainties introducing an asymptote at about 0.5 for the probability of false alarm. It is possible to state that by fixing the threshold in both CFAR and CDR, the noise uncertainty does not guarantee the desired probabilities. In particular, by using CFAR and a given false alarm probability

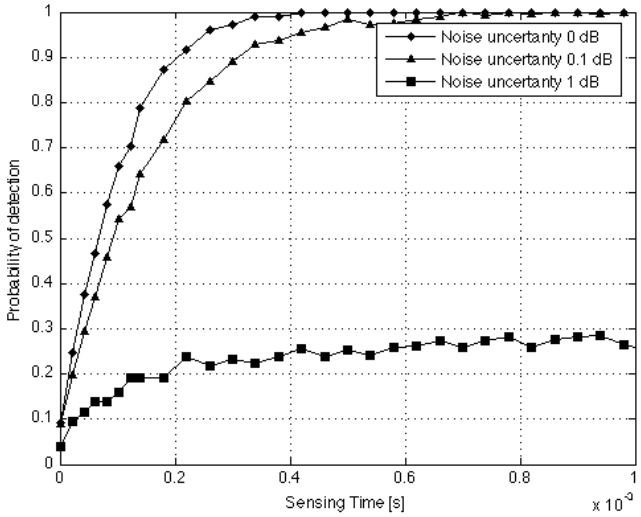

FIGURE 3.20: P_d for a given SNR equal to the I/N threshold (-10 dB) by varying the sensing time T_{oss} with different noise uncertainty levels in the CFAR approach.

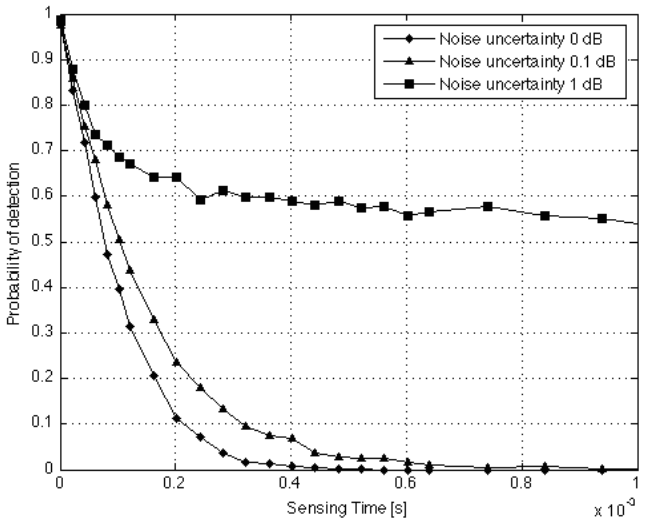

FIGURE 3.21: P_d for a given I/N threshold by varying the sensing time T_{oss} with different noise uncertainty levels in the CDR approach.

equal to 0.1, we can reach a detection probability higher than 0.9 if the sensing time is about 0.3 ms or more. On the contrary, the CDR needs more the same sensing time to guarantee a probability of false alarm of about 0.1 with a desired probability of detection equal to 0.9 and the I/N threshold fixed at - 10 dB at the antenna input as the worst case interference. Moreover, in the simulations we have considered that the RF chain will introduce an additional noise contribution besides the noise uncertainties that it may cause. All the noise contributions are considered into the equivalent system noise temperature but we have to point out that in satellite receivers pointing to the sky, noise levels are very low and small changes in the noise figure may result in much more changes of the SNR. The first results are obtained in an ideal case where no uncertainty in noise estimation is present. From the numerical results, it is possible to state that, due to the given interference

power levels, a reduced level of the noise uncertainty is needed in order to achieve the target detection probability. If we consider the ideal case or very small errors in estimating noise power, the choice between CFAR and CDR is given by the trade-off in spectrum efficiency. If we want to exploit unused incumbent user resources as much as possible even if an incumbent user is present but not detected, the CFAR methodology would be preferred rather than the CDR that guarantees the absence of the incumbent user but not the exploitation of all the possible spectrum holes.

Cyclostationary Detection Another typical detection technique is Cyclostationary Feature-based Detection (CDF). Differently from the ED, it exploits periodic features that could be present in the wireless communication signals to be detected. These periodicities could be introduced by:

- Pilots, preambles, cyclic prefixes introduced in order to aid synchronization or channel estimation;
- Coding
- Modulation schemes, symbol rate, frequency carries

A CFD technique allows to discern among different incumbent signals, thus not only detecting whether they are present or not, but also distinguishing them from noise, which has no cyclic features. The SNR wall phenomenon is not present, and the CFD provides good performance in low SNR regimes. On the other hand, it is quite complex from a computational point of view, as it requires the computation of the Fourier series of the autocorrelation function of the incoming signal: this function presents peaks in the frequency domain at multiples of some cyclic frequencies, which are related to the built-in periodicity of the signal. By building the Spectral Correlation Density (SCD) function, these second-order correlations can be detected, thus allowing to discern among different type of signals and between incumbent signals and noise. The SCD $S_x^\alpha(f)$ is given by equation (3.46), where $\{\mathcal{R}_x^\alpha(\tau)\}_{-\inf}^{\inf}$ are the Fourier series coefficients of the signal autocorrelation function, α is the generic cyclic frequency, and $x(t)$ is the incoming signal. A signal $x(t)$ is considered wide sense second-order cyclostationary if its temporal mean and autocorrelation functions are periodic with period T_0, see reference [80].

$$\mathbb{E}[x(t)] = \mathbb{E}[x(t - T_0)] \tag{3.43}$$

$$\mathcal{R}_x(tau) = \mathbb{E}[x(\tau + T_0)] \tag{3.44}$$

It follows that the autocorrelation function is periodic and it can be expressed with a Fourier series [81].

$$\mathcal{R}_x(t, \tau) = \sum_\alpha \mathcal{R}_x^\alpha(\tau) e^{j2\pi\alpha t} \tag{3.45}$$

whose coefficients are the harmonics of the fundamental cyclic frequency α_0 equal to the inverse of the period T_0 and $\mathcal{R}_x^\alpha(\tau)$ is called Cyclic Autocorrelation Function (CAF). Hence, a signal is said to be cyclostationary if exist at least one cyclic frequency $\alpha \neq 0$ such that $\mathcal{R}_x^\alpha(\tau) \neq 0$, i.e. a signal

presents cyclostationarity if and only if the signal is correlated with certain frequency shift of itself. On the contrary, a signal for which all the cyclic frequencies $\alpha \neq 0$ present $\mathcal{R}_x^\alpha(\tau) = 0$ is called purely stationary on the second order. Therefore the knowledge of the cyclic frequencies that present cyclostationary is fundamental in distinguishing the incumbent signal from the noise. Cyclostationary features in the frequency domain are evaluated from the Spectral Correlation Density (SCD) function as the Fourier transform of the CAF. In the discrete time domain, the estimation of the SCD is implemented by means of the FFT Accumulation Method (FAM).

$$\mathcal{S}_x^\alpha(f) = \sum_{\tau=-\inf}^{+\inf} \mathcal{R}_x^\alpha(\tau) e^{-j2\pi\alpha f} \tag{3.46}$$

$$\mathcal{I}(\alpha) = \max_f | \mathcal{S}_x^\alpha(f) | \tag{3.47}$$

For Scenario 1 and 2 where spectrum sensing seems to be feasible we should take into account different features that would exhibit cyclostationarity and need to prove its detection feasibility. For example, in Scenario 2 where no a priori assumption on the incumbent signal structure is possible the only information that we should exploit to determine the signal cyclostationarities is the incumbent modulation scheme. In fact it is known that FS links generally operate with M-QAM modulations. For digital signals with symbol rate Bs and oversampling them at the receiver, the SCD would present some cyclostationarities at m*Bs where m is an integer. On the contrary, in scenario 1 where the structure of the incumbent signal is well known, not only the cyclostationarities of the modulation scheme but also its periodic patterns could be exploited. In the considered scenario, the incumbent signal is a DVB-S2 like signal, and thus the following periodicities can be detected: i) Start of Frame sequence, which is always present; ii) pilot sequences, which are optional; and iii) different modcod schemes. In particular, these periodicities can be detected by means of the cyclic profile domain $\mathcal{I}(\alpha)$, defined in (3.47) and which would present detectable peaks for values of $\alpha \neq 0$.

Also in case of the CDF technique, some analysis are carried out. The signal, if present, will show peaks at all the multiple integers of the symbol rate, which is considered as periodicity to be detected. Figure 3.22 shows the frequency availability obtained with CFD with $\rho_N = 0dB$ and targeting $P_{fa} = 0.1$. The results are also compared with the application to the same scenario of the ED technique. Figure 3.23 shows the application of the CFAR approach while scanning the available bandwidths as a function of the sensing time. Noise uncertainty is also considered. It can be noticed that the same sub-bands are identified as available. However, this detector requires longer observation periods to converge to the correct detection ($20ms$ compared to $4ms$ in the ED case). This confirms that the CFD needs larger values of T_{oss}, but it allows to distinguish the different type of incumbent signals. Moreover, the CFD does not suffer from the SNR wall phenomenon, and thus provides good performance at slow SNRs.

Thanks to the estimation of the presence of possible interferer by means of its cyclostationary features it is also possible to discriminate between different Incumbent Users. However, in the SatCom scenario, the choice in

using a cyclostationary based detector is mainly driven by its ability in operating in low SNR environment. In fact, as explained in the case of the energy detector, we have to detect both for scenario 1 and 2 an interferer signal $-10[dB]$ under the noise level. Its ability in distinguish a signal also under low SNR conditions is due to the lack of cyclostationary features by the noise, which is most of the time considered stationary. An additional drawback is the required a priori knowledge of some periodicities built within the signal to be detected.

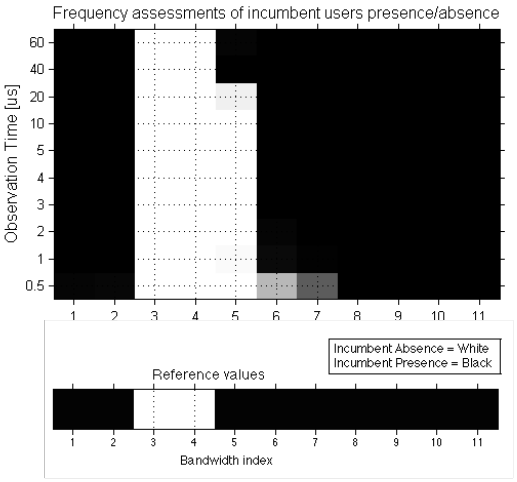

FIGURE 3.22: CFD: frequency assessment ($\rho_N = 0$ $[dB]$, $P_{fa} = 0.1$).

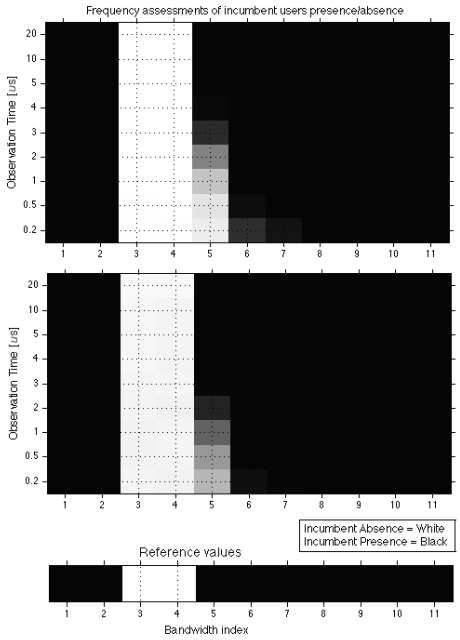

FIGURE 3.23: ED-CFAR: frequency assessment $\rho_N = 0$ $[dB]$, $P_{fa} = 0.01$ above, $P_{fa} = 0.1$ below).

Chapter 4

Spectrum Exploitation

4.1 Introduction and Rationale

Chapter 4 focusses on the application of spectrum exploitation techniques aiming at system efficiency improvements. The application of cognitive exploitation techniques in Scenario 1 and 2 of section 2.2, where different systems coexist, are investigated. In addition, techniques for spectral efficiency improvements in spectrum limited scenario, e.g., Scenario 3, are proposed. The analysis carried out for the third scenario, in particular, addresses flexible configurations of the available resources for L-band Mobile Satellite Systems (MSS) as described in section 2.3.2.

An overall improvement is foreseen when proper techniques are designed either in case of presence of other systems activities, *i.e.*, Scenarios 1 and 2, or due to a limited availability of spectrum, *i.e.*, Scenario 3. Regardless the scenario, what enables the improved exploitation of the spectrum is the knowledge of the channel state. The knowledge of the spectrum activities of the incumbent users is essential in CRs and it is usually based on spectrum sensing techniques or databases queries [2]. Such knowledge enables the following phases of the cognitive cycle to exploit the spectrum opportunities. Thus, spectrum awareness techniques as the one proposed in Chapter 3, are considered the baseline for exploitation purposes also in case of the cognitive-based satellite system. In these scenarios, avoid mutually interference is the main objective for a correct and more efficient use of the spectrum. As harmful interference is generated by the PUs against cognitive users, techniques that avoid the exploitation of the same bands in the vicinities of the PUs, are necessary. With this aim, two proposed carrier allocation schemes are investigated in this chapter. On the contrary, the third scenario, which does not foresee the coexistence of different systems in the same spectrum, is affected by its limited availability with respect to the demanded rate and the common functioning of the system. Thus, it is shown that a more efficient use of the spectrum is possible taking into account the flexibility that the system can provide. In fact, a higher frequency reuse, up to a Full Frequency Reuse (FFR), the joint exploitation of interference mitigation techniques, and system flexibility can provide higher performance in terms of achievable throughput.

The state of the art of the resource management techniques in SatCom environments and the motivations for the development of the proposed techniques in the considered scenarios, is presented in 4.2. In 4.3, the proposed carrier allocation techniques for Scenario 1 and 2 are described. The system model and a brief resume of the scenarios taken into account for the

evaluations is included in section 4.3.1, while the two techniques are detailed in section 4.3.2 and section 4.3.3, respectively. Both analytical analysis and simulations are included. In section 4.4, Scenario 3 is addressed. The proposed framework that copes with the limited spectrum issue of the considered scenario, is included also providing a general mathematical formulation of the problem. Following, several solutions and numerical results are provided with respect to the considered case of studies. The importance of spectrum exploitation techniques aiming at an improved spectrum efficiency, is also reported in the concluding remarks of 4.5, which resume, in accordance with the three scenarios, the results obtained.

4.2 Motivation and State of the Art

The efficient use of the spectrum enables higher capacities that will comply with the challenging demands of future markets. Either in case of systems coexisting in the same bandwidth or in case of the exclusive use of the spectrum, which however is becoming limited, the main objective is to exploit the available resources efficiently and according to the demands. In particular, Dynamic Spectrum Access (DSA) and Cognitive Radio (CR) exploitation techniques are seen as major solutions in the former scenarios, whereas higher frequency reuse for an improved spectral efficiency and interference mitigation techniques are foreseen in the latter.

Several resource management techniques for SatComs, not related to cognitive scenarios, have been taken into account in the last years. A detailed review and analysis of optimization and cross-layer strategies for satellite communications are presented in [82]. In [83] authors derive the optimum power allocation for multibeam satellite downlink transmission under total power constraints and different QoS requirements. Both capacity maximization and proportional fairness among users are addressed. In [84], results provided in [83] are extended with respect to minimum service requirements. In addition, it is depicted and assessed the proposed power allocation technique in a real scenario. With a particular focus on power allocation, capacity maximization problems and the related algorithms have been addressed in [85, 86, 87, 88] more recently. In particular, authors propose some algorithms to cope with power allocation and capacity maximization problems. Also bandwidth [89] or beam [90] allocation problems have been considered in literature. Generally, it is recognized that these approaches can achieve significant improvements and can efficiently use on-board resources assuring high Quality of Service (QoS) levels to end users at the expense of higher complexity. On the other side, resource management techniques have been widely addressed in case of cognitive terrestrial scenarios, while few works cope with the coexistance between terrestrial and satellite systems. Authors in [91, 92] depict a hybrid scenario in which the terrestrial system plays the role of the cognitive user and propose for it a power allocation strategy. In particular, authors in [92] develop a power allocation strategy by exploiting game theory for uplink communications of terrestrial users communicating with the base station, whereas in [91] authors consider a similar scenario while proposing a power allocation strategy aiming at maximizing the rate of the terrestrial link in the downlink case. Techniques for cognitive satellite systems

have been recently presented in [66, 67, 93] in case of uplink and downlink scenarios.

In scenarios where the satellite system act as cognitive user, *i.e.*, Scenario 1 and 2, the exploitation for broadband downlinks toward the users of frequencies not used by the PUs, is possible. As demonstrated in the previous chapter, interference levels are unbalanced along the available user bandwidth resulting in varying SINRs for the UTs. In these scenarios, an effective reuse of bandwidths non exploited by terrestrial systems, which are not interfered by the satellite links, would be effective if a reliable transmission can be provided to the cognitive users. Thus, in the considered underlay [3] SatCom based cognitive scenarios, *i.e.*, Scenario 1 and 2, optimize the SatCom links allocation in order to avoid an harmful interference against the *unprotected* satellite users is of main importance. To cope with the strong interferences that can make spectrum unusable, it has been shown that carrier allocation techniques, which allow users to be assigned to different carriers along those available, are promising techniques to be investigated [66, 67, 93]. As shown in chapter 3, the spatial distribution of the PUs and the directivity of their links, generate strong interferences only in their vicinity and make the SINRs levels of a selected user widely varying. Thus, spectrum opportunities can be limited with respect to the whole considered spectrum and vary from UT to UT, which need to be allocated in the proper carrier. The proposed carrier allocation algorithms aim at scheduling the SatCom users in the time-frequency domain according to their Quality of Service (QoS) requirements and the spatial diversity caused by the presence of the PU links.

The first proposed carrier allocation technique relies on a complete knowledge of the channel status of the different carriers. Similarly to [93, 67, 66], the technique is based on the Hungarian Algorithm. However, the proposed version of the algorithm takes into account Quality of Service requirements of the users and investigates a power allocation strategy at the transmitter. The technique requires complete knowledge of the interfering levels in each carrier. However, in the considered scenarios, these information can be redundant since can be identified zones with high spectrum opportunities and zones with lower ones. Thus, these information can be minimized focussing in providing the only needed information, where, especially in case of unknown or uncertain knowledge at the GW, wrong information can affect the performance of the carrier allocation algorithm. The second proposed carrier allocation technique is based on a genetic algorithm, which relies on a reduced knowledge of the channel information to be fed back at the GW. The algorithm relies on channel state information from the users, which have direct knowledge of the environment. Assuming that spectrum awareness is carried out autonomously by each ET, the proposed algorithm, based on a genetic approach, allows a suitable and low complexity solution by aiming at optimizing the carrier allocation of each user also reducing the amount of information to be fed back to the Network Control Center (NCC). Genetic algorithms (GA) are a family of algorithms inspired by evolution, which can encode and solve optimization problems by means of genetic-like structures [94, 95].

Contrary to Scenario 1 and 2, where the proposed techniques mainly aim at avoiding inter-system interferences, in the third scenario the focus

is put on the application of techniques that enable an higher spectral efficiency preventing intra-system interference. The followed approach, in particular, has higher impact on limited spectrum scenarios as those considered in 2.3.2. The development of *flexible configurations* allows an efficient assignment of the available spectrum with respect to the demanded rates of the users. In particular, to counteract the issue of having a limited spectrum that prevent the system to assign channels to all the users, higher frequency reuse and interference mitigation techniques are exploited.

4.3 Cognitive Exploitation Techniques

4.3.1 System Model and Problem Formulation

Due to the similarities of Scenario 1 and 2, the proposed techniques take into account the general applicability to either Scenario 1 or 2. However, assessment of the two techniques are provided for Scenario 2, which is here briefly resumed. We consider the heterogeneous scenario in which terrestrial and satellite links share the same frequencies. The focus is on the frequency interval in the Ka-band from 17.7 to 19.7 GHz, which has been assigned to terrestrial FS and can be shared in a non exclusive way with space-to-Earth satellite user links. With respect to the cognitive system, we consider the multibeam satellite architecture described in section 2.1. We assume a number of beams equal to N_B operating on the forward link with a frequency reuse plan of four colors and able to exploit with a specific SatNet the bands from 17.7 to 19.7 GHz. Thus, the total bandwidth of the SatNet is divided in four sub-bands, each further divided in K carriers of 36 MHz each. In each carrier Time Division Multiplexing (TDM) is considered to provide service to the users. The DVB-S2X standard [34], able to allocate multiple users in adjacent time-frames thus providing efficient broadband communications, is considered as the reference air interface for the satellite links. For sake of simplicity, the analysis carried out takes into account the allocation of N users in only one beam, without preventing the extension to the overall system.

Extremely different spectrum opportunities may occur according to the location of the Earth terminals, due to the directivity of the FS links and their different bandwidths. This condition is even more evident in case of SatComs because of the wide coverage of the beam, which is typically thousands of square kilometers. Thus, users either in remote and urban areas may be illuminated by the same beam giving rise to spatial diversity. In addition, a power level unbalance between the two systems is present since, in the considered underlay SatCom based cognitive scenario [3], the interference against the incumbent users is limited and negligible due to the emission limits defined in the Article S21 of the ITU Radio Regulations [48]. Thus, contrary to the limited impact that the satellite forward link has in terms of harmful interference towards the terrestrial links, protecting the satellite users from the harmful interference and their allocation in carriers able to satisfy their demands is of main importance.

In the depicted scenarios, the focus resides on optimizing carrier allocation of each transmission for the capacity maximization based on twofold requirements. On one hand, it is necessary to avoid the additional source of interference that the incumbent systems introduce, and, on the other hand,

to respect QoS requirements that each user has. To this aim, we consider an on-demand assignment of the resources [31] and the need to respect a minimum target QoS in terms of minimum signal to noise plus interference ratio (SINR) for all the active users.

The SINR of the n-th user in the k-th carrier can be written as:

$$\text{SINR}_{nk} = \frac{P_{nk}^{rx}}{N_0 + I_{nk}} \tag{4.1}$$

where i) P_{nk}^{rx} is the received power at the antenna input, ii) N_0 the thermal noise power of the terminal, and iii) I_{nk} the overall interference suffered by the user in that carrier. Due to the presence of several interference contributions, I_{nk} can be decomposed into several components, which include i) the external interference generated by other systems transmitting in the same carriers, I_{nk}^{EX}, ii) the co-channel interference generated by the same k-th carriers reused in other beams, I_{nk}^{CO}, iii) the adjacent channel interference caused by imperfect filtering, I_{nk}^{AC}, and iv) other interference contributions, I_{nk}^{other}. The main source of interference, if present, can be I_{nk}^{EX}, which corresponds to the transmission of the incumbent terrestrial links. I_{nk}^{EX} is scenario dependent and the interference generated by incumbent FS terrestrial users can be calculated from the interference model ITU-P 452-15 [77]. In the following we will consider also the presence of I_{nk}^{CO} and I_{nk}^{AC}, whereas I_{nk}^{other} is considered as a negligible contribution for system evaluations. Starting from these assumptions, the two proposed techniques develop a framework that include the definition of an optimization problem and strategies to solve it.

4.3.2 Hungarian Carrier Allocation and Waterfilling

Definition of the optimization problem

We assume that the satellite payload can use an amount of power equal to P^{tot}, which has to be properly allocated in a per-beam and per-carrier basis in order to satisfy the QoS requirements in terms of minimum SINR. Thus, we should set a constraint on the total power P^{tot} available at the satellite for transmission that has to be distributed among the N_B beams and the K carriers:

$$\sum_{b=1}^{N_B} \sum_{k=1}^{K} P_{b,k} \leq P^{tot}, \tag{4.2}$$

and a constraint on the power allocated among the K carriers of the b-th beam

$$\sum_{k=1}^{K} P_{b,k} \leq P_b^{max} \tag{4.3}$$

where P_b^{max} is the maximum power assigned to the b-th beam. Moreover, the power allocated in the k-th carrier in the b-th beam is limited by the saturation power level P^{sat}:

$$P_{b,k} \leq P^{sat} \tag{4.4}$$

In the following the subscript b will be omitted since the algorithm is performed in a per beam basis.

Assuming the knowledge of the SINRs experienced by the users from a database or from a previous sensing operation [18], we aim at identifying the carriers and the power levels that allow to maximize the total system capacity, and, at the same time, finding a compromise in satisfying the users' QoS. Due to the frequency selectivity of the SatCom channels generated by the presence of the incumbent users, the selection of a proper carrier has a key role for maximizing the SINR level and, subsequently, the system capacity. On the other hand, an efficient power allocation is fundamental from a system point of view.

The total achievable system capacity C_{tot} can be expressed as the sum of the capacities of the users C_n^{user} [65]:

$$\begin{aligned} C_{tot} &= \sum_{n=1}^{N}\sum_{k=1}^{K} C_{nk}^{\text{user}} \\ &= \sum_{n=1}^{N}\sum_{k=1}^{K} w_{nk}\frac{B_K}{N_k}\log_2\left(1+\text{SINR}_{nk}^{a}\right) \\ &= \sum_{n=1}^{N}\sum_{k=1}^{K} w_{nk}\frac{B_K}{N_k}\log_2\left(1+\frac{P_{nk}|h_{nk}|^2}{N_0+I_{nk}}\right) \end{aligned} \tag{4.5}$$

where i) B_K is the total bandwidth per carrier, ii) K the number of carriers, iii) N_k the number of users allocated in the k-th carrier, iv) $w_{nk} \in \{0,1\}$ defines the allocation in the k-th carrier of the n-th user, and v) SINR_{nk}^{a} is the signal to noise plus interference ratio of the n-th user in the k-th assigned carrier, and the Shannon formula is considered. The SINR_{nk}^{a} is also affected by the variability of the received power, P_{nk}^{rx}, that corresponds to the product of the satellite transmitted power P_k and the channel coefficient $|h_{nk}|^2$, which includes the transmitter and receiver antenna gains and the free space and atmospheric losses.

In order to correctly formulate the optimization problem, we need also to define i) the matrix $\mathbf{S}_{N\times K}$ whose elements SINR_{nk} represent the SINR level of the n-th user along the k-th carrier in which they can be allocated, ii) $\mathbf{W}_{N\times K}$ as the matrix composed by w_{nk}, iii) $\mathbf{Q}_{N\times 1}$ as the vector composed by the minimum SINR values to be guaranteed for each user, *i.e.*, Q_n^{min}, iv) the vector $\mathbf{P}_{N\times 1}$, which includes the transmission power associated to the users, v) $\mathbf{S}^a = ||\mathbf{S}\circ\mathbf{W}||_1$ as the vector of the SINR values experienced by users in the assigned carriers *i.e.*, SINR_{nk}^{a}, and vi) $\mathbf{T}_{N\times 1}^{a}$, a vector whose elements indicate the slot assigned to the n-th users.

The maximization of the total system capacity C_{tot} is considered as the objective function of the optimization problem that should also respect the constraints above. Thus, taking into account the quantities introduced previously and the system constraints, the overall problem formulation can be outlined as:

TABLE 4.1: Joint carrier and power allocation technique: system reference parameters symbols.

Parameter	Symbol
Number of beams	N_B
Number of carriers	K
Number of Users	N
Number of Users allocated per carrier	N_U
Beam Index	b
Carrier Index	k
User Index	n
Signal to noise plus interference ratio	$SINR_{n,k}$
Minimum SINR	Q_n^{min}
Total System Transmission Power	P^{tot}
Beam Transmission Power	P_b^{max}
Carrier Transmission Power	P_k
Carrier Received Power	P_{nk}^{rx}
Carrier Saturation Power	P^{sat}
Channel Gain	$\|h_{nk}\|^2$
Noise Power	N_0
Co-channel Interference Power Density	I_{nk}^{CO}
Adjacent Interference Power Density	I_{nk}^{AC}
External Interference Power Density	I_{nk}^{EX}
Other Contribution Interference Power Density	I_{nk}^{other}
User Capacity	C_n^{user}
Total Capacity	C_{tot}
Total Beam Bandwidth	B
Allocation Index	w_{nk}

$$\max_{w_{nk},P_k} \{C_{tot}\} \tag{4.6}$$

$$\text{subject to } \sum_{k=1}^{K} w_{nk} = 1, \quad w_{nk} \in \mathbf{W}_{N\times K} \tag{4.7}$$

$$\sum_{k=1}^{K} P_k \leq P^{max} \tag{4.8}$$

$$P_{nk} \leq P^{sat}, \quad P_{nk} \in \mathbf{P}_{N\times 1} \tag{4.9}$$

$$\text{SINR}_{nk}^{a} \geq Q_n^{min}, \quad Q_n^{min} \in \mathbf{Q}_{N\times 1} \tag{4.10}$$

where we aim at finding the allocation matrix $\mathbf{W}$, and the power vector $\mathbf{P}$ that allow to maximize the system capacity. In particular, (4.7) indicates that the n-th user can be allocated in only one carrier, (4.8) and (4.9) refer respectively to power constraints at beam and carrier level, whereas (4.10) takes into account the minimum value of the SINR to be guaranteed to the n-th user with respect to its QoS requirement.

The formulated problem is a mixed non linear programming optimization problem with multiple constraints [96, 97], which is NP-hard and for which an heuristic algorithm based on a two-step approach is proposed. All the parameters included in the mathematical formulation are also included in Table 4.1.

Proposed Technique

Due to the complexity of the optimization problem we resort to a two steps approach that separately solves the optimization problem under the constraints (4.7) and (4.10) at the first step, and further solves the power constraints (4.8) and (4.9). The proposed solution assigns the same number of users to each carrier, which corresponds to $N_U = ||\mathbf{W}||_\infty$ [1].

1) Carrier Allocation: The first step of the algorithm aims at allocating users in the carrier characterized by the highest SINR experienced by each user and minimizing the overall external interference. This problem can be solved optimally with a polynomial complexity by means of the Hungarian algorithm. However, the algorithm assumes that no more than one user per carrier can be assigned corresponding to the additional constraint:

$$\sum_{n=1}^{N} w_{nk} \leq 1 \qquad k = 1, .., K \tag{4.11}$$

In case of K equal to N, the problem is known as *Assignment Problem* [97]. Only K users can be allocated at the same time and, therefore, in case of a grater number of users with respect to the number of carriers, these latter have to be shared by exploiting Time Division Multiplexing (TDM). In this case, it is possible to resort to the algorithm proposed in [98], which is efficiently implemented for solving the *Assignment Problem* in case of rectangular matrices where $N \neq K$ and (4.11) is no more respected. Thus, performing iteratively N_U times the Hungarian algorithm, at each iteration K users are allocated until all the users are assigned. The algorithm allocates N_U users in each carrier and aims at maximizing the profit, *i.e.*, the average SINR of the overall system.

Nevertheless, the algorithm does not prevent a user to be allocated in a carrier, that does not satisfy the constraint introduced in (4.7). Therefore, in order to avoid this issue, the algorithm is constrained to not choose such carriers. To do this, we introduce a modified version of the matrix $\mathbf{S}$, *i.e.*, $\hat{\mathbf{S}}$, whose SINR_{nk} elements not satisfying the constraint in (4.10) are associated to a null profit. This modification defines "Step 0" of the algorithm. Following, the application of the Hungarian algorithm will assign proper carriers to each user avoiding those that not satisfy the QoS constraint.

2) Power Allocation: As output of the modified Hungarian algorithm applied to the matrix $\hat{\mathbf{S}}$, we have that a specific carrier and time slot is assigned to each user. Due to the frequency-selectivity of the fading channels and considering independent channels, we aim in this second stage of the algorithm at balancing the available power in each carrier and time slot in order to maximize the overall system capacity with respect to the SINRs that the users experience in the carriers. The problem under power constraints (4.8) and (4.9) can be solved by means of the waterfilling process [65]. The optimal power allocation, derived by applying the Lagrangian multipliers

[1] The norm $||\mathbf{W}||_\infty$ is constant only if N is a multiple of K, otherwise we assume that the users per carriers differ no more than one from N_U.

method, in the k-th carrier is:

$$\frac{P_k}{P^{max}} = \begin{cases} \frac{1}{\gamma_0} - \frac{1}{\gamma_k}, & \text{if } \gamma_k \geq \gamma_0 \\ 0, & \text{if } \gamma_k \leq \gamma_0 \end{cases} \tag{4.12}$$

where γ_0 is the cut-off value and γ_k the SINR of the k-th user assuming that all the available power P^{max} is assigned to it. In particular the cut-off value can be calculated as

$$\frac{1}{\gamma_0} = \frac{1}{K} \sum_{k=1}^{K} \frac{1}{\gamma_k} \tag{4.13}$$

The waterfilling allows to maximize the capacity by increasing power and data rates when the channel conditions are favorable and decreasing them conversely. Therefore, in case of a limited amount of total power per beam, some carriers may be switched off due to the impossibility of providing the amount of required power. We assume, without loss of generality, that the total power per beam available is sufficient to be distributed among all the carriers fulfilling the minimum Q_n^{min}. In this case, the waterfilling aims at equalizing the power of the carriers in order to refine the capacity maximization.

The joint carrier and power allocation algorithm is represented in Algorithm 1 where the initialization step, Step 0, the carrier allocation, Step 1, and the power allocation, Step 2, are highlighted.

Algorithm 1 Carrier and Power Allocation

Input: $\mathbf{S}$, $\mathbf{Q}$, P^{max}
Output: $\mathbf{W}$, $\mathbf{P}$
Initialize: $\mathbf{S}^a, \mathbf{T}^a \leftarrow 0$; $\hat{\mathbf{S}} \leftarrow \mathbf{S}$
STEP 0: Modified $\mathbf{S}$ matrix. All the carriers in which the QoS is not satisfied are forced to have null profit.
for $n = 1 : N$ **do**
  if $\{\mathbf{S}_{nk}\}_{k=1}^{K} < \mathbf{Q}_n$ **then**
    $\hat{\mathbf{S}}_{nk} \leftarrow 0$
  end if
end for
STEP 1: Hungarian Algorithm. Allocate users in carriers that provides maximum average SINR w.r.t. $\hat{\mathbf{S}}$.
$\mathbf{T^a}, \mathbf{W} \leftarrow$ *Modified Hungarian*$\{\hat{\mathbf{S}}\}$
$\mathbf{S}^a_{N\times 1} \leftarrow ||\mathbf{S} \circ \mathbf{W}||_1$
STEP 2: Waterfilling Algorithm. Provide an equalization among the carriers.
for $j = 1 : N_U$ **do**
  $\mathbf{P} \leftarrow$ *Waterfilling*$\{\mathbf{S}^a * (T^a == j), P^{max}\}$
end for

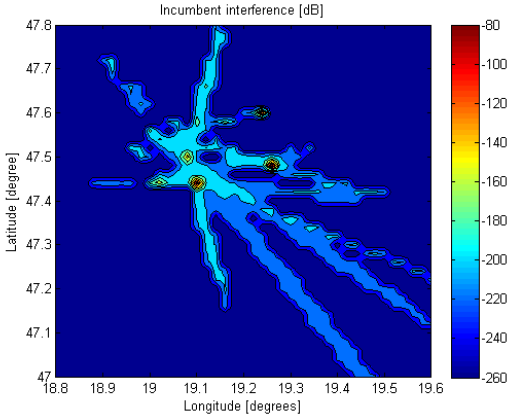

FIGURE 4.1: Scenario 2: interference density power levels in the considered region.

Numerical Results

Numerical analysis of the proposed technique are assessed according to the Scenario 2 presented in section 2.1. The area taken into account for evaluations consists of the region between $47°$N to $47.8°$N of latitude and $18.8°$E to $19.6°$E of longitude, corresponding to a portion of Hungary in which multiple incumbent users are present and occupy different carriers along the spectrum portions. Analysis on the interference generated by the FS incumbent users against FSS Earth terminals have been carried out in [22] considering the ITU-R Recommendation P.452 propagation model [77]. The performance of the proposed algorithm are evaluated in a scenario where the two systems share the bandwidth from 18.4 GHz to 18.8 GHz. Taking into account the grid points with an external interference generated by the incumbent users, a spectrum occupancy, in terms of $[\text{Hz/Km}^2]$, of about 30% occurs [2]. An example of the spectrum occupancy is given in Figure 4.1 where the aggregated power density levels of the FS links within the carrier centered in 18.418 GHz are shown. Further, we assume that a GEO multibeam cognitive satellite system positioned in $13°$E of longitude covers Europe with a frequency reuse factor of four colors, and that the selected region is illuminated by one beam having a bandwidth of 400 MHz. The sub-band is divided in 11 carriers of 36 MHz each, which are assigned to users for service provision. Each carrier is further divided in time slots, each of them assigned to a user according to the output of the proposed algorithm.

The parameters used for system evaluation are listed in Table 4.2. Different levels of the total power available per beam P^{max} and a saturated power level per carrier P_k^{sat} fixed at 55W are considered. With respect to users' demands, three different values of Q_n^{min} to be guaranteed are randomly assigned from a selection of chosen values. These values are set to -2, 5 and 8 dB, which are the lowest values associated to the lowest rate of QPSK, 8PSK, and 16APSK modulations, in order to have Quasi Error Free in AWGN conditions in case of DVB-S2X communications [34].

[2]Spectrum occupancy is defined as the area for which a INR above -10 dB is present. The limit is derived by Recommendation ITU-R S.1432-1 [76].

TABLE 4.2: Joint carrier and power allocation technique: System reference parameters.

Parameter	Value
Region of interest, latitude	47°N to 47.8°N
Region of interest, longitude	18.8°E to 19.6°E
GEO satellite longitude	13°E
P^{max}	200, 400, 610 W
P_k^{sat}	55 W
Q_n^{min}	$\{-2, 5, 8\}$ dB
Spectrum occupancy	30%
Frequency range (GHz)	[18.4, 18.8]
Beam sub-bandwidth	400 MHz
Carrier bandwidth B_W	36 MHz
Number of carriers K	11
Number of Active Users N	From 11 to 110

The histograms in Figure 4.2 provide a comparison between different techniques in terms of total capacity C_{tot} (4.5). In particular, a random assignment of carriers with equal power allocation, a carrier assignment by mean of the Hungarian algorithm together with equal power allocation, and the proposed joint Hungarian and Waterfilling approach are evaluated under the same scenario. For the sake of completeness, the obtained results are also compared with the maximum achievable capacity considering each user allocated in the most favorable carrier. Considering a number of users equal to $N = 11$ and $N = 110$ in each figure, the total capacity achieved by the techniques in case of values of available maximum power per beam P^{max} equal to 200 W and 610 W are showed. As expected, the Hungarian algorithm allows to avoid interfered carriers and outperforms the random assignment, which does not consider the presence of interfered carriers. The advantage of considering also the Waterfilling approach is confirmed in case of a high number of users but limited available power as in case of $N = 110$ in the left figure. In this case, an higher total capacity is achieved due to the better exploitation of the power.

In Figure 4.3, the Cumulative Density Function (CDF) of the average capacity of the users is showed. The figures, provide a comparison between the application of the only Hungarian algorithm, the application of the proposed joint carrier and power allocation, and the achievable maximum in different markers. In particular, the results obtained in case of $N = 11$ and P^{max} equal to 200 W and 610 W, and those in case of $N = 110$ for the same available powers, are showed in the left and the right figure, respectively. It can be noticed that the effect of the waterfilling is remarkable when the number of users is high and the available power is low. Indeed, in case of a higher available power the two approaches achieve a similar capacity.

In Figure 4.4 the CDF of the SINRs of the users is assessed. In particular, the left figure and the one on the right show the CDFs of the SINR values of the whole allocated users for which the required QoS is guaranteed, and those achieved by specific users, respectively. Both the figures consider a maximum power P^{max} equal to 400W sufficient for serving all the users. QoS constraints are guaranteed even in case of the highest SINR constraint. Moreover, in case of a higher number of users, it further seems the algorithm better allocates the users. Analysis on specific users, *i.e*, User_1, User_2,

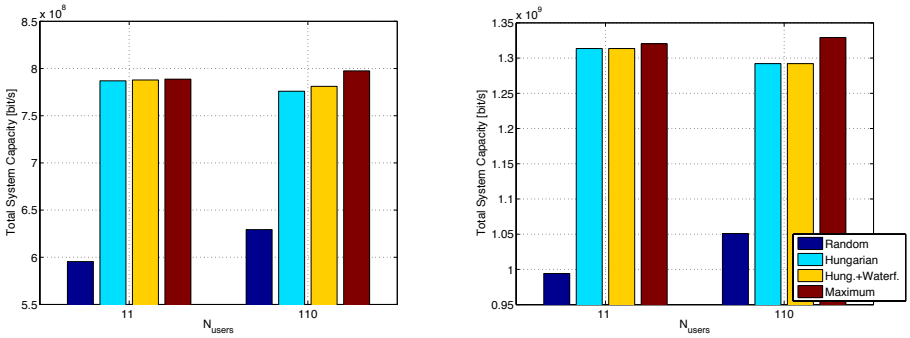

(A) *Case 1:* $P^{max} = 200W$ (B) *Case 2:* $P^{max} = 610W$

FIGURE 4.2: Joint carrier and power allocation technique: achieved total system capacity.

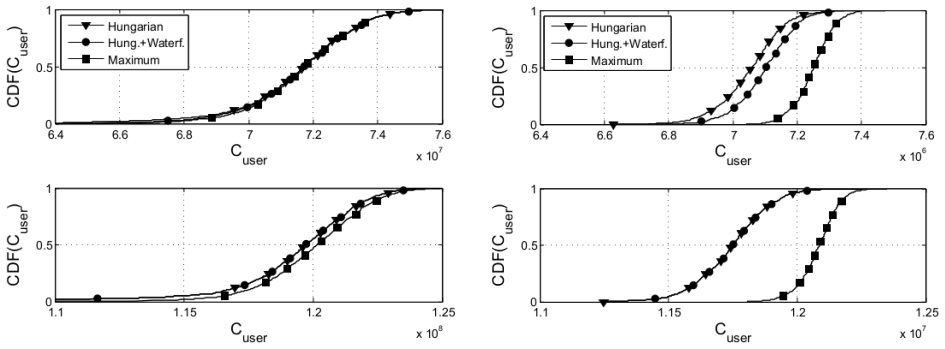

(A) *Case 1:* $N = 11$ (B) *Case 2:* $N = 110$

FIGURE 4.3: Joint carrier and power allocation technique: CDF - Average users capacity. $P^{max} = 200W$ (figures above) and $P^{max} = 610W$ (figures below).

and User_3 for which location and QoS are specified in Table 4.3, demonstrate that QoSs are guaranteed but different values of SINR are achieved depending on the number of users N, their requirements, and the scenario.

Due to the limited availability of free carriers and the fact that users are randomly chosen from the selected area, in Figure 4.5 the CDF of the percentage of users effectively allocated respecting their QoS constraint is shown. The results obtained in case of a total power P^{max} equal to 400 W and 610 W are showed. The overall number of allocated users N is equal to 110 but the minimum SINR may not be guaranteed to the whole set of users which may achieve lower values due to the limited amount of resources. Thus, not all the users, which require a higher QoS, can be satisfied in case of limited power. On the contrary, those users with lower QoS can be easily satisfied and are in both cases allocated by the algorithm, which fails only if the user is strongly interfered and does not have available carriers.

TABLE 4.3: Joint carrier and power allocation technique: Specific Users reference parameters.

Parameter	**User$_1$**	**User$_2$**	**User$_3$**
Location - latitude	47.38	47.38	47.60
Location - longitude	19.36	19.22	19.41
QoS $[dB]$	-2	5	8

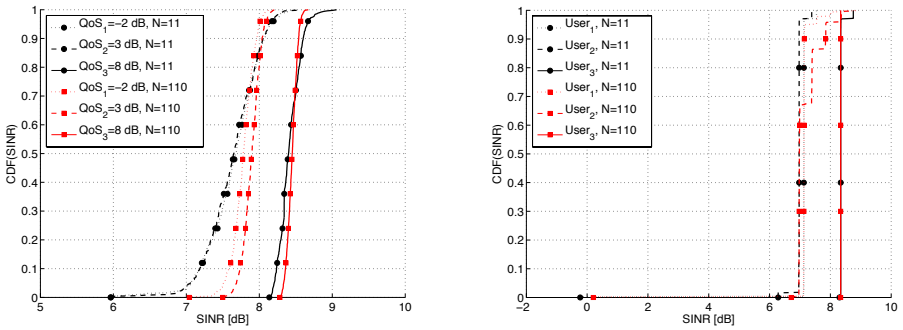

(A) *Case 1: Average SINR.* (B) *Case 2: Specific User SINR.*

FIGURE 4.4: Joint carrier and power allocation technique: SINR Cumulative Density Functions.

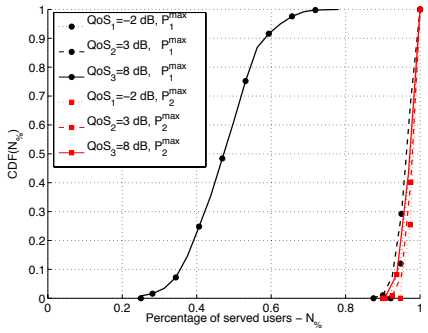

FIGURE 4.5: Joint carrier and power allocation technique: CDF - Percentage of allocated users. $\left(P_1^{max} = 400W, P_2^{max} = 610W\right)$.

4.3.3 Genetic Algorithm for scheduling

Distributed carrier selection and centralized carrier allocation

A new system level cognitive exploitation framework, which considers a distributed carrier selection and a centralized carrier allocation, is proposed. We assume that the ETs are able to autonomously select the best transmission parameters with respect to the sensed environment conditions. This choice is driven by the fact that the ETs are directly facing with the changes of the environment and their service demands. The autonomous selection is done after the sensing phase, that can be performed, e.g., by exploiting the technique introduced in chapter 3 that allows to estimate the interference level at the ET side. Moreover, it is a general assumption to consider a complete knowledge of the status of the channels at the central entity. However, in case of cognitive based SatComs, where spatial diversity raises, this approach may be redundant and not necessary. Thus, it is possible to limit the amount of information that each user has to provide to the NCC.

The set of information that the m-th user has to feed back to the NCC for performing the proposed centralized scheduling algorithm, includes i) the selected carrier k, *i.e.*, the one with the highest signal to noise plus interference ratio (SINR), ii) the MODCOD associated to the SINR γ_{km} estimated in the selected carrier k, iii) a minimum number of time slots N_m to be reserved to the user according to the required rate $\hat{R}_m$, and iv) the availability in changing the carrier, identified by the parameter t_m. These parameters, necessary to perform the proposed algorithm, are introduced in following together with the mathematical problem formulation of the problem and of the proposed solution.

Thus, we assume that the ETs feed back by means of the return channel to the NCC the set of defined information. Then, the NCC is in charge of elaborating the received information in order to identify the allocation scheme in the time/frequency domain that satisfies demands and serve all the requesting users. To do this, a carrier assignment and user scheduling procedure with the aim of minimizing the difference between the demanded and provided user data rates, is considered. To this aim our proposal is to resort to a GA based scheduling algorithm, which is particularly suited to solve optimization problems starting from a potential solution and iteratively modifying it, seeking a better one.

Problem Formulation and Proposed Solution

1) Problem Formulation Following a similar approach to the previous problem, a new optimization problem in accordance with those solved be Genetic Algorithms, is defined. The problem can be formulated as:

$$\min \sum_{m=1}^{M} \sum_{k=1}^{K} \left(\hat{R}_m - R_{km} \right) \tag{4.14}$$

$$s.t. \sum_{k=1}^{K} w_{km} = 1, \quad w_{mk} \in \mathbf{W}_{K \times M} \tag{4.15}$$

$$R_{km} \geq \hat{R}_m, \quad \hat{R}_m \in \mathbf{R}_{1 \times M}, \forall k \tag{4.16}$$

where i) $\hat{R}_m$ is the target rate of the m-th user, ii) R_{km} is the rate that the satellite system provides to the m-th user in the k-th carrier, iii) w_{km} is an element of the allocation matrix $\mathbf{W}_{K\times M}$, equal to one if the m-th user is allocated in the k-th carrier, and iv) $\mathbf{R}_{1\times M}$ is the vector of the QoS requirements in terms of minimum data rate. The difference between the target and the achieved rate per user is considered as the objective function of the optimization problem. The constraints are (4.15), which represents the capability of the system to allocate the user in only one carrier, and (4.16), the QoS constraint on the minimum rate per user.

Due to the time-frequency duality [86], we can achieve the same rate either allocating users in multiple carriers or in adjacent time slots. Broadband satellite systems consider time division multiplexing (TDM) and allocate the whole available bandwidth of the carrier to the users. According to the frame structure of the DVB-S2X and the allocation of bursts in variable size [31], it is possible to flexibly allocate time slots to each user regardless the total number of slots in each carrier. Hence, we assume that a number of multiple adjacent time slots equal to N_m can be assigned to the m-th user according to its QoS requirements. On the other hand, by considering a total number of time slots N_{max} in each frame, it is possible to define the achieved rate R_{km} on the k-th channel by the m-th user and its requested rate $\hat{R}_m$ as:

$$R_{km} = B_W \frac{N_m}{N_{tot,k}} \eta_{km} \tag{4.17}$$

$$\hat{R}_m = B_W \frac{N_m}{N_{max}} \eta_m \tag{4.18}$$

where i) B_W is the total bandwidth per carrier, ii) N_m are the slots assigned to the m-th user, iii) $N_{tot,k}$ is the sum of all the slots of the users allocated in the k-th carrier, *i.e.*, $\sum_{m=1}^{M} w_{km} N_{km}$, iv) N_{max} is the maximum number of available slots in each carrier, and v) η_{km} is the spectral efficiency of the MODCOD of the DVB-S2X standard associated to the m-th user and selected according to the estimated signal to noise plus interference ratio. Subsequently, the sum-rate achieved in the k-th carrier is equal to:

$$R_k^T = \sum_{m=1}^{M} w_{km} R_{km}, \ \forall k, \tag{4.19}$$

whereas the sum-rate of the total system is calculated as sum of the rates achieved in all the carriers:

$$R^S = \sum_{k=1}^{K} R_k^T . \tag{4.20}$$

With reference to the problem previously formulated, we can define the set of information that the ETs have to select and to feed back to the NCC. Thus, each ET, which has sensed the spectrum and estimated the SINR in

all the available carriers, selects the desired transmission parameters as:

$$k = \arg\max_{k} \{\gamma_{km}\} \tag{4.21}$$

$$\eta_{km} = f\left(\gamma_{km}\right)_{DVB-S2X} \tag{4.22}$$

$$N_m = \left\lceil \frac{\hat{R}_m N_{max}}{B_W \eta_{km}} \right\rceil \tag{4.23}$$

where the carrier index k is selected according to the maximum estimated SINR γ_{km}, the spectral efficiency η_{km} of the MODCOD is derived from the DVB-S2X standard as a function of the estimated SINR, and the number of slots N_m as the minimum integer number of slots that satisfies the demanded rate (4.18). Finally, the parameter expressing the availability of the user in changing the selected carrier, which is necessary to perform the proposed algorithm, is included and defined as:

$$t_m = \begin{cases} -\log_b \left\{ \frac{\max_k \{\gamma_{km}\} - \hat{\gamma}_m}{\max_k \{\gamma_{km}\}} + \frac{1}{b} \right\} & \text{if } t_m > 0 \\ 0 & \text{if } t_m \leq 0 \end{cases} \tag{4.24}$$

where $\hat{\gamma}_m$ is the average signal to noise plus interference ratio along the sensed carriers, and b the base of the logarithm, which identifies the value $\xi = 1 - 1/b$ that allows to separate the users available to change the carrier from those who have not availability in other carriers apart from that already chosen. Thus, for users that have similar SINRs along the carriers, t_m will tend to 1 highlighting that they can be moved in other carriers without losing in performance, whereas, getting t_m close to zero corresponds to have few carriers available and to be prone to remain in the one selected.

2) Proposed Genetic Based Solution The proposed solution is inspired by GAs, which are adaptive, flexible, and low complexity heuristic search algorithms robust against changing environments [95]. GAs have basic features that can be exploited in various applications through slight modifications [94]. The structure of the proposed genetic algorithm for carrier allocation is presented in Algorithm 2 and is designed according to the basic structure of GAs.

As a first step, the carrier allocation algorithm takes into account the carriers autonomously selected and fed back to the NCC with the other parameters by the ETs. This first step, in which the NCC just allocates the carriers based on the requests of the users, is also used as a benchmark comparison in the following Section, where numerical results are provided. Subsequently, the NCC searches for the best solution with respect to a defined fitness function F_T in the search space, *i.e.*, the set of feasible solutions. According to the formulated problem, the fitness function is defined as:

$$F_T = \sum_{m=1}^{M} \sum_{k=1}^{K} \left(\hat{R}_m - R_{km} \right). \tag{4.25}$$

We associate the following terminology of GAs with the variables of the proposed problem: i) the population is a possible allocation of $\mathbf{W}$ ii) a chromosome, which is a set of genes and constitutes the population, is the vector

containing the users allocated in the same carrier, and iii) a gene is the pair user and its assigned carrier. The proposed carrier allocation algorithm is inspired by GAs since it is a common assumption to identify the chromosome as a string of bits and, therefore, it is possible to map the rows of the matrix **W**, which identifies the population, as chromosomes. On the other hand, the common genetic operations performed by the algorithm are i) selection of genes evaluating the fitness function of each, ii) recombination of the chromosomes that contains the selected genes to breed new chromosomes, which may be better than their parents, and iii) mutation, which is not considered in the proposed algorithm and alters genes for avoiding stagnation in local optima.

In the proposed algorithm, the selection of the gene, *i.e.*, the m-th user to be reallocated at each iteration of the loop, takes place according to:

$$m = \arg\max_{m} \left\{ t_m \left(\hat{R}_m - R_m \right) \right\} \tag{4.26}$$

where the argument of the maximum function represent the product of the availability of the user to change the carrier and the difference between the achieved rate and the one demanded. This corresponds to maximize the tradeoff between the availability of changing the carrier versus the advantage in terms of increased data rate.

Subsequently, recombination between the carrier, *i.e.*, the chromosome in which the selected gene is, and the one that offers maximum availability in terms of time slots, is performed. Since the selection of the gene is executed deterministically according to (4.26), a mechanisms that avoids the selection of the same user at each iteration should be considered. It has been chosen to reduce the parameter t_m by β, which is a value a priori set to make the gene less attractive during the selection phase. Thus, for the selected gene the availability value at the next iteration becomes $t'_m = t_m - \beta$. Finally, we consider as end condition the satisfaction of all the users or, in case this can not be possible, a maximum number of iteration N_I^{max}.

Algorithm 2 Proposed Genetic Algorithm

Input: $(k, t_m, \eta_{km}, N_m) \ \forall m$
Output: W
STEP 1: Initialization. Derivation of a feasible solution (population) from the autonomous selection of the parameters performed by the users.
STEP 2: Evaluation of the defined fitness function F_T.
loop
STEP 3: Generation of a new population repeating the following steps:
3a: Selection of the user (gene) and the carrier (chromosome) available for recombination,
3b: Recombination (cross-over) of the selected gene and chromosome to generate a new solution,
3c: Availability parameter reduction,
3d: Evaluate the new population,
STEP 4: Test the end condition. End if satisfied.
end loop.

TABLE 4.4: Genetic algorithm: system and scenario reference parameters.

System Parameter	Value
Illuminated Area	$7800[Km^2]$
Frequency	18-18.5 GHz
Number of carriers K	11
L_{sat}	13 degE
Air Interface	DVB-S2X
Carrier Bandwidth B_W	36 MHz
Number of users M	From 10 to 100
Target Rate $\hat{R}_m$	From 1 Mbps to 15 Mbps
FSS antenna pattern	ITU-R S.465-6 [99]
FS antenna pattern	ITU-R F.699-7 [50]
Algorithm Parameter	**Value**
N_I^{max}	100
b	10
β	0.5

Numerical Results

In this section we discuss the numerical results of the proposed algorithm in order to demonstrate its feasibility with respect to the considered cognitive based SatCom scenario. With respect to the cognitive system, M users are placed randomly in the selected area and different QoS requirements in terms of minimum rate to be guaranteed are assigned. Thus, assessments as function of the number of users and their demands are taken into account. With respect to the total capacity of the satellite system, we consider three different study cases. In particular, a low, a medium, and a high load in terms of number of users and rates are taken into account.

As in case of the previous analysis, the same system and scenario are taken into consideration. The M users placed in an area of about $7800[Km^2]$ at mid latitudes, are illuminated by the same beam. Thus, the sub-band from 18 to 18.5 GHz, which is allocated to the beam, results in a number of carriers K with a bandwidth of 36 MHz each, equal to 11.

On the other hand, the FS transmitters are randomly placed according to a Poisson Point Process (PPP) in the same area of the ETs, while their azimuth angles are uniformly distributed. The ITU-R F.699-7 [50] antenna pattern is considered for the FS links and the carriers occupied by the FSs and their bandwidths are uniformly distributed between tens to hundreds Megahertz. According to the proposed scenario, we define as *spectrum availability* the percentage of available carriers in terms of $\frac{Hz}{Km^2}$ and we use this parameter to evaluate the performance of the proposed algorithm. Its opposite is defined as *spectrum occupancy*, and we assume as occupied those carriers in which an harmful interference against the ETs is present. To determine if an interferer is harmful, the ITU Recommendation ITU-R S.1432-1 [76] defines reference values of interference to noise ratio (I/N) related to the maximum allowable error performance and availability degradations of digital satellite paths to be respected. The selected I/N threshold is equal to -10 dB. The parameters used for the system assessment are listed in Table 4.4.

The Figure 4.6a and 4.6b represent the cumulative density function (CDF)

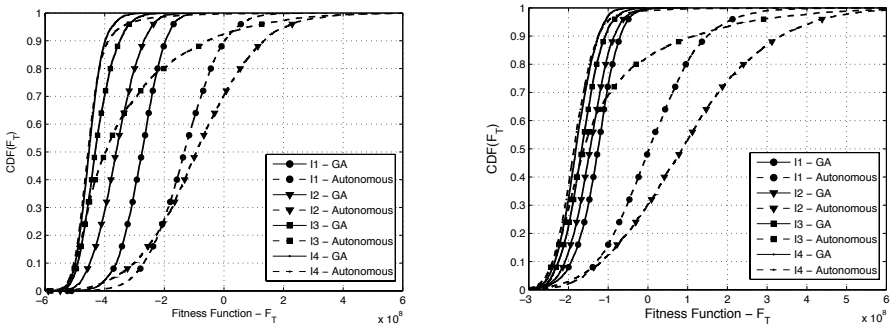

(A) *Case 1, Medium User Load* (B) *Case 2, High User Load*

FIGURE 4.6: Genetic algorithm: CDF of the fitness function F_T

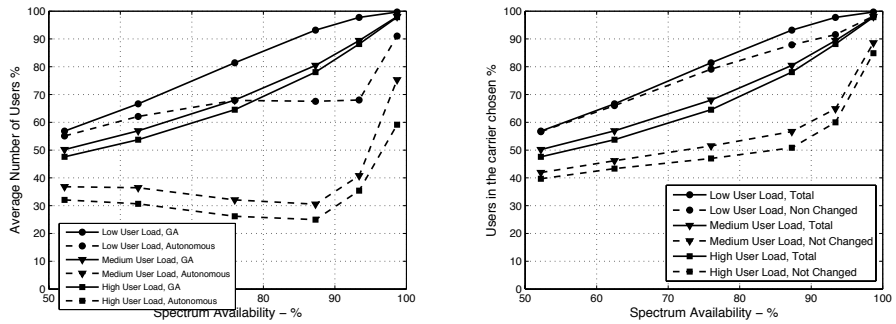

(A) *Proposed GA vs. Autonomous carrier selection allocation* (B) *Users not to be reallocated*

FIGURE 4.7: Genetic algorithm: users assessments

of the fitness function F_T in case of medium and high user loads, respectively. The figures compare the results obtained in case of the autonomous selection, with dashed lines, and after having performed the proposed algorithm, with solid lines, of the fitness function F_T. As a reminder, the autonomous selection foresees the assignment of the carriers based only on the user requests without any optimization, as performed by the GA based carrier allocation. Different markers highlight the results obtained in case of different environmental conditions, for which different percentages of spectrum occupancy, listed in Table 4.5, are considered. With respect to both the figures, we can state that the proposed algorithm achieves better, *i.e.*, with lower values of the fitness function. Moreover, in case of the non optimized assignment, F_T can assume positive values for highly interfered scenarios. This result, as confirmed in the following, shows that not all the users are able to achieve the desired rate according to the autonomous carrier selection, even if each ET has selected its best carrier. With respect to the total number of users, it can be further noticed that the fitness function is increasing for an increasing user load. In fact, the opportunity to serve all the users with the requested rate becomes more difficult in case of a higher number of total users, *i.e.*, higher user loads.

According to the results obtained for the fitness function, assessments on the average number of served users are carried out in Figure 4.7. In

TABLE 4.5: Genetic algorithm: spectrum occupancy reference parameters.

Parameter	Average number of FSs	Spectrum Occupancy
$I1$	38.7	47.8%
$I2$	15.5	24.0%
$I3$	3.8	6.6%
$I4$	0.8	1.3%

Figure 4.7a the percentage of the average number of users correctly allocated, *i.e.*, users having the minimum rate constraint satisfied, by the non optimized and the GA based scheduling are compared. On the other hand, Figure 4.7b shows the percentage of users that do not have to change the autonomously selected carrier performing the proposed genetic algorithm and compares it to the total number of users allocated. In both figures, the increasing number of users that can be allocated on average is depending on the spectrum availability of the scenario. In fact, users may have no carriers available for transmission in case of highly interfered scenarios, whereas all the users have at least one carrier in which they can be scheduled, reaching a 100% availability. In Figure 4.7a, solid lines represent the application of the GA, while dashed lines stand for the results obtained with the autonomous assignment. The difference between the two approaches is less noticeable in case of low user loads. In fact, both the spectrum occupancy and the total number of users influences how users are scheduled due to the limited number of resources. The effectiveness of the algorithm can be highlighted, since it always schedules correctly a higher number of users, especially in case of medium and high user loads, contrary to the carrier allocation based on the autonomous selection. For the sake of completeness, in Figure 4.7b the average number of users that have not to change the carrier, is assessed (dashed lines) and compared with the total (solid lines). Three different behaviors of the algorithm can be noted according to the spectrum availability in both the figures of Figure 4.7. First, in highly interfered scenarios a smaller number of users can be allocated and do not have to change the carrier from those chosen by the ETs, due to the limited number of available spectrum opportunities. Second, in partially interfered environments we have more recombinations due to a higher number of carriers in which users that not achieve the required rate can be reallocated, while, in case of more spectrum opportunities, users achieve the demanded rate without being reallocated.

Finally, we performed an analysis on the average number of iterations that the algorithm has to perform in order to schedule the users. In Figure 4.8, the average number of iterations is showed as a function of the spectrum availability and for different user loads, represented with different markers. The results show that the number of iterations is an increasing function of the total demand. Considering a fixed user load, it can be noticed that the algorithm in case of limited spectrum opportunities performs a limited number of iterations due to the impossibility in allocating highly interfered users, whereas, for scenarios with a high availability, a very low number of iterations achieves a good schedule of the users due to the high

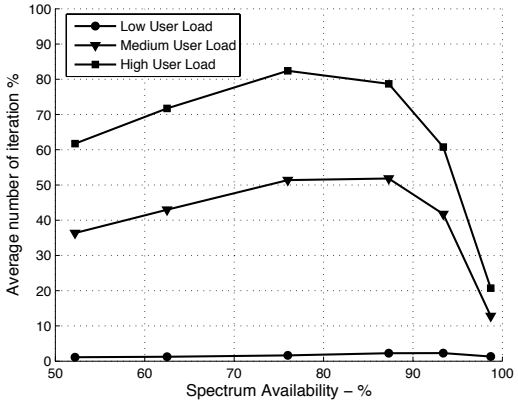

FIGURE 4.8: Genetic algorithm: average number of iterations

percentage of free spectrum. The highest number of iteration occurs in partial interfered scenarios where better performance can be achieved recombining the users in new carriers.

4.4 Exploitation in spectrum limited scenarios

The high flexibility typically incorporated in the considered mobile satellite payload (see section 2.3), which performs on-board beamforming and allocates users in orthogonal channels according to the available bandwidth and processing capability, can already offer several degrees of freedom. On the other side, L-band systems are mainly affected by an unbalanced service demand with respect to the wide coverage area of the system. In such scenarios, even the channelization of the available spectrum and a not fixed deployment of the channels with respect to a specific frequency reuse, which allow the system to add channels where needed, may not deal with the demanded rate.

In the following sections, we propose a new strategy to cope with the depicted issue in mobile satellite systems operating in L-band. These new solutions jointly exploit the flexible payload and precoding techniques, for which the feasibility has been already proved in Ka-band systems [11, 12, 13, 14, 15], in order to achieve a better use of the overall available resources and better performance. In particular, violating the principle of not reusing the same color among adjacent beams and exploiting partial or Full Frequency Reuse (FFR), the concept of beams becomes irrelevant and all the resources that previously were restricted to be assigned within the respective beam are now gathered and flexibly exploited in a specific area.

With particular interest to the hot spots scenario [100] (also described in 2.2), the proposed strategy foresees the definition of several zones within the hot spot area to whom channels are assigned according to the availability of the spectrum and a desired configuration. The configuration, in particular, defines how the channels are allocated among the zones and how precoding techniques are applied to reduce the interference introduced by the higher frequency reuse. The definition of different configurations aims at enabling an even more flexible use of the resources and achieving gain in terms of overall capacity in the selected scenario.

4.4.1 System Flexibility

The concept of beam and of frequency reuse have been introduced aiming at improving the isolation level, and thus reduce the co-channel interference, of multi beams satellite payloads. Each beam illuminates a specific geographic area and serves the users within it. In case of full frequency reuse, this one-to-one relationship between beams and users can be displaced. The generalization of the concept of beam implies that resources from the payload can be associated to any users irrespectively to their location. Avoiding the boundaries of the standard coverage of the beam, users are no more related to a specific beam. Thus, resources of the adjacent beams can be in principle allocated to users, especially those in the borders, that have limited resources from the respective beam. This approach can overcome the power and spectrum congestion problem, which affects particular areas in which the assigned beam has limited resources available with respect the demand. These areas, which are located in few beams with respect to the whole coverage since a not uniform distribution is present along the wide coverage of the satellite, are called HOT SPOTS. Although the system already achieves high levels of flexibility, the objective of this section is to identify if and in which scenarios, precoding can provide additional advantages in case of resource-limited scenarios.

In Figure 4.9, a basic resource-limited scenario is represented. In this scenario, six users are located within two beams, which, however, have only 2 available channels each (4 orthogonal channels in total). In the figures, the green area represents the standard coverage of the beam, whereas the yellow line the extended area that can be considered if the concept of beam is removed. The red and grey stars are the users served and those not, respectively. Of course, TDM (Time Division Multiplexing) can be considered in order to allow also the grey users to be served. However, the example here provided, shows the advantages of the different approaches regardless the time. In fact, precoding can provide gain due to the wider bandwidth exploited "in parallel". The reference configuration with one-to-one relationship between beams and users; the one with flexible exploitation of the resources from adjacent beams; and the one in which precoding is applied; are showed. In particular, in the first configuration, only two users in Beam 1 and one in Beam 2 can be served. In the second configuration, since some users of Beam 1 are at the border, the adjacent Beam 2, which has an available channel, can serve them. However, only one of them can exploit resources from Beam 2, which has only one channel still available. In the precoded configuration it is possible to precode two users together in the same channel (precoding can transmit the same channel from the two beams). Thus, three couples of users in three different channels are allocated also saving an additional channel. Considering the precoded flexible configuration, several configurations, which foresee the exploitation of mixed configurations of precoded and non precoded channels, can be also developed.

Starting from this simple example, different scenarios in which precoding can provide an additional gain, are considered. In particular, this example is based on the limited availability of channels. However, the system can be limited either in terms of power or available spectrum. With particular focus on power and spectrum limited scenarios, the objective of the

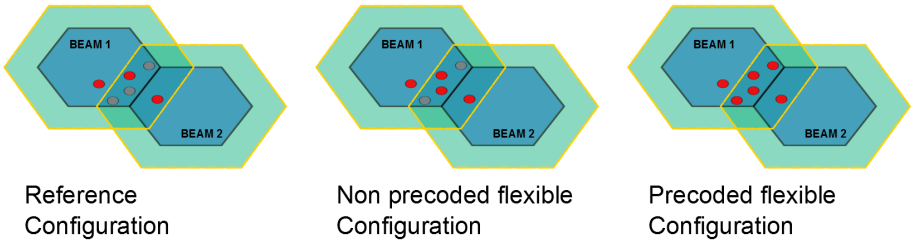

FIGURE 4.9: Spectrum limited scenario: example of sistem flexibility application

next section is to evaluate the gain provided by precoding configurations in areas, i.e., clusters with a limited number of beams, with limited resources availability. In case of high demand over an area covered approximately to only one beam, which, however, does not have sufficient resources, the six adjacent beams can be exploited as already showed in the example. The considered cluster of 7 beams will be the reference scenario in which the different configurations are assessed. With HOT SPOT we refer to the central beam, i.e., the beam, which has higher demand with respect to the other beams and for which the adjacent beams provide additional resources.

In the considered hot spot scenario[3], the *reference configuration* (refer to 2.3.2) achieves the best performance assuming only the central beam active while the others are switched off. According to the proposed configuration, the assignment of all the available channels in the central beam guarantees that all the UTs are served by the actual beam that illuminates the users' location. In this configuration the frequency reuse factor is maintained since the 6 adjacent beams are off. Assuming an orthogonal available bandwidth B_w^{ort}, this can be divided in N_{ch}^{ort} orthogonal channels with bandwidth B_w equal to 200 KHz each. On the other side, the processor capability on the payload limits the total number of channels N_{ch} that can be processed and assigned in the hot spot. When $N_{ch}^{ort} < N_{ch}$, the maximum number of channels that can be assigned by the system in the hot spot is equal to N_{ch}^{ort}.

This limitation, however, can be overcome with a higher frequency reuse and the application of precoding techniques enabling the other beams to illuminate the hot spot and exploiting spatial diversity. Toward this, new configurations are here proposed. Allowing the adjacent beams to provide resources advantageously to the demands of the hot spot, each user is illuminated by all the beams, in theory. Thus, the concept of beam, which was limiting the resource allocation is now removed. In contrast, their allocation based on the demands of specific areas is taken into account. The selected area, in particular, can be separated in different zones. The strategy proposed for the considered scenario, is to divide the hot spot, *i.e*, the central beam, in 7 zones. This approach takes into account the definition of an outer R and of an inner r radius. In particular, the former is fixed to be the radius that limits the standard 3 dB coverage of the beam, whereas the latter can be varied. In Figure 2.10b, a graphical representation of how the zones are selected is provided. The different colors and the indexes represent the zones. Specifically, the central zone, *i.e.*, zone 4, is defined as the area for which the module of channel coefficient from the central beam of

[3]where it is assumed that all the active users of the hot spot are limited within the central beam coverage,

the cluster is equal or higher than a value a-priori fixed h_r. Consequently, the external zones are the areas limited between r, which is function of the selected h_r, and R. Thus, the module of the channel coefficient from the central beam is lower than h_r in the external zones. The choice of selecting the zones with respect to the channel coefficients can take place at the GW after each user has fed back the channel coefficients. According to the definition of zones based on h_r, the higher the value of h_r the wider the inner area will be.

Having replaced the notion of beams in the *reference configuration* with zones in the *flexible configuration*, we can assign the same orthogonal channel to more users within the hot spot assuming that these users are in different zones since associated to different beams. The same channel can be reused k times, up to 7 as the number of beams that contribute to illuminate the hot spot. To cope with the increased level of co-channel interference suffered by the users, interference management techniques can be exploited. In particular, linear precoding techniques are here applied on a per channel basis. With this strategy that avoids the constraints posed by the *reference configuration*, the number of channels that can be assigned to the central beam, which now is illuminated by all the beams of the selected cluster, is no more limited by N_{ch}^{ort} but N_{ch}. The additional gain is foreseen due to the flexible allocation of a wider bandwidth. Thus, new configurations can be defined with the following approach: i) define h_r and the zones within the hot spot; ii) assign to the zones the N_{ch} available channels according a specific criterion; iii) exploit precoding in case the same channel is used in multiple zones.

4.4.2 Mathematical Formulation

The system performance needs to be analyzed according to the new defined configurations. The total system capacity depends on several parameters and can achieve different points within the capacity region [100]. From a theoretical point of view, each channel can be considered separately. Thus, the capacity of each link is computed taking into account the maximum achievable rate at the receiver. However, the rates of the users are strictly affected by the *access scheme* of the assigned channel. With *access scheme* we refer to channels that can be either orthogonal or reused in several zones and precoded. Different rates, which are represented with C_{ort} and C_{pr} respectively, are achieved because of the different interference environment.

Thus, the configuration and the *access scheme* of each channel affect the achievable sum rate capacity C_{tot}. According to a general formulation, we define for the proposed configuration a number y of channels that are orthogonal and can not be reused, and a number x of orthogonal channels that are reused k times. C_{tot} is then calculated by considering the aggregation of each user capacity. The sum, which takes into account both orthogonal and precoded channels, is expressed as:

$$C_{tot} = \sum_{i}^{kx} C_{pr,i} + \sum_{i}^{y} C_{ort,i} \tag{4.27}$$

Considering the Shannon formula, the achievable rate of the i-th user in case of orthogonal or precoded channels, respectively $C_{ort,i}$ and $C_{pr,i}$, is

defined as:

$$C_{ort,i} = B_w \log_2(1 + |h_{ij}|^2 P_i) \tag{4.28}$$

$$C_{pr,i} = B_w \log_2 \left(1 + \frac{|\mathbf{h_i u_i}|^2 P_i}{1 + \sum_{j \neq i}^{k} |\mathbf{h_i u_j}|^2 P_j} \right) \tag{4.29}$$

where B_w is the channel bandwidth, h_{ij} the channel coefficient from the j-th beam to the i-th user, P_i the power allocated to the user, $\mathbf{h_i}$ and $\mathbf{u_i}$ the channel coefficients and precoding weights vectors of the i-th user, respectively. In the proposed formulation, the noise power is assumed normalized. It is assumed that no or negligible co-channel interference from the beams outside the considered cluster occurs and, thus, for the users allocated in the orthogonal channels no co-channel interference occurs.

In addition, the sum rate C_{tot} is strictly related to the number of channels. These are subject to a limited spectrum availability and at the same time to a limited process capability. Respectively, we obtain

$$x + y \leq N_{ch}^{ort} \tag{4.30}$$

$$kx + y \leq N_{ch} \tag{4.31}$$

where (4.30), assumes a maximum bandwidth B_w^{ort} and consequently a maximum number of orthogonal channels N_{ch}^{ort} due to the channel granularity of $200\ KHz$, whereas (4.31) restricts the total number of channels to be no more than N_{ch}.

The power allocated to each user is considered equal for all of them. Thus, the power per channel per beam allocated to each user, with respect to the total power P, is proportional to the number of active channels:

$$P_i[dB] = P[dB] - 10 \log_{10}(kx + y) \tag{4.32}$$

Thanks to the proposed formulation, for each configuration the achievable sum rate, which depends on $k, x,$ and y and the access scheme of each user, can be calculated. Finding the optimum configuration based on the definition of an objective function as the sum rate maximization, however, is not a trivial task. In fact, due to the several constraints and dependency, the problem is a Mixed-Integer Non Linear Programming (MINLP) optimization problem [101], which are known to be NP-hard problems that involve both continuous and integer variables and both linear and non linear functions. Moreover, finding the optimal solution with respect to all the parameters that are involved is out of scope. In fact, the analysis aims at giving the general formulation of the achievable rates in accordance with the proposed scheme strategies, and a possible framework to define new configurations with respect to $k, x,$ and y for a better exploitation of the available resources of the system with respect to the hot spot scenario.

In the following, we propose a more pragmatic approach to the problem. Assuming uniform user distribution within the hot spot, $k, x,$ and y can be fixed in order to have a uniform number of channels with respect to the area of the zone. In fact, selecting the inner radius r such as the 7 zones have approximately an equal area, the same number of channels per zone should be considered. Driven by this general assumption, specific configurations are derived and investigated fixing $k, x,$ and y with respect to N_{ch}^{ort}

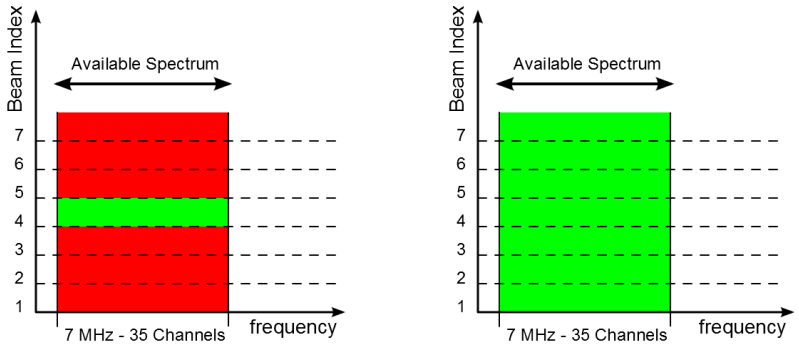

(A) *Reference configuration* (B) *FFR configuration*

FIGURE 4.10: Spectrum limited scenario: 7 MHz Scenario - configurations

and N_{ch}. Thus, without considering a global optimization of the configuration with respect to all the variables but under general and reasonable assumptions, adequate configurations can be identified. In the following, these configurations are presented and assessed with respect to the considered scenarios.

4.4.3 Proposed configurations and numerical Results

The analysis is carried out with respect two different scenarios in terms of spectrum availability and for different power constraints. For both scenarios, different configurations are proposed and assessed. The same cluster of 7 adjacent beams selected within the whole coverage is taken into account. For sake of simplicity, any additional interfering contribution from the external beams and payload non linear distortions contribution have been set equal to 17 dB. The main parameters used for the assessment and link budget calculation are also resumed in Table 4.6.

The assessment of the proposed configurations includes the evaluation of the average total capacity C_{tot} of equation (4.1). The users are selected randomly within the different zones and associated to the channels. Their capacities are subsequently computed according to equations (4.28) and (4.29) and the access scheme considered for each zone. The total power P and the parameters $k, x,$ and y are derived after having defined the specific configuration in relation to the scenario assessed. Linear unicast UpConst MMSE (Minimum Mean Square Error) precoding [14] is taken into account in case of channels that are reused among the zones.

7 MHz scenario

The first scenario considers an available bandwidth of 7 MHz, which is the maximum allocated spectrum portion in some regions. In this scenario and according the *reference configuration*, the best performance are achieved allocating all the orthogonal channels, which are 35, in the central beam. The orthogonal channels can be assigned to any user within the coverage of the hot spot. In case of precoded beams, the other beams are reused up to a frequency reuse of 1. In case of FFR, to each beam are assigned 35 channels

TABLE 4.6: Spectrum limited scenario: simulation parameters.

Parameter	Value
Frequency f_0	1.6 GHz
Channel Bandwidth B_w	200 KHz
Maximum EIRP per spot beam	67 [dBW]
Additional link budget interference contribution	17 [dBW]
Antenna gain to noise temperature G_{rx}/T	-13.5 [dB]
Free Space Loss L_{FLS}	$\left(\frac{4\pi d f_0}{c}\right)^2$
Channel coefficient h_{ij}	$\sqrt{\frac{G_{ij}^{tx}}{L_{FSL} k B_w} \frac{G_{rx}}{T}}$

TABLE 4.7: Spectrum limited scenario: configuration parameters resume in the 7 MHz scenario

Parameter	Reference	FFR
k	0	7
x	0	35
y	35	0

resulting in 245 total channels. In particular, 7 users from the 7 different zones, which are derived selecting a desired h_r, are precoded together in the same channel over the beams of the cluster. The two assessed configurations are called *reference* and *FFR* and are represented in Figure 4.10a and 4.10b, respectively. In the figure, the allocated channels and the respective beams are represented in green. The parameters that characterize the configurations, are also reported in Table 4.7.

For the 7 MHz scenario, we assess the performance in terms of total average capacity of the hot spot for different values of power and as a function of the dimension of the zones. In Figure 4.11, the total capacity is showed as a function of the inner radius r normalized with respect to the radius of the standard coverage R. The blue solid lines represent the *reference configuration*, for which different markers are used for the different values of total EIRP. Since a fair comparison in terms of equal power for both the configuration has to be guaranteed scaling the power per channel accordingly, two different values of total EIRP are considered. The *FFR configuration* is represented with dashed and solid lines in the case of without and with the application of precoding, respectively. Markers and colors represent different EIRPs.

The results show that the zone selection slightly affects the performance of the FFR configuration. On the other hand, it does not affect the *reference configuration* for which, the users are always selected within the whole coverage of the central beam. The increased capacity in case of a higher central zone is due to the fact that precoded users are selected from zone which are far from each other and closer to the adjacent beam that serves that specific zone. However, it has to be noted that, reducing the external zones, a lower number of users to be served is present if a uniform distribution is considered. This results in a higher user throughput unbalance between the users in the external and the central zones. As expected, an increasing power provides higher capacities in case of FFR with a proportional higher gain with respect to the *reference configuration*.

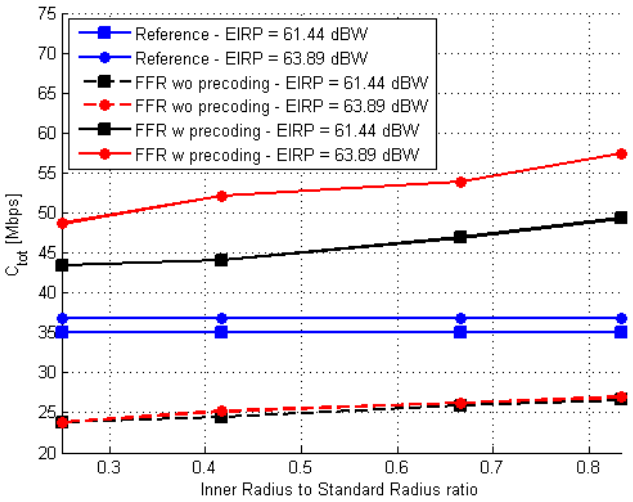

FIGURE 4.11: Spectrum limited scenario: total capacity as function of r/R in the 7 MHz scenario.

41 MHz scenario

In this second scenario, we assume that the available spectrum is equal to 41 MHz, which is the maximum available from a regulatory point of view. Since we had assumed that the payload does not have any data processing constraint, all the available spectrum can be assigned to the central beam resulting in 205 orthogonal channels. As for the previous scenario, this configuration is considered the reference one. Considering FFR, the six adjacent beams can be reused. However, due to the limitation of 630 maximum channels that can be processed by the payload, only 90 orthogonal channels can be exploited. In this configuration, only 18 MHz are occupied with respect to the 41 MHz available. These two configurations are represented in Figure 4.12. In a further scenario (Figure 4.13), in order to occupy all the available spectrum and exploit all the N_{ch} channels, we assign orthogonal channels in the central zone whereas we exploit a two color reuse among the six external zones, resulting in three co-channel zones. In this configuration, precoding can be applied to the co-channel zones in order to avoid interference, which can be present due to the lower frequency reuse.

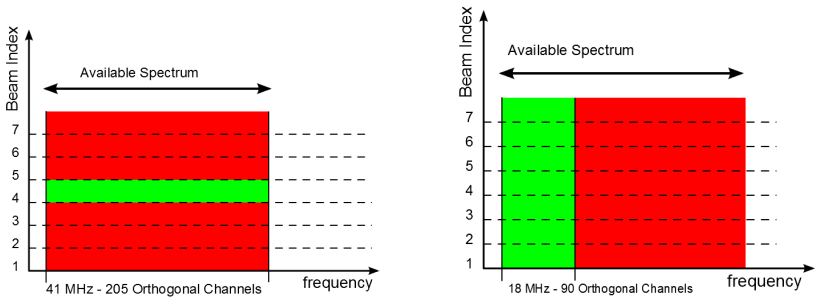

(A) *Reference configuration* (B) *FFR configuration*

FIGURE 4.12: Spectrum limited scenario: 41 MHz Scenario - configurations

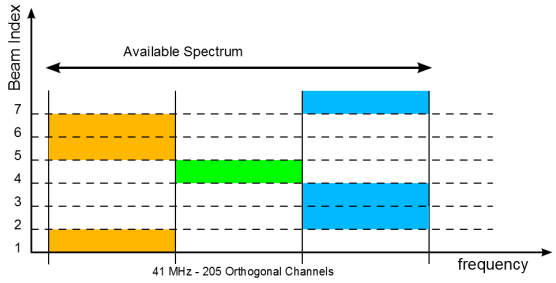

FIGURE 4.13: Spectrum limited scenario: 41 MHz Scenario - Mixort configuration

In Figure 4.13, the proposed configuration is depicted where different colors represent the co-channel zones. The beam indexes refer to Figure 2.10b and the coloring is chosen to maintain symmetry. In this first analysis, which assumes uniform distribution of the users within the hot spot, we divide the hot spot in zones with equal area and, consequently, we assign an equal number of channels to them. In Table 4.8 the parameters of the three proposed configurations are also reported. We compare the total capacity achieved by the proposed configurations for different powers and a fixed radius of the central zone, which is chosen to have equal areas of the zones. The results are showed in Figure 4.14.

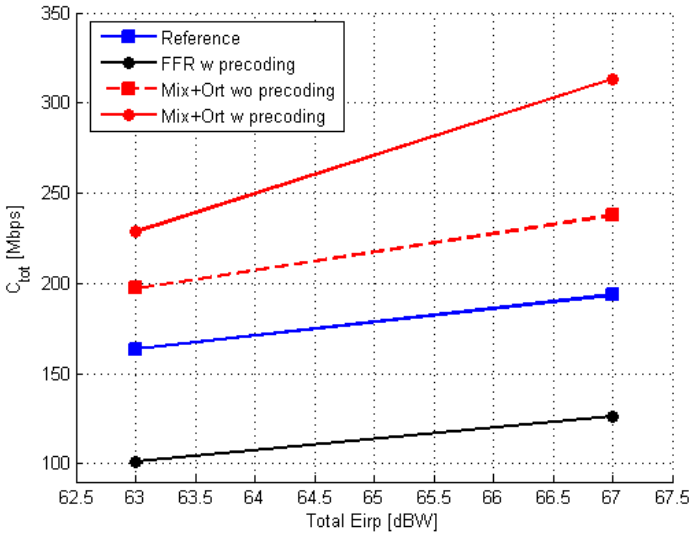

FIGURE 4.14: Spectrum limited scenario: total capacity as function of total EIRP in the 41 MHz scenario.

TABLE 4.8: Spectrum limited scenario: configuration parameters resume in the 41MHz scenario

Parameter	Reference	FFR	MixOrt w/o precoding	MixOrt w precoding
k	0	7	3	3
x	0	90	136	136
y	205	0	68	68

TABLE 4.9: Spectrum limited scenario: gain with respect to the reference configuration

Total EIRP [dBW]	FFR	MixOrt w/o precoding	MixOrt w precoding
63.89 dBW	-37.98%	20.61%	39.81%
67 dBW	-34.64%	22.96%	62.10%

The results show that the FFR configuration does not provide gain with respect to the *reference configuration*. This is mainly due to the limitation in the occupied spectrum, which is reduced from 41 MHz to 18 MHz. In this scenario, in fact, the FFR is not fully exploited and the precoded configuration does not provide a similar gain as in the 7 MHz scenario. On the contrary, the proposed configuration, which exploits both all the available spectrum and a higher frequency reuse, achieves good results. Both when precoding is used or not, the total capacity is higher than the capacity achieved by the *reference configuration*. The gain with respect to the *reference configuration* in percentage is presented in Table 4.9.

4.4.4 Specific User Analysis

In this section results with respect to specific users and their performance are presented. The analysis includes the evaluation of all the configurations considered for the 41 MHz. The central cluster with a fixed radius of the central zone for which the r/R ratio equals 0.34 is considered. Total EIRP is fixed in order to have 15 dB of SNR in the center of the beam.

Simulations have been performed in order to assess the performance of a single user. This specific user is a priori selected according its location (the grid points). In case of precoded channels, the other users are selected randomly in the other zones according to the configuration under assessment. Then, the average SINR, SNR, CIR, and capacity of the specific user are assessed. In each simulation, the specific user is selected according a fixed trajectory. As an example, having fixed the longitude and varying the latitude or vice versa. In Figure 4.15, the grid points that have been evaluated are showed. The grid points belong to the central beam coverage of the central cluster and the different colors represent the 7 zones.

The following figures show the results obtained for the different configurations as a function of the distance from the center of the selected beam. The x axis approximately represents the distance between the center of the beam and the points that are assessed. Each grid point is 0.5 degree both in latitude and longitude. However, the distance in Km of two points that differ in longitude from the same angle in degrees depends on the latitude, in case of the latitude it is possible to state the 0.5 degrees are approximately 50 Km regardless the longitude considered. Thus, the analysis here proposed, takes into account grid points for a fixed longitude and varying latitude.

In Figure 4.16, Figure 4.17, Figure 4.18, and Figure 4.19 are showed the figure of merits of the Reference, the FFR in the hot spot, the FFR in the standard coverage, and the MixOrt configurations, respectively. Per each configuration, the SINR (top left), the capacity (top right), the SNR (bottom left), and the CIR (bottom right) are represented. The non precoded and precoded values are both represented for the configurations that foresee precoded channels in black and red solid lines, respectively. The obtained

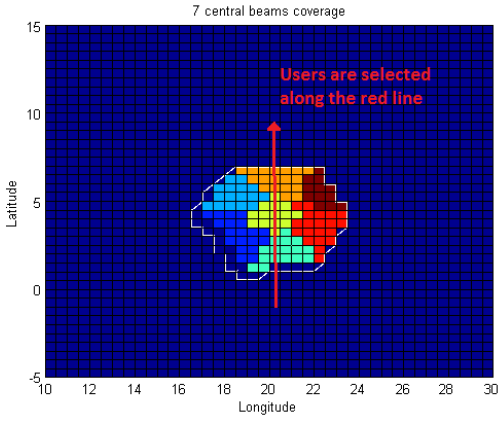

FIGURE 4.15: Hot Spot scenario: selected user analysis. Grid points from which the users are selected.

results confirm those concerning the total capacity of the previous sections. However, it has to be noted that applying precoding can provide for the hot spot worst results than the non precoded scenario. In particular, users in the central zone achieve worst SINR in both the FFR and Mix configurations. This results can be due to the ill conditioned channel matrix from which the precoding matrix is calculated. The ill conditioned channel matrix is due to the considered beam pattern, which can affect the performance of precoding.

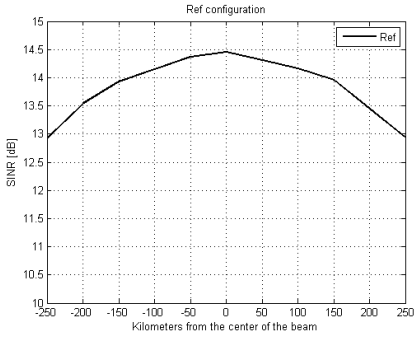

(A) *SNIR*

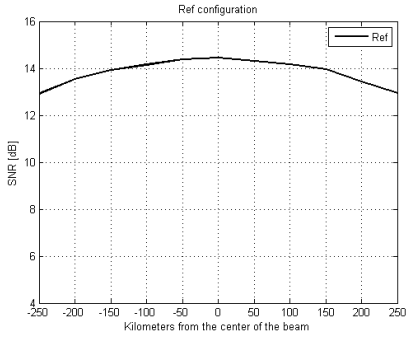

(B) *SNR*

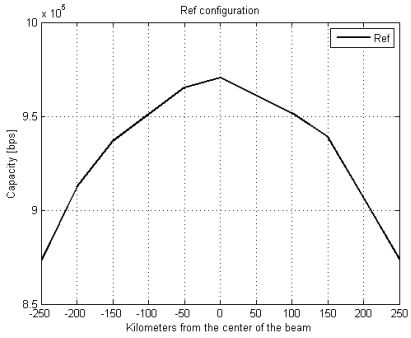

(C) *Capacity*

FIGURE 4.16: Spectrum limited scenario: reference configuration

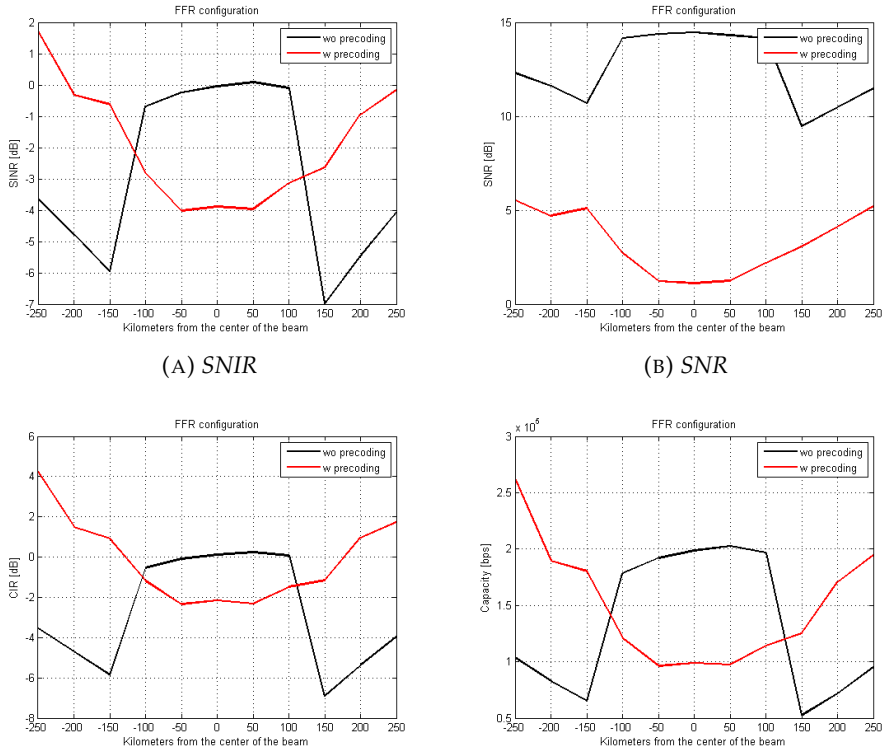

(A) *SNIR* (B) *SNR*

(C) *CIR* (D) *Capacity*

FIGURE 4.17: Spectrum limited scenario: FFR hot spot configuration

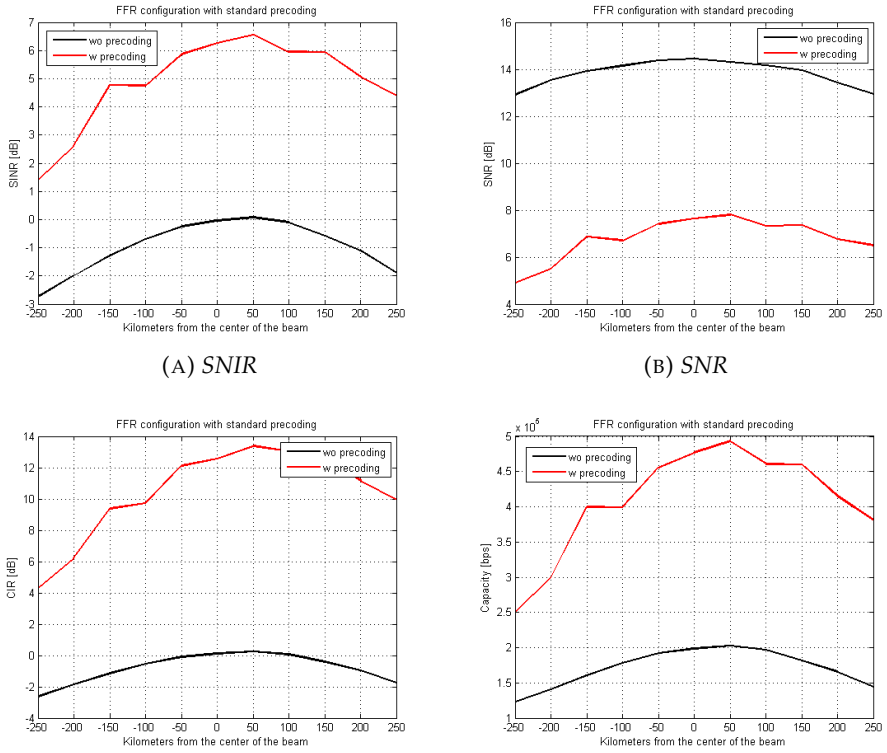

(A) *SNIR* (B) *SNR*

(C) *CIR* (D) *Capacity*

FIGURE 4.18: Spectrum limited scenario: FFR standard configuration

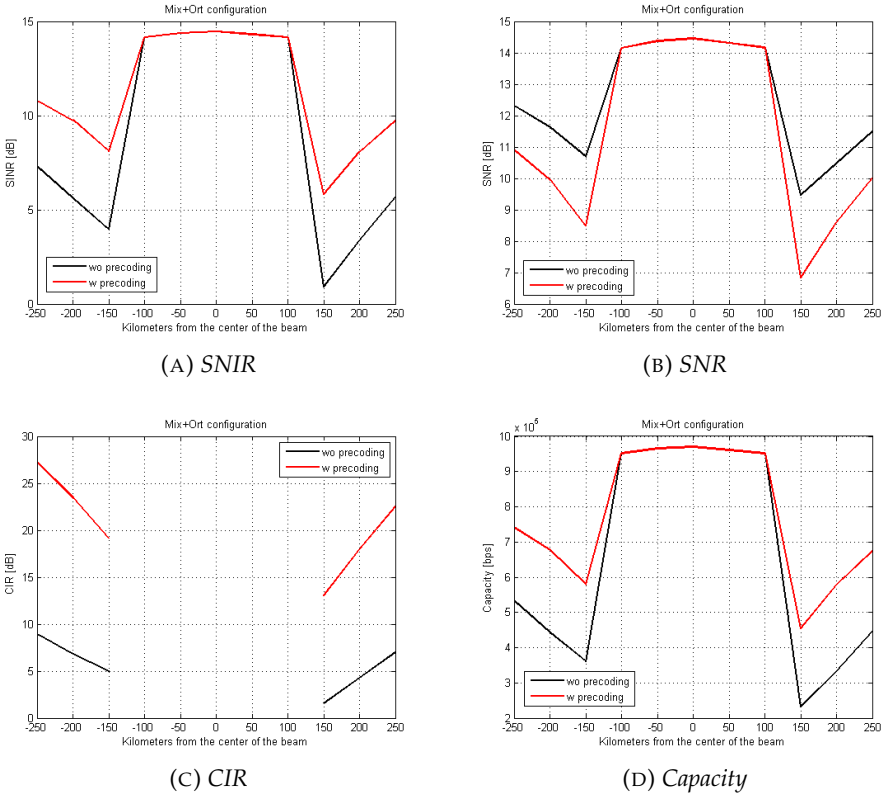

(A) *SNIR* (B) *SNR*

(C) *CIR* (D) *Capacity*

FIGURE 4.19: Spectrum limited scenario: Mixort configuration

4.4.5 Spectral Efficiency Analysis

Regardless the scenario in which performance of precoding techniques are evaluated, an effective metric to assess the gain they provide, is the spectral efficiency. Considering the Shannon capacity formula, the spectral efficiency achieved by each user is calculated as

$$\eta = log_2(1 + SINR) \tag{4.33}$$

and it is expressed in $[bit/s/Hz]$. On the other side, the total spectral efficiency of the system is equivalent to the ratio between the total capacity and the user bandwidth and represents the average spectral efficiency of the system. Thus, by means of the spectral efficiency metric would be possible to compare the different configurations regardless the effective bandwidth utilization. Moreover, the spectral efficiency is only dependent on the SINR of the users. Thus, it also provides an indication on how precoding performs.

In Table 4.10, the average spectral efficiencies achieved by the different configurations in the 41 MHz scenario are reported. The two different total EIRPs considered for the numerical analysis are both included. The configurations proposed for the 7 MHz scenario achieve similar results if same total power is considered. This confirms that the same configuration, *e.g.*, the FFR configuration in the hot spot scenario, will provide the same spectrum efficiency regardless the spectrum utilization. As can be noted, the spectral efficiency in case of the FFR configuration is higher than the reference configuration. This demonstrates that the FFR exploits better the available

bandwidth and that the lower total capacity is due to the limited spectrum exploited (18 MHz against 41 MHz for the FFR and reference configuration, respectively). In addition, the results show how the user selection impacts the performance of precoding techniques. In fact, the spectral efficiency of the FFR in the hot spot and in the standard configuration differ.

TABLE 4.10: Spectrum limited scenario: spectral efficiency η analysis

Configuration	**EIRP = 63.11 dBW**		**EIRP = 67 dBW**	
	w/o precoding	**w precoding**	**w/o precoding**	**w precoding**
Reference	3.99		4.72	
FFR Hot Spot	-	5.63	-	7.02
FFR Standard	7.9	11.57	8.9	15.7
Mix+Ort	4.83	5.6	5.8	7.65

4.4.6 Analysis on Precoding Bounds

In this section, the different performance of precoding techniques according to the considered scenarios are discussed. It has been shown in the results of Table 4.10 that, on average, different gains are obtained in case of different scenarios even with the same configuration, *e.g.*, the FFR configuration with standard selection of the users from the beams versus the selection from the zones of the hot spot scenario.

The application of precoding techniques, as shown in the following, is mainly affected by the channel matrix, *i.e.*, the channel signatures of the users that are selected and precoded together. In this context, users are selected randomly within the area of interest. Some criteria for user selection should be considered. However, they are usually referred to the scheduling part of the system and, thus, they will not considered in the following.

Considering the general formulation of the SINR of the i-th user

$$SINR_i = \frac{P_i |\mathbf{h_i u_i}|^2}{1 + \sum_{j \neq i} P_j |\mathbf{h_i u_j}|^2} \tag{4.34}$$

where P_i is the power allocated, $\mathbf{h_i}$ the vector of the channel signatures, and $\mathbf{u_i}$ the vector of precoding weights of the i-th user. We assume that the columns of the precoding matrix have unitary norm. Thus, the total power constraint $\sum_{i=1}^{N} P_i = P_{tot}$ is satisfied.

By definition, we can reformulate the SNR as

$$|\mathbf{h_i u_i}|^2 = ||\mathbf{h_i}||^2 ||\mathbf{u_i}||^2 |\cos(\theta(\mathbf{h_i}, \mathbf{u_i}))|^2 \tag{4.35}$$

where $||\cdot||$ is the 2-norm operator and $\theta(\mathbf{h_i}, \mathbf{u_i})$ is the angle between the two vectors and the absolute value of its cosine assumes values between 0 if orthogonal and 1 if the vectors are parallel. Taking into account this last

formulation, the i-th user SINR can also be reformulated as

$$SINR_i = \frac{P_i |\mathbf{h_i u_i}|^2}{1 + \sum_{j \neq i} P_j |\mathbf{h_i u_j}|^2} = \tag{4.36}$$

$$= \frac{P_i \left(||\mathbf{h_i}|| ||\mathbf{u_i}|| |\cos(\theta(\mathbf{h_i}, \mathbf{u_i}))| \right)^2}{1 + \sum_{j \neq i} P_j \left(||\mathbf{h_i}|| ||\mathbf{u_i}|| |\cos(\theta(\mathbf{h_i}, \mathbf{u_j}))| \right)^2} = \tag{4.37}$$

$$= \frac{P_i ||\mathbf{h_i}||^2 |\cos(\theta(\mathbf{h_i}, \mathbf{u_i}))|^2}{1 + \sum_{j \neq i} P_j ||\mathbf{h_i}||^2 |\cos(\theta(\mathbf{h_i}, \mathbf{u_j}))|^2} \tag{4.38}$$

where the norm of the precoding matrix columns have been simplified. From the latter formulation, $|\cos(\theta(\mathbf{h_i}, \mathbf{u_i}))|$ and $|\cos(\theta(\mathbf{h_i}, \mathbf{u_j}))|$ can be interpreted as the SNR reduction and the amount of interference that has not been cancelled out by the application of precoding, respectively.

As a consequence, in order to evaluate the performance of precoding is necessary to define a metric able to describe either the reduction of the SNR and the interfering contribution, which has not been cancelled out with respect to the selected channel matrix and the precoding matrix derived.

In the numerical assessments, the considered technique [14] assigns to each user equal power, $P_i = P$, and applies constraints on the maximum level of EIRP per channel per beam. For sake of simplicity, the same assumptions are made in the following. According to the previous assumption, the SINR of the i-th user simplifies in

$$SINR_i = \frac{||\mathbf{h_i}||^2 |\cos(\theta(\mathbf{h_i}, \mathbf{u_i}))|^2}{1 + \sum_{j \neq i} ||\mathbf{h_i}||^2 |\cos(\theta(\mathbf{h_i}, \mathbf{u_j}))|^2} \tag{4.39}$$

$$= \frac{|\cos(\theta(\mathbf{h_i}, \mathbf{u_i}))|^2}{\frac{1}{||\mathbf{h_i}||^2} + \sum_{j \neq i} |\cos(\theta(\mathbf{h_i}, \mathbf{u_j}))|^2} \tag{4.40}$$

Taking into account the SNR, $|\mathbf{h_i u_i}|^2$, the maximum achievable SNR is achieved if and only if the cosine is one. Thus, $\mathbf{u_i}$ and $\mathbf{h_i}$ need to be linearly dependent, *i.e.*, one of the vector's magnitudes is zero or one is a scalar multiple of the other. Thus, this translates into

$$\mathbf{u_i} = \frac{\mathbf{h_i}^*}{||\mathbf{h_i}||} \tag{4.41}$$

which means that the rows of the precoding matrix $\mathbf{U}$ are the transpose conjugate of the normalized rows of $\mathbf{H}$.

On the contrary, in order to have null interference, *i.e.*, $\sum_{j \neq i} |\mathbf{h_i u_j}|^2 = 0$, all the elements $|\mathbf{h_i u_j}|^2$ need to be 0 since sum of positive elements or, equivalently, the cosine of their angles $\theta(\mathbf{h_i}, \mathbf{u_j})$ $\forall j \neq i$ to be $90^{\cdot}$.

$$\sum_{j \neq i} |\mathbf{h_i u_j}|^2 = 0 \; \forall j \neq i \tag{4.42}$$

Thus, $|\mathbf{h_i u_j}|^2 = 0$ if and only if the two vectors are orthogonal. Considering $\mathbf{h_i} \perp \mathbf{u_j}$ $\forall j \neq i$ implies that $\mathbf{U}$ is calculated as the inverse or (pseudo-inverse in case of rectangular matrices) of the channel matrix

$$\mathbf{U} = \mathbf{H}^{\dagger} = \left(\mathbf{H}^* \mathbf{H}\right)^{-1} \mathbf{H}^* \tag{4.43}$$

and its columns are normalized such as

$$\mathbf{u_i} = \frac{\mathbf{u_i}}{||\mathbf{u_i}||} \tag{4.44}$$

The considered approach is exactly Zero-Forcing (ZF) precoding.

Both maximum SNR and null interference are, therefore, achieved if the matrix $\mathbf{H}$ is unitary, i.e., $\mathbf{H}\mathbf{H}^* = \mathbf{H}^*\mathbf{H} = \mathbf{I}$. This translates into $\mathbf{H}^* = \mathbf{H}^{-1}$ and both maximum SNR and null interference are achieved. On the contrary, for matrices non unitary and closer to singularity either a reduction of the SNR and an increment of the interference are foreseen taking into account the two approaches described.

The condition number of a matrix $\mathbf{A}$ could be a good metric for measuring the level of singularity of a matrix. In fact, a unitary matrix has all the eigenvalues on the unitary circle, thus, with module equal to 1, while are increasing when approaching singular matrices. From its definition, the condition number of the matrix equals to

$$\kappa(\mathbf{A}) = ||\mathbf{A}||_p||\mathbf{A}^{-1}||_p \tag{4.45}$$

where $||\cdot||_p$ is the p-th norm of the matrix $\mathbf{A}$.

Contrary to Single User MIMO (SU-MIMO) in which a relationship between condition number of the channel matrix and the user capacity has been established [102], for the Multi User MIMO (MU-MIMO) scenario, the capacity formula is not straightforward. Thus, some heuristic metrics that could provide a qualitative indication of the performance of precoding should be defined. As noted, precoding techniques achieve higher performance in case of unitary channel matrices that consequently translate into linearly independent channel signatures, *i.e.*, the rows of the channel matrix. Defining as metric the Frobenius-norm of $\mathbf{H}\mathbf{H}^*$, it would be possible to highlight the dependency of the performance of the selected precoding technique from the singularity of the matrix. The Frobenius-norm $||\cdot||_F$ of the square matrix $\mathbf{A}_N$ is defined as the sum of the power two of the absolute value of the elements of $\mathbf{A}$.

$$||\mathbf{A}||_F = \sqrt{\sum_{j=1}^{N}\sum_{j=1}^{N}|a_{ij}|^2} = \sqrt{\text{Trace}\,(\mathbf{A}^*\mathbf{A})} \tag{4.46}$$

Thus, the Frobenius-norm would be equal to the N in case of unitary matrices, whereas it would be higher in case of non unitary matrices since the elements over the diagonal of the matrix $\mathbf{H}\mathbf{H}^*$ will be one, while the off-diagonal will be always positive non zero elements. The defined metric has low complexity and depends only on the channel matrix.

In Figure 4.20, the spectral efficiencies achieved by selecting random sets of users in the standard scenario and in the hot spot scenario, are compared. The red and the blue points represent 1000 different sets of users randomly selected from the respective beams and the zones of the hot spot scenario, respectively. In order to fairly compare the two scenarios, a total EIRP equal to 63.89 dBW for the FFR configuration in the 41 MHz scenario is considered for both. The power constraint per channel per beam is considered as well. The analysis provides only a qualitative example on how

the spectral efficiency is affected by the channel matrix since there is no simple relationship between the matrix and the spectral efficiency. However, although the variability of the results for a given norm, the selected metric on the Frobenius-norm still gives a trend on how precoding techniques applied to the different scenarios perform.

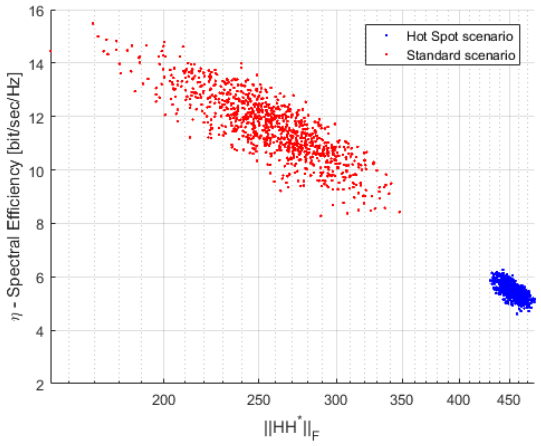

FIGURE 4.20: Spectral efficiency versus Frobenius norm of the channel matrix. Comparison between the standard application of precoding and its application in hot spots scenarios.

The same analysis on the spectral efficiency is also performed with respect to the additional metric $\kappa(\mathbf{H}^*\mathbf{P}\mathbf{H} + \mathbf{I})_F$. The metric is defined as

$$\kappa(\mathbf{H}^*\mathbf{P}\mathbf{H} + \mathbf{I})_F = ||\mathbf{H}^*\mathbf{P}\mathbf{H} + \mathbf{I}||_F|| \left(\mathbf{H}^*\mathbf{P}\mathbf{H} + \mathbf{I}\right)^{-1} ||_F \tag{4.47}$$

The metric is based on the regularized version of the channel matrix that is involved in the MMSE precoding matrix $\mathbf{U}$ calculation. Even if the selected metric depends on the total available power and, thus, is dependent on the scenario, it has a more precise relationship with the spectral efficiency. In the analysis the same sets of users and parameters are selected in the simulation.

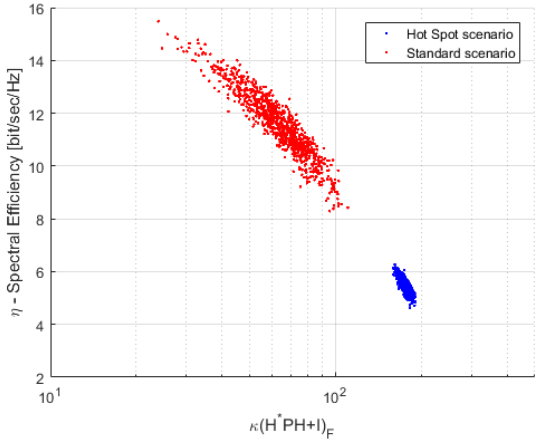

FIGURE 4.21: Spectral efficiency versus $\kappa(\mathbf{H}^*\mathbf{P}\mathbf{H} + \mathbf{I})_F$. Comparison between the standard application of precoding and its application in hot spots scenarios.

The results in 4.21 show similar trends as in the previous case. However, the proposed metric achieves less variability. The analysis confirms that a proper set of users to be precoded together is fundamental in order to achieve higher spectral efficiencies. For sake of completeness, the cumulative density function of the condition numbers evaluated in the simulation are plotted in Figure 4.22. With respect to the scenario, the cumulative function gives an indication in terms of percentage of the matrices that can achieve higher spectral efficiencies, *i.e.*, the lower the condition number the higher the spectral efficiency, when selected.

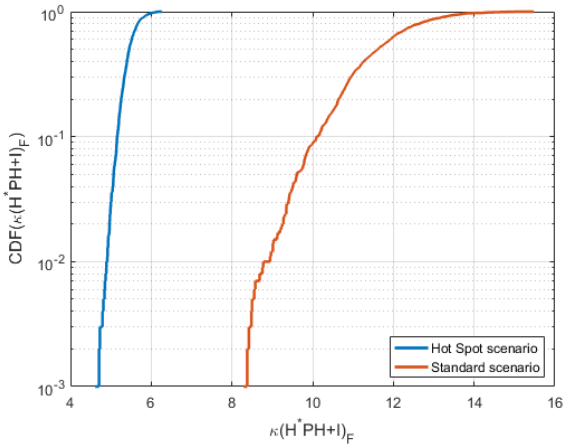

FIGURE 4.22: CDF of the condition number of the selected metric in the standard application of precoding and its application in hot spots scenarios.

4.5 Concluding Remarks

The chapter investigates techniques for an improved spectral efficiency according to the different scenarios presented in chapter 2. The proposed techniques are adapted and assessed to the scenarios aiming at improving system performance either in case of *shared* or *exclusive* spectrum. This improved spectrum efficiency is enabled by the knowledge of the environment in the form of experienced SINR at the user side and Channel State Information.

With particular focus on the cognitive-based SatCom scenarios 1 and 2, two different carrier allocation schemes are investigated. Numerical results are provided with respect to their application in scenario 2. First, a joint carrier and power allocation algorithm that aims at maximizing total system capacity and providing a fair allocation of the resources with respect to different QoS requirements from the users, is proposed. Results show that the algorithm outperforms a random assignment and in case of limited amount of available power also performs slightly better than the application of the only Hungarian algorithm, especially in case of a high number of users to be scheduled. The QoS constraints are also ensured, confirming that the algorithm can achieve a good fair allocation of the resources among all the active users. A genetic inspired algorithm that schedules users according their environment conditions and service demands, is also proposed. In this

case, the operations needed to perform the algorithm are assigned among the entities of the system. Awareness is therefore performed by the ETs, which have direct knowledge of the spectrum activities of the FSs, whereas the exploitation phase is in charge of the NCC, which has global knowledge of the system status. The proposed technique aims at reducing the number of information that the UTs have to feed back to the GW since most of them are redundant and can avoided. Results show that the proposed algorithm achieves good performance in terms of scheduled users and achieved rates without the need of feed back complete information on the status of the channels to the NCC.

The third scenario investigates higher spectrum efficiency configurations in *exclusive* bands for L-band systems. A higher frequency reuse and the application of interference mitigation techniques, *e.g*, linear precoding techniques, are investigated in spectrum limited scenarios. With particular interest in hot spots scenarios, the flexibility provided by the considered system and the application of precoding techniques, allow higher performance in terms of total capacity. A new framework from which *flexible configurations* that outperforms the *reference configuration*, is included. Analysis on selected users, and on the performance of precoding techniques with respect the different scenarios, are included as well.

Appendix A

State of the Art of cognitive-based SatCom

In the appendix is briefly resumed the state of the art of Cognitive Radio systems and its application in satellite scenarios. The topic of Cognitive Radio in a satellite communications is a topic of recent interest. In the appendix, the references and their main outcomes, from which the studies proposed in the thesis are based on, are included.

The different and specific characteristics of satellite systems have led the concepts and the techniques developed for terrestrial systems to be completely revised. Several new scenarios and new challenges to be addressed can be defined taking into account a cognitive satellite system. Challenges as the definition of proper bandwidths to be exploited, or adapt and propose techniques suitable for satellite systems are still under investigation. As an example, the low power level of the satellite signals even in Line of Sight (LoS), affects the adaptation of cognitive techniques in a SatCom environment, whose phases of the cognitive cycle need to be adapted properly. In particular, knowledge of the scenarios in which the cognitive system operates, is fundamental for this purpose.

One of the first papers that investigates application of cognitive radio in satellite communication systems is [103]. A first classification for the possible applications of cognitive satellite systems is provided. The proposed application scenarios include a) secondary use of satellite spectrum by a terrestrial system, b) secondary use of terrestrial spectrum by a satellite system, and c) a hybrid scenario where terrestrial network coverage is expanded by the use of satellite spots. Key challenges and enabling technologies for each scenario are discussed. Link budget analyses and assessments on the operational limits for interference management in the mentioned scenarios show that CR techniques should be applied with caution in satellite bands. However, potential to improve the spectrum efficiency is foreseen. In [104] the three main paradigm of cognitive radios are presented and addressed in SatCom. The *interweave* paradigm allows the secondary (unlicensed) users to occupy the portions of the spectrum left temporarily free by the primary (licensed) users. According to the *underlay* paradigm, the secondary transmitter overlaps in frequency with the primary user, after making sure that the interference level it causes is below a given threshold. The *overlay* paradigm uses the secondary user's knowledge of the primary users transmission scheme and of the channel to choose a transmission scheme that causes an acceptable amount of interference. In [105] different cognitive techniques such as underlay, overlay, interweave and database

related techniques are discussed by reviewing the current state of art. Interference modelling between terrestrial Base Station (BS) and satellite terminal is carried out on the basis of interference power level. Strong and weak links can be defined. Primary links should be always strong and from the level of interference that the secondary link generates against them, applicable techniques can be identified. As an example, underlay techniques are possible in case of weak secondary links, whereas interweave techniques if the primary and secondary links are similar. Furthermore, suitable cognitive techniques are proposed in high and low interference regions in the context of satellite cognitive communication. In [106], the authors study the main aspects of satellite cognitive communications and present possible practical scenarios for hybrid/dual cognitive satellite systems. Furthermore, suitable cognitive techniques for the considered scenarios are identified. Spectrum Sensing (SS), interference modelling, and beamforming techniques are discussed for hybrid cognitive scenario and SS, interference alignment, and cognitive beamhopping techniques are discussed for dual satellite systems. The paper includes interesting open research issues on the topic. The authors of [107] describe cognitive satellite terrestrial radios for hybrid satellite-terrestrial systems. The key issues are addressed and the concepts of developing CR based satellite ground terminals in the considered scenario are presented. The concept of tridimensional reuse of the spectrum is introduced. The importance of the additional bandwidth that could be exploited in case of shared spectrum scenarios, is addressed in [9], where are demonstrated the advantages of applying cognitive radio techniques in satellite communications (SatCom) in order to increase the spectrum opportunities for future generations of satellite networks without interfering with the operation of incumbent services.

With particular attention to the *awareness* techniques in SatCom scenarios, the sensing phase needs more reliable algorithms due to the lower power levels, the longer distances of the links, and the wider bandwidths. However, additional domains that enable spectrum holes to be exploited as the third angular dimension, are unique for the SatCom case of study. For the sensing phase the directivity of the antenna needs to be taken into account. This aspect can be either beneficial or detrimental since a directive antenna would be less interfered by other systems and the interference will be related to its direction of arrival. On the contrary, this also reduces the sensing capability of the terminal. With respect to the directivity of the antenna, in [105], a study on the interference between satellite and terrestrial links is carried out. Satellite uplinks in low elevation angles are demonstrated to interfere more terrestrial systems. In addition, satellite receivers at high latitudes are more interfered by terrestrial systems. Other sensing domains as polarization are investigated in [108, 109] as well. However, the long propagation time that characterises satellite communications also affects cognitive transmissions. Thus, sensing information on the presence of other systems can become easily obsolete. To counteract this issue, the cognitive systems can rely on database information [**tang2015** , 39, 40, 41]. Radio Enviroment Maps (REM) can be built in order to have a priori or statistical information on spectrum activities of other systems that will ease the operations during the sensing phase and even allow the exploitation phase. The combined used of databases

and spectrum sensing techniques can therefore provide both static and dynamic information on the spectrum and allow a more efficient use of it. The authors in [43] address the problem of accurate analyse interference from FS against satellite UTs. Real data bases and appropriate propagation models are used. Database statistics for several European Union (EU) countries were also evaluated and the importance of using accurate terrain profiles and accurate propagation models are discussed. The definition of Exclusion Zone is presented in [46]. Cognitive zones around incumbent users beyond which the cognitive terminals can utilize the same frequency band are considered. The study on the feasibility of the coexistance between the two systems is included. In [110], the impact of the propagation phenomena in a co-existence scenario of satellite uplink FSS and terrestrial FS systems operating in Ka-band are investigated. Specifically, the authors derive analytically the Signal-to-Interference Ratio (SIR) and the Signal-to-Noise plus Interference Ratio (SNIR) statistical distributions considering an accurate space-time dependent propagation channel model. Taking into account the propagation phenomena, interference statistical distribution is obtained for cognitive satellite communication systems operating above 10 GHz in [111]. The authors investigate a dual cognitive satellite systems, operating at Ku-band and above scenarios. The Signal-to-Interference Ratio statistical distribution under rainfall conditions and under the assumption that the link under consideration is available is analytically obtained and verified. The performance of both incumbent and cognitive users is examined. Spectrum Sensing (SS) techniques for a dual polarized fading channel are considered in [108]. Performance of Energy Detection (ED) technique is evaluated in the context of a co-existence scenario of a satellite and a terrestrial link. Diversity combining techniques such as Equal Gain Combining (EGC) and Selection Combining (SC) are considered to enhance the SS efficiency. Furthermore, analytical expressions for probability of detection and probability of false alarm are presented for these techniques in the considered fading channel and the sensing performance is studied through analytical and simulation results. Moreover, the effect of Cross Polar Discrimination on the sensing performance is presented and it is shown that SS efficiency improves for low values of it. New techniques for spectrum sensing (SS) in cognitive SatComs has been proposed in [109]. The analysis of different combining techniques has been carried out for SS using dual polarized antenna. Furthermore, polarization states of received signals are exploited and based on obtained polarization states, Optimum Polarization Based Combining (OPBC) technique has been used for carrying out SS in the satellite terminal. The sensing performance of OPBC technique has been compared to Selection Combining (SC), Equal Gain Combining (EGC) and Maximum Ratio Combining (MRC) techniques. The simulation results show that OPBC technique achieves a great improvement in sensing efficiency over other considered techniques at the expense of complexity in a dual polarized AWGN channel.

The problem of resource allocation in the context of cognitive Satellite Communications (SatCom) has also been addressed in several papers. As an example, coexistence of geostationary FSS downlink and BSS feeder links in the Ka-band from 17.3 to 18.1 GHz is investigated in [67]. The authors investigate, assuming the availability of an accurate Radio Environment Map (REM), the application of carrier allocation and beamforming

in the considered scenario. The additional spectrum allows an increased system throughput and availability. In [66], cognitive downlink access for geostationary FSS terminals in the band from 17.7 to 19.7 GHz, where FS microwave links are considered as primary users, is investigated. Joint receiver beamforming techniques and carrier allocation is proposed at the cognitive FSS terminal side. The problem addresses maximization of the overall throughput. It is shown that, using non-exclusive bandwidths for the FSS downlinks, improves the overall system throughput. In [112], the authors consider overlaying a secondary-user signal over a satellite communication channel occupied by a primary user. The objective is to find the jointly optimal transmitter and receiver pair of a secondary system to minimize the mean squared error (MSE) at the output of the secondary receiver, subject to zero interference induced at the output samples of the primary receiver. In [113], a mechanism combining Spectrum Sensing and Power Control is proposed to allow a cognitive user to access the frequency band of a Primary User (PU) operating based on an Adaptive Coding and Modulation (ACM) protocol. The suggested SS technique considers Higher Order Statistical (HOS) features of the signal and an efficient machine learning detector in order to constantly monitor the modulation scheme of the PU. The proposed algorithm converges to the interference limit and guarantees preservation of the PU link QoS. Considering cognitive satellite terrestrial networks architecture, in [91], an efficient resource management mechanism for the terrestrial network acting as secondary system is proposed. Authors introduce a new power allocation algorithm that optimizes the effective capacity of the terrestrial link for given Quality of Service (QoS) requirements while guaranteeing a specified outage probability for the satellite link. Both perfect and imperfect channel estimation cases are considered in the power allocation scheme and analytical results are presented. A dual satellite scenario is considered in [114]. For this scenario, Interference Alignment (IA) is investigated for spectral coexistence of different wireless systems in an underlay scenario and Frequency Packing (FP) for enhancing spectrum efficiency. The effect of FP on the performance of multi-carrier based IA technique are addressed. Different IA techniques have been considered. The effect of FP on the performance of different IA techniques in the considered scenario is evaluated in terms of system sum rate and primary rate protection ratio. The proposed framework achieves higher sum rates according to the FP technique while the primary rate is perfectly protected with the coordinated IA technique even with dense FP. Spectral coexistence scenario of two multibeam satellites over a common coverage area is studied in [115]. A primary satellite having larger beams than the secondary satellite having smaller beams. Beamhopping is considered as exploitation technique. A further scenario of the presence of multiple secondary users within an inactive primary beam is considered with power control on the secondary transmission. The system performance is evaluated by considering partial and full frequency sharing approaches. It is noted that the total spectral efficiency increases with the number of secondary users in the full frequency reuse approach.

Bibliography

[1] J. Mitola and G. Q. Maguire. "Cognitive radio: making software radios more personal". In: *IEEE Personal Communications* 6.4 (1999), pp. 13–18. ISSN: 1070-9916. DOI: 10.1109/98.788210.

[2] S. Haykin. "Cognitive radio: brain-empowered wireless communications". In: *IEEE Journal on Selected Areas in Communications* 23.2 (Feb. 2005), pp. 201–220.

[3] A. Goldsmith et al. "Breaking Spectrum Gridlock With Cognitive Radios: An Information Theoretic Perspective". In: *Proceedings of the IEEE* 97.5 (2009), pp. 894–914.

[4] Ian F. Akyildiz et al. "NeXt Generation/Dynamic Spectrum Access/ Cognitive Radio Wireless Networks: A Survey". In: *Comput. Netw.* 50.13 (Sept. 2006), pp. 2127–2159. ISSN: 1389-1286.

[5] *5G: Challenges, Research Priorities, and Recommendations*. White Paper. NetWorld2020 ETP for Communications Networks and Services, Sept. 2014.

[6] *4G Americas Recommendations on 5G Requirements and Solutions*. White Paper. 4G Americas, Oct. 2014.

[7] *5G white paper*. White Paper. EU-China FIRE, 2014.

[9] S. Maleki et al. "Cognitive spectrum utilization in Ka band multibeam satellite communications". In: *Communications Magazine, IEEE* 53.3 (2015), pp. 24–29.

[11] Dimitrios Christopoulos et al. "Linear and nonlinear techniques for multibeam joint processing in satellite communications". In: *EURASIP Journal on Wireless Communications and Networking* 2012.1 (2012), pp. 1–13. ISSN: 1687-1499. DOI: 10.1186/1687-1499-2012-162. URL: http://dx.doi.org/10.1186/1687-1499-2012-162.

[12] Pantelis-Daniel Arapoglou et al. "DVB-S2X-enabled precoding for high throughput satellite systems". In: *International Journal of Satellite Communications and Networking* 34.3 (2016). SAT-15-0019.R1, pp. 439–455. ISSN: 1542-0981. DOI: 10.1002/sat.1122. URL: http://dx.doi.org/10.1002/sat.1122.

[13] Dimitrios Christopoulos, Pantelis-Daniel Arapoglou, and Symeon Chatzinotas. "Linear Precoding in Multibeam SatComs: Practical Constraints". In: *31st AIAA International Communications Satellite Systems Conference (ICSSC)* 2013 (2013). DOI: doi:10.2514/6.2013-5716. URL: http://dx.doi.org/10.2514/6.2013-5716.

[14] G. Taricco. "Linear Precoding Methods for Multi-Beam Broadband Satellite Systems". In: *European Wireless 2014; 20th European Wireless Conference; Proceedings of*. 2014, pp. 1–6.

[15] Jesús Arnau et al. "Performance study of multiuser interference mitigation schemes for hybrid broadband multibeam satellite architectures". In: *EURASIP Journal on Wireless Communications and Networking* 2012.1 (2012), pp. 1–19. ISSN: 1687-1499. DOI: 10.1186/1687-1499-2012-132. URL: http://dx.doi.org/10.1186/1687-1499-2012-132.

[16] *COgnitive RAdio for SATellite Communications*. White Paper. CoRaSat consortium, 2013.

[17] K. Liolis et al. "Cognitive radio scenarios for satellite communications: The CoRaSat approach". In: *Future Network and Mobile Summit (FutureNetworkSummit), 2013*. 2013, pp. 1–10.

[37] *FCC online Table Of Frequency Allocations Chart*. 47. Document. 2016. URL: https://transition.fcc.gov/oet/spectrum/table/fcctable.pdf.

[38] *Regulatory, Standardisation and Technology framework*. Deliverable D2.2. 2013. URL: http://www.ict-corasat.eu/.

[39] W. Tang, P. Thompson, and B. Evans. "A Database Approach to Extending the Usable Ka Band Spectrum for FSS Satellite Systems," in: *The 7th International Conference on Advances in Satellite and Space Communications (SPACOMM)*. 2015.

[40] W. Tang, P. Thompson, and B. Evans. "Frequency Sharing between Satellite and Terrestrial Systems in the Ka Band: A Database Approach," in: *IEEE International Conference on Communications (ICC)*. 2015, pp. 2470–2475. DOI: DOI:10.1109/ICC.2015.7248431.

[41] P. Thompson and B. Evans. "Extending the spectrum for Ka band satellite systems in the shared bands via a database approach," in: *21st Ka and Broadband Communications Conference*. 2015.

[42] W. Tang et al. *Extending the usable Ka band spectrum for FSS satellite systems using a FS Database*. 2015.

[43] P. Thompson and B. Evans. "Analysis of interference between terrestrial and satellite systems in the Band 17.7 to 19.7 GHz". In: *2015 IEEE International Conference on Communication Workshop (ICCW)*. 2015, pp. 1669–1674. DOI: 10.1109/ICCW.2015.7247420.

[46] S. Maleki et al. "Cognitive Zone for Broadband Satellite Communications in 17.3-17.7 GHz Band". In: *IEEE Wireless Communications Letters* 4.3 (2015), pp. 305–308. ISSN: 2162-2337. DOI: 10.1109/LWC.2015.2411597.

[53] J. Tronc et al. "Overview and comparison of on-ground and on-board beamforming techniques in mobile satellite service applications". In: *International Journal of Satellite Communications and Networking* 32.4 (2014), pp. 291–308. ISSN: 1542-0981. DOI: 10.1002/sat.1049. URL: http://dx.doi.org/10.1002/sat.1049.

[54] A. Franchi, A. Howell, and J. Sengupta. "Broadband mobile via satellite: inmarsat BGAN". In: *Broadband Satellite: The Critical Success Factors - Technology, Services and Markets (Ref. No. 2000/067), IEE Seminar on*. 2000, pp. 23/1–23/7. DOI: 10.1049/ic:20000547.

[55] *Inmarsat 4F2 Attachment 1. Technical Description*. URL: https://licensing.fcc.gov/myibfs/download.do?attachment_key=-94644.

[56] R. Tandra, S.M. Mishra, and A. Sahai. "What is a Spectrum Hole and What Does it Take to Recognize One?" In: *Proceedings of the IEEE* 97.5 (2009), pp. 824–848.

[57] S. Haykin, D.J. Thomson, and J.H. Reed. "Spectrum Sensing for Cognitive Radio". In: *Proceedings of the IEEE* 97.5 (2009), pp. 849–877.

[58] E. Axell et al. "Spectrum Sensing for Cognitive Radio: State-of the-Art and Recent Advances". In: *IEEE Signal Processing Magazine* 29.3 (2012), pp. 101–116.

[59] A. Ghasemi and E.S. Sousa. "Spectrum sensing in cognitive radio networks: requirements, challenges and design trade-offs". In: *IEEE Communications Magazine* 46.4 (2008), pp. 32–39.

[61] T. Yucek and H. Arslan. "A survey of spectrum sensing algorithms for cognitive radio applications". In: *IEEE Communications Surveys and Tutorials* 11.1 (2009), pp. 116–130.

[62] H. Urkowitz. "Energy detection of unknown deterministic signals". In: *Proceedings of the IEEE* 55.4 (1967), pp. 523–531.

[63] R. Tandra and A. Sahai. "SNR Walls for Signal Detection". In: *Selected Topics in Signal Processing, IEEE Journal of* 2.1 (2008), pp. 4–17.

[64] S.K. Sharma, S. Chatzinotas, and B. Ottersten. "A hybrid cognitive transceiver architecture: Sensing-throughput tradeoff". In: *Cognitive Radio Oriented Wireless Networks and Communications (CROWNCOM), 2014 9th International Conference on*. 2014, pp. 143–149.

[66] Shree Krishna Sharma et al. "Resource allocation for cognitive Satellite Communications in Ka-band (17.7-19.7 GHz)". In: *Communication Workshop (ICCW), 2015 IEEE International Conference on*. 2015, pp. 1646–1651.

[67] Shree Krishna Sharma et al. "Joint Carrier Allocation and Beamforming for cognitive SatComs in Ka-band (17.3-18.1 GHz)". In: *Communications (ICC), 2015 IEEE International Conference on*. 2015, pp. 873–878.

[68] Willian A. Gardner, Antonio Napolitano, and Luigi Paura. "Cyclostationarity: Half a century of research". In: *Signal Processing* 86.4 (2006), pp. 639–697.

[69] Ying-Chang Liang et al. "Sensing-Throughput Tradeoff for Cognitive Radio Networks". In: *Wireless Communications, IEEE Transactions on* 7.4 (2008), pp. 1326–1337.

[70] F. Benedetto et al. "Effective Monitoring of Freeloading User in the Presence of Active User in Cognitive Radio Networks". In: *Vehicular Technology, IEEE Transactions on* 63.5 (2014), pp. 2443–2450.

[71] S. Cioni, G.E. Corazza, and M. Bousquet. "An Analytical Characterization of Maximum Likelihood Signal-to-Noise Ratio Estimation". In: *Proc. of 2nd International Symposium on Wireless Communication Systems*. Sept. 2005, pp. 827–830.

[72] S. Cioni, R. De Gaudenzi, and R. Rinaldo. "Channel estimation and physical layer adaptation techniques for satellite networks exploiting adaptive coding and modulation". In: *Int. J. Satell. Commun. Network.* 26 (Mar. 2008), pp. 157–188.

[78] E. Axell et al. "Spectrum Sensing for Cognitive Radio : State-of-the-Art and Recent Advances". In: *IEEE Signal Processing Magazine* 29.3 (2012), pp. 101–116.

[79] H. Kim and K. G. Shin. "In-Band Spectrum Sensing in IEEE 802.22 WRANs for Incumbent Protection". In: *IEEE Transactions on Mobile Computing* 9.12 (2010), pp. 1766–1779.

[80] W. A. Gardner. "Exploitation of spectral redundancy in cyclostationary signals". In: *IEEE Signal Processing Magazine* 8.2 (1991), pp. 14–36.

[81] J. Lunden et al. "Spectrum Sensing in Cognitive Radios Based on Multiple Cyclic Frequencies". In: *2007 2nd International Conference on Cognitive Radio Oriented Wireless Networks and Communications*. 2007, pp. 37–43.

[83] J.P. Choi and V.W.S. Chan. "Optimum multibeam satellite downlink power allocation based on traffic demands". In: *Global Telecommunications Conference, 2002. GLOBECOM '02. IEEE*. Vol. 3. 2002, 2875–2881 vol.3. DOI: 10.1109/GLOCOM.2002.1189155.

[84] Yang Hong et al. "Optimal power allocation for multiple beam satellite systems". In: *Radio and Wireless Symposium, 2008 IEEE*. 2008, pp. 823–826. DOI: 10.1109/RWS.2008.4463619.

[85] A. Destounis and A.D. Panagopoulos. "Dynamic Power Allocation for Broadband Multi-Beam Satellite Communication Networks". In: *Communications Letters, IEEE* 15.4 (2011), pp. 380–382. ISSN: 1089-7798. DOI: 10.1109/LCOMM.2011.020111.102201.

[86] J. Lei and M.A. Vazquez-Castro. "Multibeam satellite frequency/time duality study and capacity optimization". In: *Communications and Networks, Journal of* 13.5 (2011), pp. 472–480.

[87] N.K. Srivastava and A.K. Chaturvedi. "Flexible and Dynamic Power Allocation in Broadband Multi-Beam Satellites". In: *Communications Letters, IEEE* 17.9 (2013), pp. 1722–1725. ISSN: 1089-7798. DOI: 10.1109/LCOMM.2013.080113.130615.

[88] A.I. Aravanis et al. "Power Allocation in Multibeam Satellite Systems: A Two-Stage Multi-Objective Optimization". In: *Wireless Commun., IEEE Trans. on* 14.6 (2015), pp. 3171–3182. ISSN: 1536-1276. DOI: 10.1109/TWC.2015.2402682.

[89] I. Bisio and Mario Marchese. "Power Saving Bandwidth Allocation over GEO Satellite Networks". In: *Communications Letters, IEEE* 16.5 (2012), pp. 596–599. ISSN: 1089-7798. DOI: 10.1109/LCOMM.2012.030912.111913.

[90] J.P. Choi and V.W.S. Chan. "Optimum power and beam allocation based on traffic demands and channel conditions over satellite downlinks". In: *Wireless Communications, IEEE Transactions on* 4.6 (2005), pp. 2983–2993. ISSN: 1536-1276. DOI: 10.1109/TWC.2005.858365.

[91] S. Vassaki et al. "Power Allocation in Cognitive Satellite Terrestrial Networks with QoS Constraints". In: *IEEE Communications Letters* 17.7 (2013), pp. 1344–1347. ISSN: 1089-7798. DOI: 10.1109/LCOMM.2013.051313.122923.

[92] E. Del Re et al. "A power allocation strategy using Game Theory in Cognitive Radio networks". In: *Game Theory for Networks, 2009. GameNets '09. International Conference on*. 2009, pp. 117–123. DOI: 10.1109/GAMENETS.2009.5137392.

[93] E. Lagunas et al. "Resource Allocation for Cognitive Satellite Uplink and Fixed-Service Terrestrial Coexistence in Ka-band". In: *Proc. of IEEE CROWNCOM 2015*. Doha, Qatar, 2015.

[94] M. Srinivas and L.M. Patnaik. "Genetic algorithms: a survey". In: *Computer* 27.6 (1994), pp. 17–26.

[96] Pietro Belotti et al. "Mixed-integer nonlinear optimization". In: *Acta Numerica* 22 (May 2013), pp. 1–131. ISSN: 1474-0508. DOI: 10.1017/S0962492913000032. URL: http://journals.cambridge.org/article_S0962492913000032.

[98] F. Bourgeois and J. C. Lassalle. "An extension of the Munkres algorithm for the assignment problem to rectangular matrices". In: *Communication of the ACM* 14.12 (1971).

[100] N. Alagha and A. Modenini. "On Capacity Measures for Multi-Beam Satellite Systems Analyses". In: *2016 8th Advanced Satellite Multimedia Systems Conference (ASMS) and 14th Signal Processing for Space Communications Workshop (SPSC)*. 2016.

[101] Ignacio E. Grossmann and Zdravko Kravanja. "Mixed-Integer Nonlinear Programming: A Survey of Algorithms and Applications". In: (1997). Ed. by Lorenz T. Biegler et al., pp. 73–100. DOI: 10.1007/978-1-4612-1960-6_5. URL: http://dx.doi.org/10.1007/978-1-4612-1960-6_5.

[103] M. H*öy*hty*ä* et al. "Application of cognitive radio techniques to satellite communication". In: *Dynamic Spectrum Access Networks (DYSPAN), 2012 IEEE International Symposium on*. 2012, pp. 540–551. DOI: 10.1109/DYSPAN.2012.6478178.

[104] E. Biglieri. "An overview of Cognitive Radio for satellite communications". In: *2012 IEEE First AESS European Conference on Satellite Telecommunications (ESTEL)*. 2012, pp. 1–3. DOI: 10.1109/ESTEL.2012.6400078.

[105] S. K. Sharma, S. Chatzinotas, and B. Ottersten. "Satellite cognitive communications: Interference modeling and techniques selection". In: *2012 6th Advanced Satellite Multimedia Systems Conference (ASMS) and 12th Signal Processing for Space Communications Workshop (SPSC)*. 2012, pp. 111–118. DOI: 10.1109/ASMS-SPSC.2012.6333061.

[106] S. K. Sharma, S. Chatzinotas, and B. Ottersten. "Cognitive Radio Techniques for Satellite Communication Systems". In: *Vehicular Technology Conference (VTC Fall), 2013 IEEE 78th*. 2013, pp. 1–5. DOI: 10.1109/VTCFall.2013.6692139.

[107] S. Kandeepan et al. "Cognitive Satellite Terrestrial Radios". In: *Global Telecommunications Conference (GLOBECOM 2010), 2010 IEEE*. 2010, pp. 1–6. DOI: 10.1109/GLOCOM.2010.5683428.

[108] S. K. Sharma, S. Chatzinotas, and B. Ottersten. "Spectrum sensing in dual polarized fading channels for cognitive SatComs". In: *Global Communications Conference (GLOBECOM), 2012 IEEE*. 2012, pp. 3419–3424. DOI: 10.1109/GLOCOM.2012.6503643.

[109] S. K. Sharma, S. Chatzinotas, and B. Ottersten. "Exploiting polarization for spectrum sensing in cognitive SatComs". In: *Cognitive Radio Oriented Wireless Networks and Communications (CROWNCOM), 2012 7th International ICST Conference on*. 2012, pp. 36–41. DOI: 10.4108/icst.crowncom.2012.248473.

[110] C. Kourogiorgas, A. D. Panagopoulos, and K. Liolis. "Cognitive uplink FSS and FS links coexistence in Ka-band: Propagation based interference analysis". In: *2015 IEEE International Conference on Communication Workshop (ICCW)*. 2015, pp. 1675–1680. DOI: 10.1109/ICCW.2015.7247421.

[111] C. Kourogiorgas and A. D. Panagopoulos. "Interference statistical distribution for cognitive satellite communication systems operating above 10GHz". In: *2014 7th Advanced Satellite Multimedia Systems Conference and the 13th Signal Processing for Space Communications Workshop (ASMS/SPSC)*. 2014, pp. 256–261. DOI: 10.1109/ASMS-SPSC.2014.6934552.

[112] Y. H. Yun and J. H. Cho. "An orthogonal cognitive radio for a satellite communication link". In: *2009 IEEE 20th International Symposium on Personal, Indoor and Mobile Radio Communications*. 2009, pp. 3154–3158. DOI: 10.1109/PIMRC.2009.5449826.

[113] A. Tsakmalis, S. Chatzinotas, and B. Ottersten. "Automatic Modulation Classification for adaptive Power Control in cognitive satellite communications". In: *2014 7th Advanced Satellite Multimedia Systems Conference and the 13th Signal Processing for Space Communications Workshop (ASMS/SPSC)*. 2014, pp. 234–240. DOI: 10.1109/ASMS-SPSC.2014.6934549.

[114] S. Chatzinotas, S. K. Sharma, and B. Ottersten. "Frequency Packing for Interference Alignment-Based Cognitive Dual Satellite Systems". In: *Vehicular Technology Conference (VTC Fall), 2013 IEEE 78th*. 2013, pp. 1–7. DOI: 10.1109/VTCFall.2013.6692209.

[115] S. K. Sharma, S. Chatzinotas, and B. Ottersten. "Cognitive beamhopping for spectral coexistence of multibeam satellites". In: *Future Network and Mobile Summit (FutureNetworkSummit), 2013*. 2013, pp. 1–10.

Books

[8] Hüseyin Arslan. *Cognitive radio, software defined radio, and adaptive wireless systems*. Vol. 10. Springer, 2007.

[31] Gerard Maral, Michel Bousquet, and Zhili Sun, eds. *Satellite Communications Systems: Systems, Techniques and Technology*. English. 5th. Wiley, Dec. 2009. ISBN: 978-0-470-71458-4.

[32] Giovanni Corazza, ed. *Digital Satellite Communications*. 2007. ISBN: 978-0-387-25634-4.

[60] K. Sithamparanathan and A. Giorgetti, eds. *Cognitive Radio Techniques: Spectrum Sensing, Interference Mitigation, and Localization (Mobile Communications)*. English. Artech House, 2012. ISBN: 978-1608072033.

[65] Andrea Goldsmith. *Wireless Communications*. Cambridge Univerisity Press, 2005.

[75] Van Trees and Harry L. *Detection, Estimation, and Modulation Theory -Vol.1*. John Wiley Sons, Inc. New York, NY, USA, 2004. ISBN: 978-0-471-46382-5.

[82] Giovanni Giambene. *Resource Management in Satellite Networks - Optimization and Cross-Layer Design*. Springer US, 2007.

[95] Melanie Mitchell. *An introduction to genetic algorithms*. MIT press, 1998.

[97] Silvano Martello and Paolo Toth. *Knapsack problems: algorithms and computer implementations*. John Wiley & Sons, Inc. New York, NY, USA, 1990. ISBN: 0-471-92420-2.

[102] David Tse and Pramod Viswanath. *Fundamentals of Wireless Communication*. Cambridge University Press, 2005.

Standardization and Regulation

[33] *Digital Video Broadcasting (DVB); Second generation framing structure, channel coding and modulation systems for Broadcasting, Interactive Services, News Gathering and other broadband satellite applications (DVB-S2)*. EN 302 307. European Standard. Version 1.3.1. ETSI. 2013.

[34] *Digital Video Broadcasting (DVB); Second generation framing structure, channel coding and modulation systems for Broadcasting, Interactive Services, News Gathering and other broadband satellite applications Part II: S2-Extensions (DVB-S2X)*. EN 302 307 - 2. European Standard. ETSI. 2014.

[35] *Digital Video Broadcasting (DVB); Second Generation DVB Interactive Satellite System (DVB-RCS2);* TS 101 545-1. European Standard. Version 1.2.1. ETSI. Apr. 2014.

[36] *The European table of frequency allocations and applications in the frequency range 8.3 kHz to 3000 GHz (ECA table)*. 25. ERC Report. 2013.

[44] *The availability of frequency bands for high density applications in the Fixed Satellite Service (space-to-Earth and Earth-to-space)*. (05)08. ECC Decision. 2013.

[45] *The harmonised use, free circulation and exemption from individual licensing of Earth Stations On Mobile Platforms (ESOMPs) within the frequency bands 17.3-20.2 GHz and 27.5-30.0 GHz*. (13)01. ECC Decision. 2013.

[47] *The shared use of the band 17.7-19.7 GHz by the fixed service and earth stations of the fixed-satellite service (space-to-Earth)*. (13)01. ERC Decision. 2016.

[48] *Radio Regulations - Vol. 1: Articles and Vol. 2: Appendices*. International Telecommunications Union - Radiocommunication Sector. 2012.

[49] *System parameters and considerations in the development of criteria for sharing or compatibility between digital fixed wireless systems in the fixed service and systems in other services and other sources of interference*. F.758-6. Rec. 2015.

[50] *Reference radiation patterns for fixed wireless system antennas for use in coordination studies and interference assessment in the frequency range from 100 MHz to about 70 GHz*. F.699-7. Rec. 2006.

[51] *Mathematical model of average and related radiation patterns for line-of-sight point-to-point fixed wireless system antennas for use in certain coordination studies and interference assessment in the frequency range from 1 GHz to about 70 GHz*. F.1245-2. Rec. Mar. 2012.

[52] *Reference radiation patterns of omnidirectional, sectoral and other antennas for the fixed and mobile service for use in sharing studies in the frequency range from 400 MHz to about 70 GHz*. F.1336-4. Rec. Feb. 2014.

[73] *LTE; Evolved Universal Terrestrial Radio Access (E-UTRA); User Equipment (UE) radio transmission and reception*. TS 136 101 - 10.3.0. European Standard. ETSI. 2011.

[74] *Digital Video Broadcasting (DVB); Frame structure channel coding and modulation for a second generation digital terrestrial television broadcasting system (DVB-T2)*. EN 302 755 - 1.3.1. European Standard. ETSI. 2012.

[76] *Apportionment of the allowable error performance degradations to fixed-satellite service (FSS) hypothetical reference digital paths arising from time invariant interference for systems operating below 30 GHz*. S.1432-1. Recommendation. 2006.

[77] *Prediction procedure for the evaluation of interference between stations on the surface of the Earth at frequencies above about 0.1 GHz*. P.452-15. Recommendation. 2013.

[99] *Reference radiation pattern for earth station antennas in the fixed satellite service for use in coordination and interference assessment in the frequency range from 2 to 31 GHz*. S.465-6. Rec. 2010.

Personal Contributions

[10] S. Chatzinotas et al. "Cognitive approaches to enhance spectrum availability for satellite systems". In: *International Journal of Satellite Communications and Networking* (2016).

[18] V. Icolari et al. "An interference estimation technique for Satellite cognitive radio systems". In: *2015 IEEE International Conference on Communications (ICC)*. 2015, pp. 892–897.

[19] D. Tarchi et al. "On the feasibility of Interference Estimation Techniques in Cognitive Satellite Environments with Impairments". In: *Proc. of WiSats 2015*. Bradford, UK, 2015.

[20] A. Guidotti et al. "Spectrum awareness techniques for 5G satellite communications". In: *Signal Processing Conference (EUSIPCO), 2015 23rd European*. 2015, pp. 2761–2765.

[21] *Performance evaluation of existing cognitive techniques in satellite context*. Deliverable D3.2. 2014. URL: http://www.ict-corasat.eu/.

[22] *Adaptation and design of cognitive techniques for satellite communications*. Deliverable D3.3. CoRaSat Project, 2014. URL: http://www.ict-corasat.eu/.

[23] *Comparative system evaluation and scenario-technique selection*. Deliverable D3.4. CoRaSat Project, 2015. URL: http://www.ict-corasat.eu/.

[24] V. Icolari et al. "Genetic inspired scheduling algorithm for cognitive satellite systems". In: *2016 IEEE International Conference on Communications (ICC)*. 2016, pp. 1–6.

[25] V. Icolari et al. "Flexible precoding for mobile satellite system hot spots". In: *2017 IEEE International Conference on Communications (ICC)*. 2017, accepted for publication.

[26] D. Tarchi et al. "Technical challenges for cognitive radio application in satellite communications". In: *2014 9th International Conference on Cognitive Radio Oriented Wireless Networks and Communications (CROWNCOM)*. 2014, pp. 136–142.

[27] V. Icolari et al. "An energy detector based radio environment mapping technique for cognitive satellite systems". In: *2014 IEEE Global Communications Conference*. 2014, pp. 2892–2897.

[28] A. Guidotti et al. "Spectrum awareness and exploitation for Cognitive Radio Satellite Communications". In: *Networks and Communications (EuCNC), 2015 European Conference on*. 2015, pp. 16–20.

[29] V. Icolari et al. "Beam pattern allocation strategies for satellite cognitive radio systems". In: *2015 IEEE International Conference on Communication Workshop (ICCW)*. 2015, pp. 1652–1657.

[30] Barry Evans et al. “Extending the usable Ka band spectrum for satellite communications: The CoRaSat project”. In: *International Conference on Wireless and Satellite Systems*. Springer International Publishing. 2015, pp. 119–132.